Profound Endothelial Dysfunction and Inflammation in Fabry Disease: Responses to Exercise Training

by

Jung Euy Kang

A dissertation submitted in partial fulfillment
of the requirements for the degree of
Doctor of Philosophy
(Kinesiology)
in the University of Michigan
2017

Doctoral Committee:

Clinical Assistant Professor Peter F. Bodary, Co-Chair
Professor Jeffrey F. Horowitz, Co-Chair
Professor Gregory D. Cartee
Professor James A. Shayman

Justin Jung-Euy Kang

justinjk@umich.edu

ORCID iD: 0000-0002-2907-6872

Acknowledgment

There are a number of people I need to thank for helping me to reach this point since I started my Ph.D. journey in the summer of 2011. It would only be appropriate to begin by expressing my sincere gratitude for the tremendous efforts of my mentor, Dr. Peter F. Bodary.

Dr. Bodary, I honestly cannot thank you enough for providing an amazing environment for me to grow as a scientist. The first word that comes to my mind whenever I think about you is approachable. No matter how busy you were, your door was always open to me. Whenever I came to you to discuss any data or even a harebrained idea, you never told me “no” or “wrong.” You always treated me as a colleague, not a student. I believe there is a thin line between a boss and a leader. A boss only commends and stays on the sideline. However, a leader says “we”, not “I”, always stays at the front of the pack, and leads by examples, generating enthusiasm, not fear. You are my leader and the leader of the Vascular Biology Laboratory. You have made a lasting impact on my life and have been the best possible mentor that one can be. One day, I want to become such a pattern to someone else, just like you are such a pattern to me. The time and dedication you put into me is second to none, and I can confidently say that I got your full attention during my Ph.D. I appreciate your tremendous efforts and mentorship, Dr. Bodary!

Dr. Shayman, thank you for your generous support throughout my Ph.D. and your guidance on my research. You taught me how to see a big picture and keep things in perspective. I still remember that one day you told me that “you are only limited by your time and your effort.” I am grateful for providing me an amazing research environment and giving me academic freedom.

Dr. Horowitz, thank you for your advice on my research and helpful comments and discussions. During the time of the weekly journal club in your lab, I enjoyed getting inputs from your people who have different perspectives on research. I am also thankful for your prompt responses and helps during the past couple months even though you were on sabbatical outside of the U.S.

Dr. Cartee, thank you for giving me an opportunity to have my lab rotation in your lab. I did not have much research background at that time. While being in one of the worldly renowned muscle biology laboratories, I was fortunate to learn a significant amount of research techniques including, but not limited to, western blot and murine muscle dissection skills, which have greatly assisted my dissertation studies.

And of course, special thanks to the small army of undergrad and grad students, and research fellows known as the Shayman lab. I thank everyone for bearing with me during the days of “darkness” whenever I ran the biotin switch assay, which needs to be performed in the dark. Dr.

Robert Kelly, thank you for your help in everything but especially for teaching me general research techniques and ordering research supplies for me. I know Shayman lab would not function without your efforts! Dr. Hinkovska-Galcheva (my lab mother), not only did you provide your invaluable advice on my experiments, but you have always put students before you. You have your own way of enlightening the mood, and I like your “enjoy your life” lessons. Nayiri, thank you for being my go-to colleague in the lab for methodology and data discussion, and I sincerely grateful for sharing your “sexy” CRISPR cell lines. Another special thanks to Taylour Treadwell for collecting voluntary wheel data. I know a lot of efforts went into it, and I would not have been able to finish the exercise study without your help.

To the past members of the Vascular Biology Laboratory, I want to thank you for your assistance, support, and patience. Xiaoya, I was able to pass through my coursework and the comprehensive exam during the first couple years of my Ph.D. with you learning together. And to the awesome crews of VBL, the big “sac parties” were never boring because of all of you.

I need to also thank the neighboring labs in the basement of the CCRB for helping me on a regular basis. Dr. Edward Arias, thank you for teaching me muscle dissection skills and letting me monopolize the glass homogenizer. Carlos, thank you for being so approachable and helping me with a number of lab, grant, and career-related questions. I cannot wait to play golf with you in Dallas! Doug and Alison, the basement of the CCRB has been a surprisingly entertaining place to

work because of you guys. It has been always a pleasure to have you guys around to chat about science- and non-science-related topics any times.

Dr. James Park, I am thankful for your invaluable research advice on the studies of vascular function and teaching me the “fancy” myograph technique. Charlene, thank you for your support and help for each step of my doctoral process. Whenever I had questions related to any requirements or important processes during my Ph.D., you were the first one to ask, and you always had the answers. Dr. Justin Jeon, I am grateful for your support, and I believe that I have absorbed some of your “Why not? Let’s do it.”-spirit.

Seung-young, Kyung-hwan, Jung-woon, Bum-hyun, and “eagles”, you guys are like brothers to me. I know I can always count on you guys. When I need to talk to someone, you guys are there. Whenever I need someone to unwind together, you guys are there. Wherever I go, it makes me easier to move forward knowing that you guys were and continue to have my back.

To my friends in church in Ann Arbor. To list the contributions of all of you guys would surely require a separate volume. Here I especially thank Ching-shih and Edwina, Daniel and Edith, Floyd and Caroline, Bong-chae, Anthony and Priscilla, and EJ. I was able to get through some difficult times because of your tremendous support, love, and prayers. You guys are like my family, and

thank you for taking care of Jenny and me and keeping us always in your prayer. We will always have a room for you to visit us in Dallas.

Last, but by no means least, to my family. Jenny, you are an amazing woman and wife. You have made numerous sacrifices to help me get to where I am, and I appreciate every one of them. I was able to stay focused on my work, not worrying about anything else because of you. You are the best cook I know, and I am thankful for your incredible heart and invaluable support. I love you so much, and I am excited to see what our future holds. Mom and Dad, I appreciate everything you have done for me. You are all extraordinary people and I would not have been able to do this without your sacrifices that you have made to provide me as many opportunities as possible. I will continue to strive to be the best possible person that I can be to ensure that your sacrifices were worthwhile. I love you and miss you so much. To my in-laws, Charles and Amber, I really feel that I am lucky to be a part of your family. You all have been extremely supportive of me ever since we met. Jiyoung and Sanglim, thank you for your prayers and being there for me. You have always had confidence in me and have always put my best interests before yours. I love you all.

Table of Contents

List of Figures

List of Appendices

ABSTRACT

Cardiovascular disease is the leading cause of death in the United States and globally. Atherosclerosis is an important basis for coronary heart disease and stroke, the two major types of cardiovascular disorders. Fabry disease promotes accelerated atherogenesis and thrombogenesis by loss of activity of the lysosomal hydrolase, α-Galactosidase A (GLA), resulting in the accumulation of globotriaosylceramide (Gb3) in vascular endothelial cells. Although endothelial dysfunction, characterized by decreased nitric oxide bioavailability, is believed to be the basis for the vasculopathy in Fabry disease, the pathophysiological mechanisms underlying GLA deficiency remain elusive. Using Fabry disease as a model to study accelerated vascular disease, the overall purpose of my dissertation was to further characterize endothelial dysfunction and inflammation using murine and *in vitro* endothelial cell models of Fabry disease, and to examine the effects of 12 weeks of voluntary exercise on endothelial function in the setting of eNOS dysregulation. The major findings of my dissertation studies include that: 1) GLA deficiency in mice resulted in early, profound endothelial dysfunction in the mesenteric artery, which was associated with eNOS uncoupling and changes in eNOS activating and inhibitory phosphorylation sites; 2) the *in vitro* disruption of GLA in endothelial cells with siRNA or CRISPR/Cas9 directly promoted a decrease in eNOS activity and robustly elevated the secretion of von Willebrand factor (VWF), which plays an important role in thrombi formation; 3) pharmacological approaches that improve exogenous or endogenous NO availability or reduce reactive oxygen species (ROS) completely normalized

the elevated VWF secretion in the setting of GLA deficiency; and 4) 12 weeks of voluntary wheel exercise did not significantly improve endothelium-mediated vasodilation or the oxidative stress profile despite increased p-Akt (Ser473), AMPK (Thr172), and eNOS (Ser1177) signaling cascades in the aorta of 12-14 month old GLA deficient mice. Overall, the findings from these dissertation projects suggest that in Fabry disease: 1) decreased NO availability due to eNOS uncoupling and elevated ROS may exacerbate endothelial dysfunction and inflammation; 2) VWF release from the endothelium appears to be mediated by the profound endothelial dysfunction present in GLA deficiency; 3) strategies that increase NO bioavailability and/or decrease ROS, such as sepiapterin, tempol, and ebselen lead to an attenuation in VWF secretion; and 4) exercise mediated activation of Akt/AMPK/eNOS signaling cascades without significant improvement in aortic endothelial function in 12-14 month old GLA deficient mice. In summary, this dissertation compliments the prior hypothesis that GLA deficiency-mediated eNOS dysregulation is an important basis for endothelial inflammation and questions whether current treatment strategies for Fabry disease are optimal for improving the underlying vasculopathy.

CHAPTER 1

Statement of the Problem

Heart disease is the leading cause of death in the United States, and cardiovascular disease accounts for nearly 30% of all deaths annually (7). However, many heart disease and stroke deaths could be delayed through treatment of risk factors and improvements in lifestyle behaviors.

Fabry disease is an X-linked inborn error of glycosphingolipid metabolism caused by a defect in the gene encoding the lysosomal enzyme α-Galactosidase A (GLA), resulting in a toxic accumulation of globotriaosylceramide (Gb3) in various organ systems (1, 6). This accumulation of Gb3, especially in the vascular endothelium, is coupled with impaired endothelial function in patients with Fabry disease, ultimately leading to premature death from cardiac disease and strokes (4). The current standard of care for Fabry patients is enzyme replacement therapy (ERT) using recombinant human GLA. Although this treatment is effective in reducing Gb3 accumulation in multiple cell types, the average cost per patient of the ERT is tremendous (over $215,000 / year), which makes therapy difficult to obtain for these patients (4). In addition, emerging evidence suggests that ERT does not prevent the natural course of cardiac disease, cerebrovascular disease, or nephropathy in all patients once the damage from this disease is far advanced (8, 10). In contrast, Gaucher disease, the most common of the lysosomal storage disorders, is effectively treated with replacement of its defective enzyme, beta-glucocerebrosidase (2). This indicates that the vascular complications in Fabry disease do not entirely depend on Gb3 accumulation. It is, therefore,

important to investigate the cellular mechanism(s) underlying the Fabry vasculopathy and to identify better treatment strategies. A recent study that screened more than 1,400 patients with common forms of heart disease, such as coronary artery disease and cardiomyopathy, has reported that elevated urinary Gb3 is positively associated with and predicts near-term mortality in heart disease patients who do not have Fabry disease (9). This suggests that heart disease in common clinical settings is associated with glycolipid metabolism abnormalities. Therefore, although Fabry disease is a very rare genetic condition, a greater appreciation of the role of this glycosphingolipid storage disease on endothelial dysfunction may have broad implications for our understanding of cardiovascular disease pathophysiology.

The outline of my dissertation is as follows:

A. Endothelial dysfunction and inflammation in the setting of GLA deficiency.
    - **PROJECT 1:** Determination of endothelium-dependent dilation and signaling alterations of the endothelial nitric oxide synthase in the mesenteric artery in younger and older mice deficient in GLA compared to age-matched wild type mice.
    - **PROJECT 2:** Examination of endothelial inflammation and possible mechanisms of alterations in von Willebrand factor secretion in cellular models of Fabry disease.
B. Effects of exercise on endothelial dysfunction and inflammation in the setting of GLA deficiency.
    - **PROJECT 3:** Investigation of the effects of 12 weeks of voluntary wheel running on endothelial nitric oxide synthase uncoupling and endothelial inflammation in the mouse model of Fabry disease.

The overall objective of my dissertation projects is to advance understanding of endothelial dysfunction and inflammation in murine and cellular models of Fabry disease and to examine possible roles of voluntary wheel exercise on endothelial nitric oxide synthase dysregulation in the setting of GLA deficiency. History has revealed that the study of rare lipid disorders can lead to the discovery of specific mechanisms and/or therapeutic interventions for cardiovascular disease. For example, previous studies on rare familial hypercholesterolemia characterized by LDL receptor deficiency led to the discovery of the regulation of cholesterol metabolism (5) and the current class of medications (i.e. statins) that have proven useful for reducing cardiovascular disease mortality in high risk patients (3). Therefore, the findings of these dissertation projects have important implications for identifying new strategies for preventive and therapeutic interventions for vasculopathy in Fabry disease, in addition to fundamentally advancing the fields of cardiovascular disease and vascular complications.

References

1. **Brady RO.** Enzymatic abnormalities in diseases of sphingolipid metabolism. *Clin Chem* 13: 565-577, 1967.

2. **Chinetti-Gbaguidi G and Staels B.** Macrophage polarization in metabolic disorders: functions and regulation. *Curr Opin Lipidol* 22: 365-372, 2011.

3. **Chou R, Dana T, Blazina I, Daeges M, and Jeanne TL.** Statins for Prevention of Cardiovascular Disease in Adults: Evidence Report and Systematic Review for the US Preventive Services Task Force. *Jama* 316: 2008-2024, 2016.

4. **Eng CM, Fletcher J, Wilcox WR, Waldek S, Scott CR, Sillence DO, Breunig F, Charrow J, Germain DP, Nicholls K, and Banikazemi M.** Fabry disease: baseline medical characteristics of a cohort of 1765 males and females in the Fabry Registry. *Journal of inherited metabolic disease* 30: 184-192, 2007.

5. **Goldstein JL and Brown MS.** The low-density lipoprotein pathway and its relation to atherosclerosis. *Annual review of biochemistry* 46: 897-930, 1977.

6. **Kint JA.** Fabry's disease: alpha-galactosidase deficiency. *Science* 167: 1268-1269, 1970.

7. **Mozaffarian D, Benjamin EJ, Go AS, Arnett DK, Blaha MJ, Cushman M, de Ferranti S, Despres JP, Fullerton HJ, Howard VJ, Huffman MD, Judd SE, Kissela BM, Lackland DT, Lichtman JH, Lisabeth LD, Liu S, Mackey RH, Matchar DB, McGuire DK, Mohler ER, 3rd, Moy CS, Muntner P, Mussolino ME, Nasir K, Neumar RW, Nichol G, Palaniappan L, Pandey DK, Reeves MJ, Rodriguez CJ, Sorlie PD, Stein J, Towfighi A, Turan TN, Virani SS, Willey JZ, Woo D, Yeh RW, Turner MB, American Heart Association Statistics C, and Stroke Statistics S.** Heart disease and stroke statistics--2015 update: a report from the American Heart Association. *Circulation* 131: e29-322, 2015.

8. **Rombach SM, Smid BE, Bouwman MG, Linthorst GE, Dijkgraaf MG, and Hollak CE.** Long term enzyme replacement therapy for Fabry disease: effectiveness on kidney, heart and brain. *Orphanet journal of rare diseases* 8: 47, 2013.

9. **Schiffmann R, Forni S, Swift C, Brignol N, Wu X, Lockhart DJ, Blankenship D, Wang X, Grayburn PA, Taylor MR, Lowes BD, Fuller M, Benjamin ER, and Sweetman L.** Risk of death in heart disease is associated with elevated urinary globotriaosylceramide. *Journal of the American Heart Association* 3: e000394, 2014.

10. **Terryn W, Cochat P, Froissart R, Ortiz A, Pirson Y, Poppe B, Serra A, Van Biesen W, Vanholder R, and Wanner C.** Fabry nephropathy: indications for screening and guidance for diagnosis and treatment by the European Renal Best Practice. *Nephrology, dialysis, transplantation : official publication of the European Dialysis and Transplant Association - European Renal Association* 28: 505-517, 2013.

CHAPTER 2

Review of Literature

Despite the success in reducing the mortality from acute cardiovascular events, cardiovascular disease (CVD) and its complications still produce immense health and economic burdens as the main cause of death in the United States and globally (115). Compelling scientific evidence suggests that the endothelium plays a pivotal role in the regulation of vascular tone, growth, thrombogenicity, atherogenicity, and inflammation (90). Moreover, it is evident that the presence of endothelial dysfunction is associated with cardiovascular events (66). Therefore, it is important to understand how the endothelium regulates vascular homeostasis in physiological and pathophysiological conditions. Strategies designed to prevent endothelial dysfunction may therefore reduce cardiovascular complications.

Endothelial nitric oxide synthase in normal physiologic condition

Human vasculature is composed of three layers: the endothelium (intima), smooth muscle cells (media), and surrounding elastic and connective tissues (adventitia). The innermost monolayer of the endothelial cells sense hemodynamic forces and respond to physiologic and pathologic stimuli (51, 52, 66, 85). Also, the endothelium, as the primary interface between the blood and body tissues, governs several important aspects of vascular responses through the generation of nitric oxide (NO), a gas produced by nitric oxide synthase (NOS) enzymes (43, 50-52, 133). There are three

major isoforms of NOS: neuronal NOS (nNOS), or type 1 NOS; inducible NOS (iNOS), or type 2 NOS; and endothelial NOS (eNOS), or type 3 NOS (66). eNOS is the predominant NOS isoform in the vasculature and is responsible for most of the NO produced in this tissue (42). As a multi-domain enzyme, eNOS consists of an N-terminal oxygenase domain and a reductase domain (Figure 2 - 1). The oxygenase domain contains binding sites for heme, L-arginine, and tetrahydrobiopterin (BH_4), and the reductase domain contains binding sites for flavin mononucleotide (FMN), flavin adenine dinucleotide (FAD), nicotinamide adenine dinucleotide phosphate (NADPH) and calmodulin (CaM) (22, 142). eNOS oxidizes its substrate L-arginine and produces L-citrulline and NO, the most prominent vasodilatory agent (3, 33). The functional eNOS requires dimerization of the enzyme, the presence of the substrate L-arginine, and the essential cofactor BH_4 (43). eNOS is classified as a constitutive enzyme that produces NO in a Ca^{2+} / CaM dependent manner (17). The CaM-binding domain of eNOS has been reported to directly bind phospholipids, and functional eNOS was found to be primarily localized in caveolae of the plasma membrane (61, 98, 144, 163). Caveolae are small invaginations of the plasma membrane, which sequester diverse receptors and function to organize various signaling transduction pathways including eNOS (93). The major structural proteins of caveolae are cholesterol, glycosphingolipids, sphingomyelin, and caveolin-1 (cav-1) (143). Cav-1 is abundant in endothelial cells and inhibits eNOS activity in the basal state by impeding the signaling of caveolae-targeted receptors that transduce eNOS-stimulatory signals as well as by antagonizing calmodulin binding to eNOS (47, 76). Heat shock protein 90 (Hsp90) is a chaperone that is involved in protein trafficking and folding and agonist-dependent eNOS activation (108). Hsp90 is known to reduce the inhibitory effects of cav-1 on eNOS (41, 55). Upon an increase in cytoplasmic calcium, CaM is thought to aid the

recruitment of Hsp90 to eNOS and facilitate the effects of Hsp90 on the dissociation of eNOS from caveolin-1.

eNOS is known to be activated by various physiological stimuli, including mechanical shear stress (23, 52, 60, 111, 169), insulin (129), acetylcholine (68), and other receptor-dependent agonists (7) (Figure 2 - 2). eNOS is regulated by post-translational phosphorylation at several serine (S) and threonine (T) residues including T495, S615, S633, and S1177 (13, 33). Among those potential phosphorylation sites, phosphorylation of eNOS at S1177 residue in the reductase domain and phosphorylation at T495 within the CaM-binding domain have been most studied. T495 is constitutively phosphorylated and associated with a decrease in enzyme activity (40, 59, 109). S1177 phosphorylation results in more active eNOS and NO production, even at resting levels of intracellular calcium (103). eNOS-derived NO serves several important functions. First, it regulates vascular tone and regional blood flow (68). Second, it modulates the expression of surface cell adhesion molecules that governs interactions with circulating cells including leukocytes, monocytes, and platelets, therefore affecting propensity or resistance to atherosclerotic plaque formation and thrombosis (21, 44, 82, 89). Finally, NO also inhibits the proliferation and injury responses of vascular smooth muscle cells, which could contribute to neointima formation during the development of atherosclerosis (114, 134, 155). Based on the combination of those effects, endothelial NO represents an important anti-atherogenic defense principle in the vasculature (42).

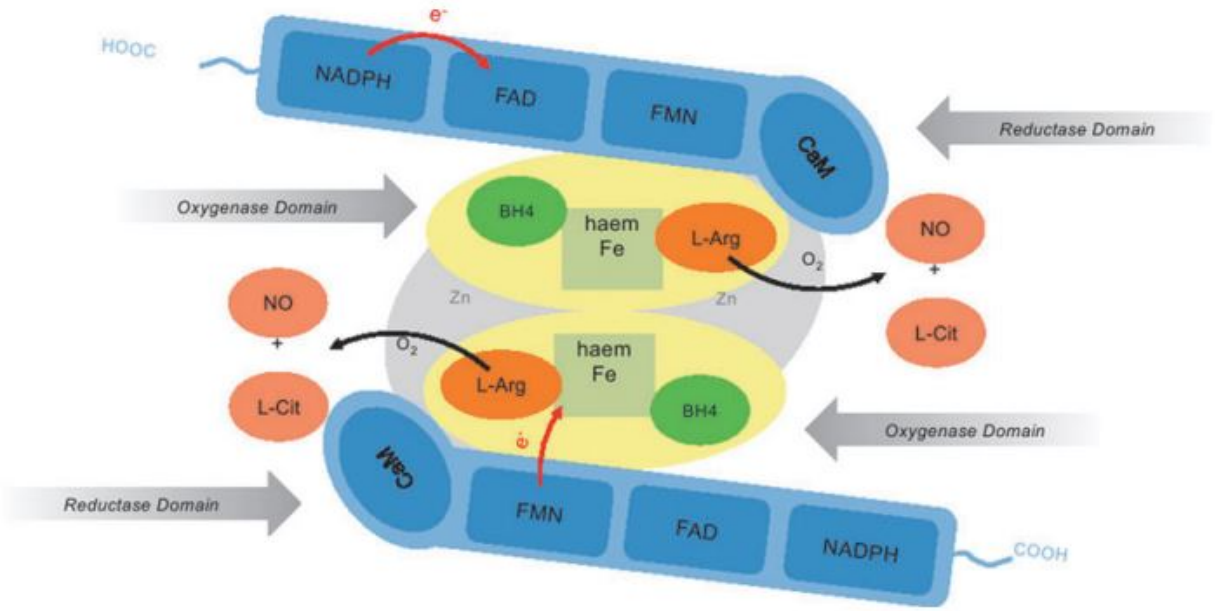

Figure 2 - 1. Catalysis of endothelial nitric oxide synthase

This figure depicts eNOS that functions as homodimers. Each monomer consists of an N-terminal oxygenase domain and a reductase domain. The oxygenase domain contains binding sites for heme, L-arginine, and tetrahydrobiopterin (BH_4). The reductase domain contains binding sites for flavin mononucleotide (FMN), flavin adenine dinucleotide (FAD), nicotinamide adenine dinucleotide phosphate (NADPH) and calmodulin (CaM). eNOS oxidizes its substrate L-arginine and produces L-citrulline and NO, the most prominent vasodilatory agent. The functional eNOS requires dimerization of the enzyme, the presence of the substrate L-arginine, and the essential cofactor BH_4. *Abbreviations:* *L-Arg*: L-arginine; *BH_4*: tetrahydrobiopterin; *CaM*: calmodulin; *FMN*: flavin mononucleotide; *FAD*: flavin adenine dinucleotide; *NADPH*: nicotinamide adenine dinucleotide phosphate. Adapted from (9).

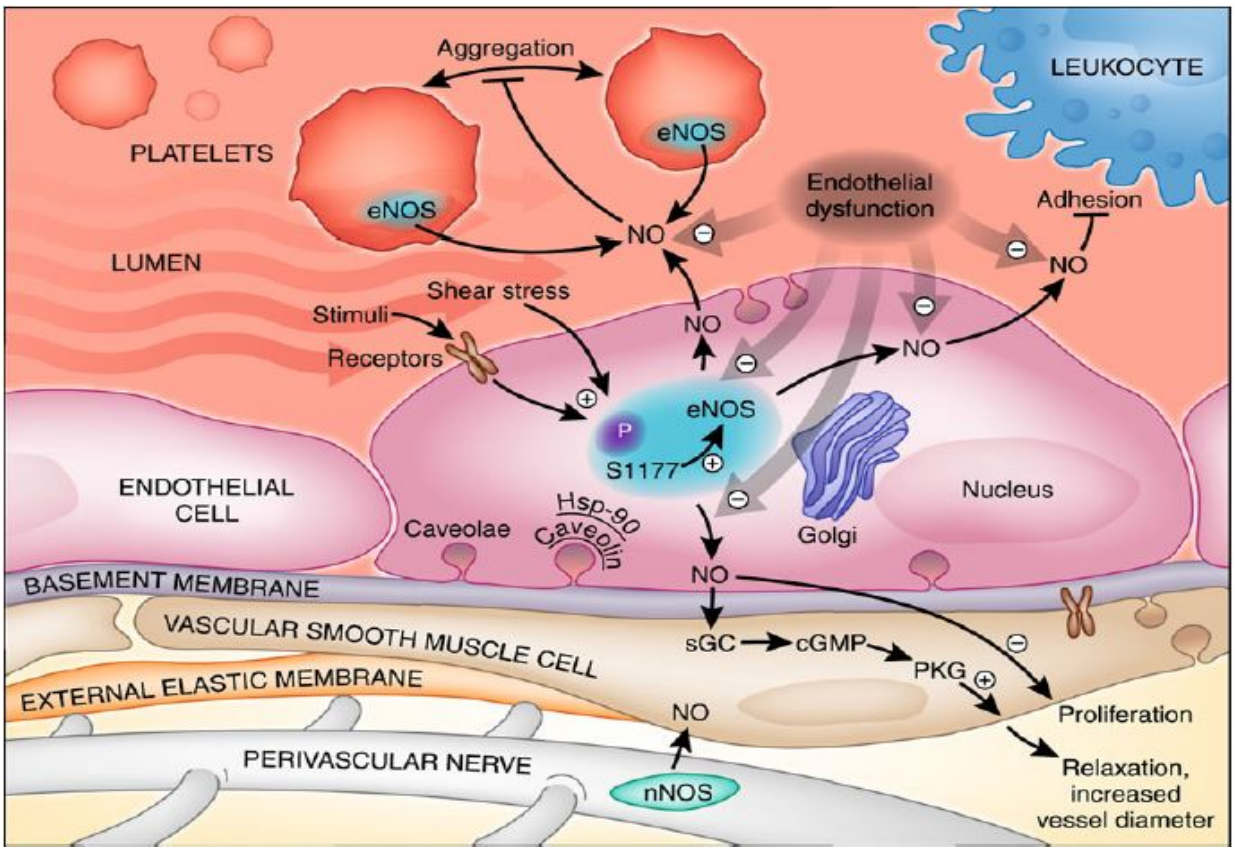

Figure 2 - 2. Biological roles of endothelial nitric oxide

This figure depicts biological roles of endothelial NO. eNOS is activated by physiological and metabolic stimuli including shear stress and receptor-dependent agonists. Phosphorylation of eNOS at S1177 increases its activity. NO generated from eNOS inhibits platelets aggregation, modulates leukocyte-endothelial cell interactions, inhibits smooth muscle cell proliferation, and regulates vascular tone. eNOS catalytic activity depends on the intracellular localization to caveolae and the protein-protein interactions with caveolins and hsp-90. NO diffuses to vascular smooth muscle cells and induces smooth muscle cell relaxation through cGMP-PKG pathway, which increases luminal diameter and blood flow. Abbreviations: P: phosphorylation; S1177: serine 1177; HSP-90: heat shock protein-90; PKG: serine-threonine-specific protein kinase G. Adapted from (6).

Protein regulation by S-nitrosylation and vesicle trafficking

As mentioned above, NO has a variety of effects on vascular cells including smooth muscle relaxation, inhibition of smooth muscle cell migration and proliferation, platelet adherence and aggregation, and vascular inflammation. Among these effects, NO may regulate vascular inflammation and thrombosis, in part, by controlling endothelial vesicle trafficking (94). Vesicle trafficking involves several discrete stages: cargo loading, budding, translocation, priming, membrane fusion, and recycling (73, 75, 107, 156). Weibel-Palade bodies (WPBs) are released from endothelial cells following this cycle of vesicle trafficking upon endothelial inflammation and injury (94). WPBs are cigar-shaped granules that contain both pro-thrombotic and pro-inflammatory factors, mainly von Willebrand Factor (VWF) and P-selectin (164, 167). The release of VWF into the blood stream promotes platelet adhesion and aggregation (135). WPB exocytosis also leads to the translocation of P-selectin to the endothelial cell plasma membrane, which regulates leukocyte rolling and extravasation (102, 104). After WPB exocytosis, the empty granule recycles back to the Golgi (94). Distinct sets of proteins regulate the cycle of WPB trafficking, including Rab family members, N-ethylmaleimide sensitive factor (NSF), soluble NSF attachment receptor proteins (SNAREs), and the Sec/Munc family (73, 75, 107, 156). Rab proteins are small GTPases that regulate vesicle tethering to target membranes (179). The SNAREs are a group of transmembrane proteins that specify fusion partners and assemble into stable ternary complexes (74). For example, one v-SNARE (VAMP-3) localized on the endothelial granule can interact with two t-SNAREs (syntaxin-4 and SNAP-23) localized to the plasma membrane, making a stable SNARE complex (99). The assembly of the SNARE complex is accelerated by Sec/Munc proteins (145). In contrast, NSF disassembles the three part SNARE complex by converting the chemical energy of ATP hydrolysis into mechanical energy (101).

NO has been reported to react with free thiol groups on cysteine residues of target proteins in a process called S-nitrosylation (153). Protein S-nitrosylation is a posttranslational modification where the binding of NO to cysteine residues can induce covalent changes in protein function (127). Out of the many proteins that regulate vesicle trafficking, NSF is a critical part of the exocytic machinery and a target of S-nitrosylation (10, 97, 99). Several experiments supported this notion by showing exogenous NO-mediated nitrosylation of 3 of the 9 cysteine residues in recombinant NSF as well as endogenous NO-mediated nitrosylation of NSF in wild type mice through blockage of NO production with NOS inhibitor or in eNOS null mice (99). Therefore, NO may inhibit WBP exocytosis by NSF nitrosylation at a cysteine 264 residue because nitrosylation or a mutation of this site blocked NSF separation of the SNARE complex (99, 100).

It is also reported that S-nitrosylation is reversible (99). Thioredoxin is a reductase that maintains redox balance within cells, and is involved in many processes (16). Thioredoxin 1 (TRX1) is expressed in the cytosol, and reduces oxidized cysteine residues on target proteins. In endothelial cells TRX1 has a pro-inflammatory role because it is recruited to nitrosylated NSF, removes NO moieties, and restores exocytosis of WPBs (72). Therefore, the relative availability of NO and the activity of TRX1 regulate NSF function, subsequently influencing WPB exocytosis.

Endothelial nitric oxide synthase in pathological condition

Endothelial dysfunction is a broadly defined term used to describe a failure of the endothelium to serve its normal physiologic and protective effects (29, 171). A common feature associated with many cardiovascular risk factors (including hypertension, diabetes, insulin resistance, obesity and hyperlipidemia) is endothelial dysfunction (66). Because the endothelium normally protects against the processes involved in atherosclerosis, smooth muscle cell proliferation, inflammation

and thrombosis using NO, endothelial dysfunction is central to the pathogenesis of atherosclerotic lesion development. A mechanism of endothelial dysfunction is insufficient endothelial NO availability (67). A decline in NO bioavailability could be caused by many different factors. These include reduced eNOS gene expression, a lack of its substrate L-arginine, inhibition of eNOS by asymmetric dimethylarginine, uncoupling of eNOS and BH_4 deficiency, metabolic intoxication by free fatty acids and inflammatory cytokines IL-6 and TNFα, alterations of intracellular signaling pathways of eNOS, and rapid scavenging of NO by superoxide anion (12, 26, 27, 66, 80, 123, 172). Two important causes of endothelial dysfunction seem to be accelerated NO degradation by reactive oxygen species (ROS) and eNOS uncoupling. There are many potential enzymatic sources of ROS in mammalian cells. These include the mitochondrial respiration, arachidonic acid pathway enzymes lipoxygenase and cyclooxygenase, cytochrome p450s, xanthine oxidase, NADPH oxidases, eNOS, peroxidases, and other hemoproteins (18). Although many of these sources could potentially produce ROS that inactivate NO, xanthine oxidase, NADPH oxidase, and eNOS have been studied rather extensively in the cardiovascular system.

Xanthine oxidase is a form of xanthine oxidoreductase, which reduces molecular oxygen to produce O_2^- and H_2O_2 (18). Studies suggested that O_2^- derived from xanthine oxidase can decrease NO bioavailability because blood pressure in spontaneously hypertensive rats was dramatically lowered by a recombinant form of superoxide dismutase or the xanthine oxidase inhibitor oxypurinol (118). Also, oxypurinol reduced O_2^- production and improved impaired acetylcholine-mediated vascular relaxation in the aorta of hyperlipidemic rabbits (120). These suggest that xanthine oxidase contributes to endothelial dysfunction by altering NO bioavailability.

NADPH oxidase (NOX) is a membrane-bound enzyme complex and catalyzes one electron transfer of oxygen from NADPH to generate O_2^- and H_2O_2 (91). The oxidases are multi-subunit

enzymes that are expressed in vascular smooth muscle cells (NOX1 and NOX4) and in endothelial cells (NOX2 and NOX4) (2, 37, 53, 84). Cardiovascular risk factors, such as hypertension, diabetes, and hypercholesterolemia, increase the expression and/or activity of NOX in the vascular wall, enhancing the production of ROS (63, 77, 91, 128, 166). Both basal and NADPH-stimulated O_2^- formation was significantly increased in the rat aorta with heart failure (8). Subsequent treatment with superoxide dismutase (SOD) improved the impaired endothelium-dependent vasorelaxation. This evidence suggests that activation of this source of O_2^- can lead to a decrease in NO bioavailability and endothelial dysfunction.

eNOS has received substantial attention as another source of vascular ROS production (18, 43, 66). There has been evidence that eNOS becomes uncoupled in various pathophysiological conditions (63, 83, 110, 112, 160). This phenomenon is named "eNOS uncoupling" because O_2^- generation mainly occurs when eNOS is not coupled with its cofactor or substrate (95). BH_4 is an essential cofactor necessary for optimal eNOS activity (4). For full enzymatic activity, eNOS requires proper dimerization (66). When BH_4 levels are inadequate, eNOS becomes unstable and produces less NO and more O_2^- (Figure 2 - 3). Under conditions of eNOS uncoupling and/or high oxidant stress, O_2^- reacts with NO to form peroxynitrite anion ($ONOO^-$) in a very rapid reaction (123). Importantly, $ONOO^-$ has multiple effects, including selective nitration of tyrosine residues in proteins (56), increased expression of inducible NOS (25), oxidation of the zinc-thiolate complex in eNOS (180), and oxidation of BH_4 to BH_2 (88). Interestingly, BH_2 also can promote eNOS uncoupling because it can competitively replace eNOS-bound BH_4 (28).

Although multiple mechanisms can lead to O_2^- generation and eNOS uncoupling simultaneously, the common feature is a reduction in the amount of NO bioavailability, which protects the

vasculature, under normal healthy physiological condition, from the molecular events that lead to endothelial dysfunction and inflammation.

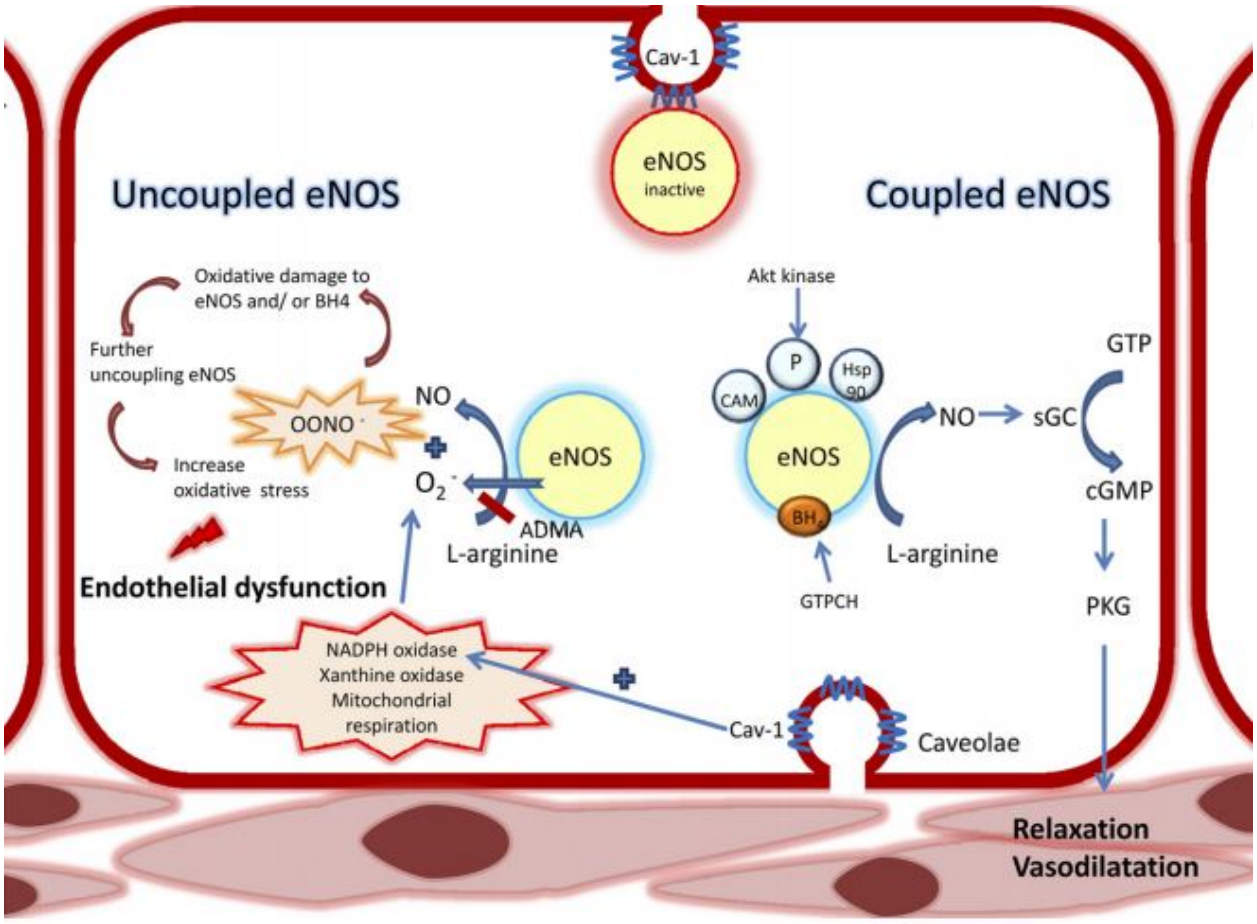

Figure 2 - 3. Coupled eNOS and uncoupled eNOS

This figure depicts the role of eNOS uncoupling in the pathogenesis of endothelial dysfunction. eNOS is inactive when it is bound to cav-1 localized to the plasma membrane. When it becomes active, eNOS disassociates from cav-1 and binds with calmodulin (CaM) and heat shock protein 90 (Hsp90) with phosphorylation at Serine1177. When availability of L-arginine or BH_4 levels are insufficient, eNOS becomes unstable, resulting in less NO production and more superoxide generation. Moreover, peroxynitrite, a potent oxidant product from NO and superoxide, further oxidizes BH_4, leading to eNOS uncoupling as a vicious cycle with subsequent endothelial dysfunction. <u>*Abbreviations:*</u> *cav-1*: caveolin-1; *BH_4*: tetrahydrobiopterin; *CaM*: calmodulin; *Hsp90*: heat shock protein 90; *P*: phosphorylation; *$ONOO^-$*: peroxynitrite. Adapted from (79).

Lipid accumulation in the endothelium and cardiovascular disease

Accumulation of lipids within the arterial wall is the principal cause and progression of atherosclerotic lesion (133). The deposition of the fatty streak precedes the influx of macrophages and T lymphocytes (154). This inflammatory response stimulates migration and proliferation of smooth-muscle cells and becomes intermixed with the area of inflammation to form an intermediate lesion. Lipid-rich advanced atherosclerotic plaques are pro-inflammatory and more prone to rupture and thrombosis than lipid-poor plaques (117). Therefore, the composition of lipid fractions within the atherosclerotic plaque may play a crucial role in the progression of atherosclerosis and in the complications of atherosclerotic vascular disease including myocardial infarction and stroke.

α-Galactosidase A deficiency (Fabry disease)

Fabry disease is caused by deficiency or absence of activity of the lysosomal enzyme α-galactosidase A (GLA) (15, 81). It was first recognized in two affected brothers as a disease characterized by abnormal vacuoles in blood vessels throughout their bodies, suggesting a storage disorder (125). Reduced GLA activity may result from multiple different GLA gene mutations, which lead to reduced or complete deficiency of enzyme activity, or dysfunctional enzyme with low activity (24, 139). Since GLA hydrolyses the substrates possessing terminal α-galactosidic residues, the glycolipid conversion of globotriaosylceramide (Gb3) to lactosylceramide is impeded in Fabry disease (113). As a result, the progressive lysosomal accumulation of neutral glycosphingolipids with terminal α-galactosyl moieties is observed. The predominant site of glycosphingolipid accumulation is the endothelium and smooth muscle cells of the vasculature, although accumulation can occur in various other organ systems such as skeletal muscle cells,

histiocytes, reticulocytes, corneal epithelial cells, glomerulus and tubules of the kidney, ganglions of autonomous nervous system, epithelial cells, and others (36, 38, 157).

Early signs and symptoms of Fabry disease include episodic acute pain (Fabry crisis) characterized by agonizing burning pain in the extremities and gastrointestinal involvement with abdominal pain, diarrhea, nausea, and vomiting (19, 64, 147). Other clinical manifestations of Fabry disease include renal failure, painful neuropathies, stroke, cardiac disease, and skin lesions (49). However, premature life-threatening complications result from cardiovascular diseases including myocardial infarction, stroke, hypertrophic cardiomyopathy, and renal failure with frequent detection in more than 60 % of affected males and heterozygous females (92, 105). Before renal dialysis and renal transplants became widely available, the average age at death among untreated males was reported as approximately 40 years (175). Although the increased availability of renal replacement therapy extended the lifespan of Fabry patients, it is still several decades shorter than the United States general population (96, 140, 165).

Prevalence rate and treatments for Fabry disease

The prevalence rate of Fabry disease was conventionally estimated to be 1 case in 40,000-117,000 male births (106). However, more recent studies of newborn screenings now suggest the incidence of Fabry disease to be between 1 in 3,100 and 1 in 1,250 with later-onset phenotypes including hemodialysis, hypertrophic cardiomyopathy and stroke, raising the clinical importance of the condition in the future (69, 152). Although inheritance of GLA is X-linked, many heterozygotes will develop early symptoms and, later on, vital organ involvement (96, 170, 174).

Several potential therapies for Fabry disease, including bone marrow transplantation, substrate deprivation, recombinant GLA enzyme replacement, and gene therapy, have shown promise in pre-clinical trials in mice (1, 71, 78, 122). Whereas enzyme replacement therapy (ERT) with recombinant GLA is the only approved therapy for Fabry disease, there is no clear evidence that ERT alters the natural course of cardiac and cerebrovascular diseases (35, 130, 161).

Basic research models of Fabry disease

Because it is a rare disease, animal and cellular models of Fabry disease have been invaluable models for exploring the vascular pathophysiology of human genetic disease as well as for the development of effective therapeutic strategies. The combined homologous recombination and embryonic stem cell technology has allowed generation of knock-out mice for Fabry disease (121). This animal model has played an important role in studies of vascular pathogenesis. Although the GLA null mouse does not display a spontaneous vascular phenotype, recent studies reported several inducible models of vasculopathy. First, mice deficient in GLA showed a significant reduction in the time to occlusive thrombus formation with age compared to wild type C57BL6/J mice when exposed to photochemical reactive oxygen species (34). Accumulation of Gb3 on the carotid artery with age was associated with the enhanced thrombotic response to photochemical injury in GLA deficient mice. No changes in the vascular phenotype with bone marrow transplantation between GLA deficient and wild type mice suggested that the pro-thrombotic phenotype was not due to an abnormality of circulating blood elements, but most likely to changes localized to the vessel wall (34). Second, because glycosphingolipids have been shown to accumulate in atherosclerotic plaques of the human aorta (116), it is also possible that Gb3 deposition in the vascular wall may promote atherogenesis. To address the potential role of GLA

deficiency in atherosclerosis, the GLA null mice were bred with apolipoprotein E deficient mice. At 45 weeks of age, Gb3 accumulation due to GLA deficiency was associated with a significant increase in total atherosclerotic burden (11). In a third model, acetylcholine mediated vascular relaxation was measured in the aortic rings from wild type and GLA-null mice pre-contracted with phenylephrine (124). The impaired vascular reactivity to acetylcholine in the GLA deficient rings was normalized with calcium ionophore-mediated NO production, suggesting a plasma membrane-based defect. Primary aortic endothelial cells from GLA deficient mice demonstrated that the increased plasma membrane Gb3 was the basis for the abnormality (148, 149). The Gb3 accumulation was associated with decreased eNOS expression, activity, and levels of high molecular weight caveolin-1 oligomers (150). These results suggest that Gb3 alters the assembly of signaling molecules with caveolin-1, including eNOS.

To study the molecular mechanisms, a cellular model of Fabry disease was also established. When the primary aortic endothelial cells from wild type and GLA null mice in various ages were compared, an age-dependent elevation in Gb3 was observed only in the GLA null cells (148). The glucosylceramide synthase inhibitor, ethylenedioxyphenyl-P4, significantly decreased Gb3 level by 96 hours of treatment. Recombinant GLA completely eliminated Gb3 accumulation by 48 hours of incubation. In addition, a single and low dose for a shorter period of incubation with a combination of ethylenedioxyphenyl-P4 and recombinant GLA had a synergistic effect. In a more recent study, GLA was transiently silenced using a RNA interference technique in an immortalized human umbilical cell line, EA.hy926 (151). An interesting finding of this study is that there was a decrease in eNOS activity consistent with the impaired formation of NO. In addition, a 50-fold increase in 3-nitrotyrosine was observed only in the GLA null cells, but not in the cells with β–glucocerebrosidase knockdown, an enzyme responsible for the most common lysosomal storage

disease Gaucher disease. This significant elevation of 3-nitrotyrosine, but not of other tyrosine adducts, was also measured in GLA null mouse plasma and aorta as well as in the plasma of classical Fabry patients, suggesting that eNOS uncoupling with reactive nitrogen species formation was specific to Fabry disease (151).

Dysregulation of endothelial nitric oxide synthase in Fabry disease

Two primary hypotheses have been proposed to explain the pathogenesis of the vasculopathy of Fabry disease. One hypothesis suggests that circulating lyso-Gb3 deposition in the medial layer of the arterial vasculature is the initiating step of the vasculopathy. This promotes smooth muscle cell proliferation in the subendothelial layer and formation of neointimal fibrotic structures. A resultant hyperdynamic circulation in a less compliant vascular wall leads to upregulation of the local renin-angiotensin system, and subsequent production of reactive oxygen species with a decrease in NO synthesis (132).

An alternative hypothesis suggests that Gb3 accumulation in the endothelium alone is sufficient to account for the dysregulation of eNOS, which leads to low NO production and eNOS uncoupling with aberrant formation of reactive oxygen species (151) (Figure 2 - 4). The potential role for eNOS dysregulation with Gb3 accumulation in the endothelium is well supported by the cellular model of Fabry disease (151). In this study GLA knockdown induced a time dependent Gb3 accumulation in human endothelial cells. This toxic deposition was associated with decreased NO activity. Uncoupling of eNOS was also confirmed by a highly robust elevation in 3-nitrotyrosine, the $ONOO^-$ nitration product, in this cell line, GLA null mouse plasma and aorta, as well as in the plasma of classical Fabry patients. Also, Gb3 loading in skin microvascular endothelial cells resulted in an increase in reactive oxygen species and the transcription of intercellular adhesion

molecule-1, vascular cellular adhesion molecule-1, and E-selectin (146). In addition, Gb3 content was markedly increased in the total plasma membrane as well as the caveolar fraction of primary mouse aortic endothelial cells from GLA null mice (148, 149). These observations were consistent with decreased eNOS expression, hormone-stimulated eNOS activity, and high molecular weight caveolin-1 oligomers, indicating increased plasma membrane Gb3 is the basis for the endothelial dysfunction (150). This hypothesis was further supported by an observation that impaired Ach-mediated vascular relaxation of GLA null mouse aorta was eliminated with calcium ionophore-stimulated dilation (124). In addition, the GLA knockout mice display increased thrombogenesis and atherogenesis when exposed to reactive oxygen species and bred on an apolipoprotein E1-deficient background, respectively (11, 34). Together, although many different factors could play a role in the vascular abnormality present in Fabry disease, common factors are an alteration of nitric oxide bioavailability and the presence of eNOS uncoupling.

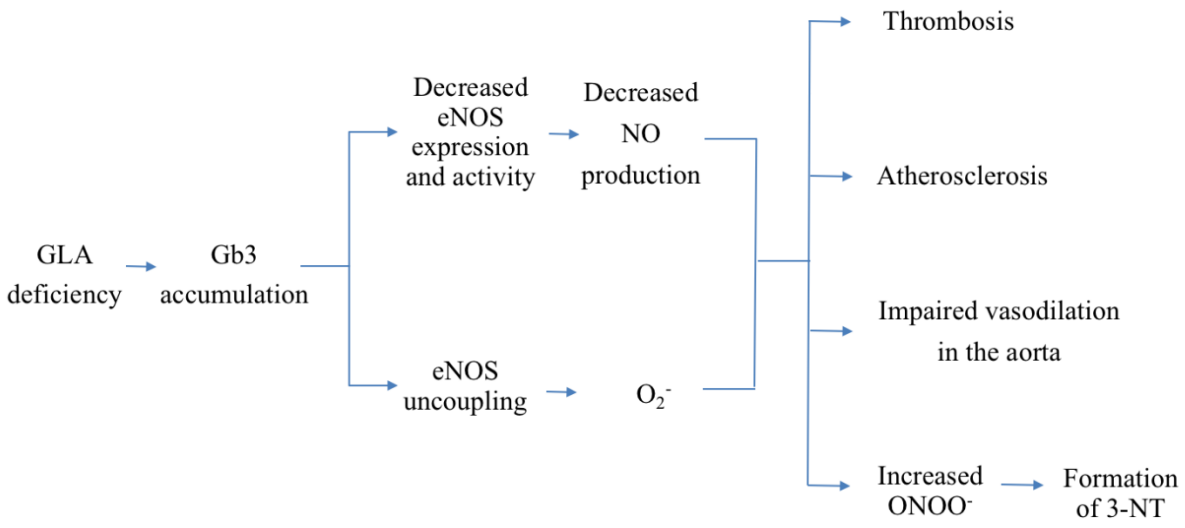

Figure 2 - 4. Gb3 deposition in the endothelium leads to endothelial dysfunction

This figure depicts the role of Gb3 accumulation in the vascular endothelial cells. Deficient or absent activity of GLA results in Gb3 accumulation in the endothelium. This leads to decreased NO bioavailability and eNOS uncoupling with the formation of reactive oxidants. These promotes thrombosis, atherosclerosis, and impaired vasodilation in the aorta. Also, NO from eNOS binds to O_2^- to generate $ONOO^-$, a highly reactive nitrogen species, resulting in protein nitration (3-NT). $ONOO^-$ can oxidize BH_4 to BH_2. BH_2 can efficiently replace eNOS-bound BH_4, resulting in further eNOS uncoupling. *Abbreviations: GLA*: α-galactosidase A; Gb3: globotriaosylceramide; eNOS: endothelial nitric oxide synthase; NO: nitric oxide; O_2^-: superoxide; $ONOO^-$: peroxinitrite; 3-NT: 3-nitrotyrosine; BH_4: tetrahydrobiopterin; BH_2: dihydrobiopterin.

Mechanisms by which exercise improves endothelial dysfunction

Many studies have demonstrated exercise to be one of the most effective non-pharmacological interventions for improving endothelial dysfunction. During the last two decades, the beneficial effects of exercise on attenuated endothelial function have been extensively studied in various aspects including aging, heart disease, hypercholesterolemia, hypertension, and type II diabetes mellitus.

Impaired endothelium-dependent dilation (EDD) with aging is thought to be mediated by reduced NO bioavailability associated with increased oxidative stress (18, 32, 159). Three months of habitual aerobic exercise improved impaired EDD in middle-aged and older adults (31, 141, 158, 159). This was thought to be mediated in part by an enhanced NO bioavailability because a greater degree of forearm vasoconstriction with intra-brachial artery infusion of an eNOS inhibitor was observed after exercise intervention (158). Also, acute administration of supraphysiological concentrations of vitamin C improved EDD only in sedentary men, but not in endurance exercise-trained men, indicating that the improvement in EDD may be secondary to reduced oxidative stress. These observations suggest that this influence is mediated by an increase in NO bioavailability and reduced oxidative stress.

A number of studies have reported that reduced EDD in hypercholesterolemia is reversed or prevented by exercise training in mice and rabbits (119, 126, 178). In a genetic mouse model of hypercholesterolemia, aortic EDD was decreased compared to wild type mice, but four weeks of treadmill training restored normal EDD (119). Six weeks of treadmill training reduced carotid artery neointima formation with an increase in eNOS expression in apo E null mice compared to sedentary apo E null mice (126). Studies using aorta, carotid, and mesenteric arteries in spontaneously hypertensive rats have consistently shown that impaired Ach mediated EDD and

NO production were improved by exercise training (6 – 22 weeks) (5, 20, 54). Additionally, reduced aortic EDD in OLETF type 2 diabetic rats was restored by 9 weeks of voluntary wheel exercise (138). In this study, urinary NO_2, a stable degradation product of NO in biological solutions, was significantly increased by exercise compared to non-diabetic OLETF and sedentary control OLETF rats, suggesting exercise-mediated improvement in NO production. Together, one of the most important molecular consequences of exercise is the absolute increase in NO bioavailability.

Exercise may exert its beneficial effect, in part, by shear stress. Shear stress induced by blood flow is one of the most important exercise-mediated physiological regulators of vascular tone (85). Numerous investigations have documented that exercise or increased shear stress up-regulates eNOS activity in cell culture, animal, and human studies (14, 57, 176). The beneficial effects of exercise on endothelial function are the result of changes in endothelial cell phenotype that involve increased eNOS expression and activity (57, 86, 87). Other markers of endothelial cell phenotype changes induced by exercise/shear stress include increased expression and activity of SOD and decreased oxidative stress (45, 136, 137). Because NO can be rapidly inactivated by reaction with O_2^- and lead to the production of the strong oxidant $ONOO^-$, SOD may regulate NO-mediated signaling by inhibiting oxidative inactivation of NO (46, 123). Shear stress may exert its beneficial effects by not only increasing NO production, but also up-regulating SOD expression. Indeed, an NO donor (DETA-NO) increased the expression of vascular extracellular SOD in a time- and dose-dependent manner in human aortic smooth muscle cells (45). This effect was prevented by a guanylate cyclase inhibitor and by a protein kinase G inhibitor, indicating NO may stimulate SOD expression and thereby prevent degradation of NO. Therefore, the beneficial effect of exercise on EDD observed in several studies may not only be due to an increase in eNOS expression (58, 62,

65), but also due to an increase in SOD expression, which decreases O_2^- reaction with NO. Importantly, unidirectional laminar shear stress significantly increased mRNA, protein content, and activity of cytosolic Cu/Zn SOD in human aortic endothelial cells, which would further enhance NO bioavailability in response to exercise/shear stress (70).

Summary of review of literature

The overall goal of my dissertation projects is to understand Gb3 accumulation on endothelial dysfunction and inflammation and to identify strategies for attenuating this progression in the setting of GLA deficiency. Although the vasculopathy is the basis for the life-threatening complications of Fabry disease, one of the early symptoms appearing in childhood is gastrointestinal involvement, which may be related to the deposition of Gb3 in the autonomic ganglia of the bowel and mesenteric blood vessels (39). However, the vascular phenotype in the mesenteric artery is unknown. Therefore, the objective of my first study is to characterize endothelial function of the mesenteric artery and to determine signaling alterations of eNOS in GLA deficient mice. Additionally, although ERT has been the standard care for Fabry disease, cerebral vascular events continue to occur in Fabry patients with advanced disease treated with long-term ERT (131, 168, 173). Endothelium-derived VWF plays a pivotal role in platelet adhesion and subsequent thrombus formation, supporting normal hemostasis and thrombosis (177). Previously, prothrombotic and proinflammatory profiles have been documented in Fabry disease (30, 48, 146, 162). However, less attention has been paid to the direct effect of GLA deficiency on the endothelium-derived coagulation factor, VWF. The second study of my dissertation projects, therefore, examines the effects of GLA disruption on VWF secretion and its association with eNOS dysregulation in *in vitro* models of Fabry disease. Finally, although exercise is known to improve

endothelial dysfunction in many conditions including diabetes, hypertension, and sedentary aging, the effects of exercise on endothelial dysfunction and inflammation in Fabry disease remain unclear. Thus, the third project uses a mouse model of Fabry disease to examine whether exercise improves endothelial dysfunction in the setting of eNOS uncoupling.

The rationale for the proposed studies is that once it is known how GLA deficiency leads to vasculopathy, factors that affect endothelial dysfunction and inflammation can be manipulated either up or down pharmacologically and/or non-pharmacologically (exercise). Therefore, findings of the proposed research have important implications for the prevention and treatment of Fabry disease in addition to expanding our understanding in the fields of cardiovascular disease and vascular complications.

References

1. **Abe A, Gregory S, Lee L, Killen PD, Brady RO, Kulkarni A, and Shayman JA.** Reduction of globotriaosylceramide in Fabry disease mice by substrate deprivation. *The Journal of clinical investigation* 105: 1563-1571, 2000.

2. **Ago T, Kitazono T, Ooboshi H, Iyama T, Han YH, Takada J, Wakisaka M, Ibayashi S, Utsumi H, and Iida M.** Nox4 as the major catalytic component of an endothelial NAD(P)H oxidase. *Circulation* 109: 227-233, 2004.

3. **Alderton WK, Cooper CE, and Knowles RG.** Nitric oxide synthases: structure, function and inhibition. *The Biochemical journal* 357: 593-615, 2001.

4. **Alp NJ and Channon KM.** Regulation of endothelial nitric oxide synthase by tetrahydrobiopterin in vascular disease. *Arteriosclerosis, thrombosis, and vascular biology* 24: 413-420, 2004.

5. **Arvola P, Wu X, Kahonen M, Makynen H, Riutta A, Mucha I, Solakivi T, Kainulainen H, and Porsti I.** Exercise enhances vasorelaxation in experimental obesity associated hypertension. *Cardiovascular research* 43: 992-1002, 1999.

6. **Atochin DN and Huang PL.** Endothelial nitric oxide synthase transgenic models of endothelial dysfunction. *Pflugers Archiv : European journal of physiology* 460: 965-974, 2010.

7. **Barton M.** Endothelial dysfunction and atherosclerosis: endothelin receptor antagonists as novel therapeutics. *Curr Hypertens Rep* 2: 84-91, 2000.

8. **Bauersachs J, Bouloumie A, Fraccarollo D, Hu K, Busse R, and Ertl G.** Endothelial dysfunction in chronic myocardial infarction despite increased vascular endothelial nitric oxide synthase and soluble guanylate cyclase expression: role of enhanced vascular superoxide production. *Circulation* 100: 292-298, 1999.

9. **Bendall JK, Douglas G, McNeill E, Channon KM, and Crabtree MJ.** Tetrahydrobiopterin in cardiovascular health and disease. *Antioxidants & redox signaling* 20: 3040-3077, 2014.

10. **Block MR, Glick BS, Wilcox CA, Wieland FT, and Rothman JE.** Purification of an N-ethylmaleimide-sensitive protein catalyzing vesicular transport. *Proceedings of the National Academy of Sciences of the United States of America* 85: 7852-7856, 1988.

11. **Bodary PF, Shen Y, Vargas FB, Bi X, Ostenso KA, Gu S, Shayman JA, and Eitzman DT.** Alpha-galactosidase A deficiency accelerates atherosclerosis in mice with apolipoprotein E deficiency. *Circulation* 111: 629-632, 2005.

12. **Bode-Boger SM, Boger RH, Kienke S, Junker W, and Frolich JC.** Elevated L-arginine/dimethylarginine ratio contributes to enhanced systemic NO production by dietary L-arginine in hypercholesterolemic rabbits. *Biochem Biophys Res Commun* 219: 598-603, 1996.

13. **Boo YC and Jo H.** Flow-dependent regulation of endothelial nitric oxide synthase: role of protein kinases. *American journal of physiology Cell physiology* 285: C499-508, 2003.

14. **Boo YC, Sorescu G, Boyd N, Shiojima I, Walsh K, Du J, and Jo H.** Shear stress stimulates phosphorylation of endothelial nitric-oxide synthase at Ser1179 by Akt-independent mechanisms: role of protein kinase A. *The Journal of biological chemistry* 277: 3388-3396, 2002.

15. **Brady RO, Gal AE, Bradley RM, Martensson E, Warshaw AL, and Laster L.** Enzymatic defect in Fabry's disease. Ceramide trihexosidase deficiency. *N Engl J Med* 276: 1163-1167, 1967.

16. **Burke-Gaffney A, Callister ME, and Nakamura H.** Thioredoxin: friend or foe in human disease? *Trends in pharmacological sciences* 26: 398-404, 2005.

17. **Busse R and Mulsch A.** Calcium-dependent nitric oxide synthesis in endothelial cytosol is mediated by calmodulin. *FEBS letters* 265: 133-136, 1990.

18. **Cai H and Harrison DG.** Endothelial dysfunction in cardiovascular diseases: the role of oxidant stress. *Circulation research* 87: 840-844, 2000.

19. **Charrow J.** A 14-year-old boy with pain in hands and feet. *Pediatric annals* 38: 190, 192, 2009.

20. **Chen HI and Chiang IP.** Chronic exercise decreases adrenergic agonist-induced vasoconstriction in spontaneously hypertensive rats. *The American journal of physiology* 271: H977-983, 1996.

21. **Chen J, Kuhlencordt PJ, Astern J, Gyurko R, and Huang PL.** Hypertension does not account for the accelerated atherosclerosis and development of aneurysms in male apolipoprotein e/endothelial nitric oxide synthase double knockout mice. *Circulation* 104: 2391-2394, 2001.

22. **Chen PF, Tsai AL, Berka V, and Wu KK.** Mutation of Glu-361 in human endothelial nitric-oxide synthase selectively abolishes L-arginine binding without perturbing the behavior of heme and other redox centers. *The Journal of biological chemistry* 272: 6114-6118, 1997.

23. **Chien S.** Mechanotransduction and endothelial cell homeostasis: the wisdom of the cell. *American journal of physiology Heart and circulatory physiology* 292: H1209-1224, 2007.

24. **Colomba P, Nucera A, Zizzo C, Albeggiani G, Francofonte D, Iemolo F, Tuttolomondo A, Pinto A, and Duro G.** Identification of a novel mutation in the alpha-galactosidase A gene in patients with Fabry disease. *Clin Biochem* 45: 839-841, 2012.

25. **Cooke CL and Davidge ST.** Peroxynitrite increases iNOS through NF-kappaB and decreases prostacyclin synthase in endothelial cells. *American journal of physiology Cell physiology* 282: C395-402, 2002.

26. **Cooke JP.** Does ADMA cause endothelial dysfunction? *Arteriosclerosis, thrombosis, and vascular biology* 20: 2032-2037, 2000.

27. **Cosentino F and Luscher TF.** Tetrahydrobiopterin and endothelial function. *European heart journal* 19 Suppl G: G3-8, 1998.

28. **Crabtree MJ, Smith CL, Lam G, Goligorsky MS, and Gross SS.** Ratio of 5,6,7,8-tetrahydrobiopterin to 7,8-dihydrobiopterin in endothelial cells determines glucose-elicited changes in NO vs. superoxide production by eNOS. *American journal of physiology Heart and circulatory physiology* 294: H1530-1540, 2008.

29. **Deanfield JE, Halcox JP, and Rabelink TJ.** Endothelial function and dysfunction: testing and clinical relevance. *Circulation* 115: 1285-1295, 2007.

30. **DeGraba T, Azhar S, Dignat-George F, Brown E, Boutiere B, Altarescu G, McCarron R, and Schiffmann R.** Profile of endothelial and leukocyte activation in Fabry patients. *Annals of neurology* 47: 229-233, 2000.

31. **DeSouza CA, Shapiro LF, Clevenger CM, Dinenno FA, Monahan KD, Tanaka H, and Seals DR.** Regular aerobic exercise prevents and restores age-related declines in endothelium-dependent vasodilation in healthy men. *Circulation* 102: 1351-1357, 2000.

32. **Donato AJ, Morgan RG, Walker AE, and Lesniewski LA.** Cellular and molecular biology of aging endothelial cells. *Journal of molecular and cellular cardiology*, 2015.

33. **Dudzinski DM, Igarashi J, Greif D, and Michel T.** The regulation and pharmacology of endothelial nitric oxide synthase. *Annu Rev Pharmacol Toxicol* 46: 235-276, 2006.

34. **Eitzman DT, Bodary PF, Shen Y, Khairallah CG, Wild SR, Abe A, Shaffer-Hartman J, and Shayman JA.** Fabry disease in mice is associated with age-dependent susceptibility to vascular thrombosis. *J Am Soc Nephrol* 14: 298-302, 2003.

35. **El Dib RP, Nascimento P, and Pastores GM.** Enzyme replacement therapy for Anderson-Fabry disease. *The Cochrane database of systematic reviews* 2: CD006663, 2013.

36. **Elleder M.** Sequelae of storage in Fabry disease--pathology and comparison with other lysosomal storage diseases. *Acta Paediatr Suppl* 92: 46-53; discussion 45, 2003.

37. **Ellmark SH, Dusting GJ, Fui MN, Guzzo-Pernell N, and Drummond GR.** The contribution of Nox4 to NADPH oxidase activity in mouse vascular smooth muscle. *Cardiovascular research* 65: 495-504, 2005.

38. **Eng CM and Desnick RJ.** Molecular basis of Fabry disease: mutations and polymorphisms in the human alpha-galactosidase A gene. *Hum Mutat* 3: 103-111, 1994.

39. **Eng CM, Germain DP, Banikazemi M, Warnock DG, Wanner C, Hopkin RJ, Bultas J, Lee P, Sims K, Brodie SE, Pastores GM, Strotmann JM, and Wilcox WR.** Fabry disease: guidelines for the evaluation and management of multi-organ system involvement. *Genetics in medicine : official journal of the American College of Medical Genetics* 8: 539-548, 2006.

40. **Fleming I, Fisslthaler B, Dimmeler S, Kemp BE, and Busse R.** Phosphorylation of Thr(495) regulates Ca(2+)/calmodulin-dependent endothelial nitric oxide synthase activity. *Circulation research* 88: E68-75, 2001.

41. **Fontana J, Fulton D, Chen Y, Fairchild TA, McCabe TJ, Fujita N, Tsuruo T, and Sessa WC.** Domain mapping studies reveal that the M domain of hsp90 serves as a molecular scaffold to regulate Akt-dependent phosphorylation of endothelial nitric oxide synthase and NO release. *Circulation research* 90: 866-873, 2002.

42. **Forstermann U, Closs EI, Pollock JS, Nakane M, Schwarz P, Gath I, and Kleinert H.** Nitric oxide synthase isozymes. Characterization, purification, molecular cloning, and functions. *Hypertension* 23: 1121-1131, 1994.

43. **Forstermann U and Munzel T.** Endothelial nitric oxide synthase in vascular disease: from marvel to menace. *Circulation* 113: 1708-1714, 2006.

44. **Freedman JE, Sauter R, Battinelli EM, Ault K, Knowles C, Huang PL, and Loscalzo J.** Deficient platelet-derived nitric oxide and enhanced hemostasis in mice lacking the NOSIII gene. *Circulation research* 84: 1416-1421, 1999.

45. **Fukai T, Siegfried MR, Ushio-Fukai M, Cheng Y, Kojda G, and Harrison DG.** Regulation of the vascular extracellular superoxide dismutase by nitric oxide and exercise training. *The Journal of clinical investigation* 105: 1631-1639, 2000.

46. **Fukai T and Ushio-Fukai M.** Superoxide dismutases: role in redox signaling, vascular function, and diseases. *Antioxidants & redox signaling* 15: 1583-1606, 2011.

47. **Garcia-Cardena G, Martasek P, Masters BS, Skidd PM, Couet J, Li S, Lisanti MP, and Sessa WC.** Dissecting the interaction between nitric oxide synthase (NOS) and

caveolin. Functional significance of the nos caveolin binding domain in vivo. *The Journal of biological chemistry* 272: 25437-25440, 1997.

48. **Gelderman MP, Schiffmann R, and Simak J.** Elevated Endothelial Microparticles in Fabry Children Decreased After Enzyme Replacement Therapy. *Arteriosclerosis, thrombosis, and vascular biology* 27: e138-e139, 2007.

49. **Germain DP.** Fabry disease. *Orphanet journal of rare diseases* 5: 30, 2010.

50. **Gimbrone MA, Jr.** Endothelial dysfunction and atherosclerosis. *J Card Surg* 4: 180-183, 1989.

51. **Gimbrone MA, Jr., Cybulsky MI, Kume N, Collins T, and Resnick N.** Vascular endothelium. An integrator of pathophysiological stimuli in atherogenesis. *Ann N Y Acad Sci* 748: 122-131; discussion 131-122, 1995.

52. **Gimbrone MA, Jr., Topper JN, Nagel T, Anderson KR, and Garcia-Cardena G.** Endothelial dysfunction, hemodynamic forces, and atherogenesis. *Ann N Y Acad Sci* 902: 230-239; discussion 239-240, 2000.

53. **Gorlach A, Brandes RP, Nguyen K, Amidi M, Dehghani F, and Busse R.** A gp91phox containing NADPH oxidase selectively expressed in endothelial cells is a major source of oxygen radical generation in the arterial wall. *Circulation research* 87: 26-32, 2000.

54. **Graham DA and Rush JW.** Exercise training improves aortic endothelium-dependent vasorelaxation and determinants of nitric oxide bioavailability in spontaneously hypertensive rats. *Journal of applied physiology* 96: 2088-2096, 2004.

55. **Gratton JP, Fontana J, O'Connor DS, Garcia-Cardena G, McCabe TJ, and Sessa WC.** Reconstitution of an endothelial nitric-oxide synthase (eNOS), hsp90, and caveolin-1 complex in vitro. Evidence that hsp90 facilitates calmodulin stimulated displacement of eNOS from caveolin-1. *The Journal of biological chemistry* 275: 22268-22272, 2000.

56. **Guo W, Adachi T, Matsui R, Xu S, Jiang B, Zou MH, Kirber M, Lieberthal W, and Cohen RA.** Quantitative assessment of tyrosine nitration of manganese superoxide dismutase in angiotensin II-infused rat kidney. *American journal of physiology Heart and circulatory physiology* 285: H1396-1403, 2003.

57. **Hambrecht R, Adams V, Erbs S, Linke A, Krankel N, Shu Y, Baither Y, Gielen S, Thiele H, Gummert JF, Mohr FW, and Schuler G.** Regular physical activity improves endothelial function in patients with coronary artery disease by increasing phosphorylation of endothelial nitric oxide synthase. *Circulation* 107: 3152-3158, 2003.

58. **Hambrecht R, Wolf A, Gielen S, Linke A, Hofer J, Erbs S, Schoene N, and Schuler G.** Effect of exercise on coronary endothelial function in patients with coronary artery disease. *N Engl J Med* 342: 454-460, 2000.

59. **Harris MB, Ju H, Venema VJ, Liang H, Zou R, Michell BJ, Chen ZP, Kemp BE, and Venema RC.** Reciprocal phosphorylation and regulation of endothelial nitric-oxide synthase in response to bradykinin stimulation. *The Journal of biological chemistry* 276: 16587-16591, 2001.

60. **Harrison DG, Widder J, Grumbach I, Chen W, Weber M, and Searles C.** Endothelial mechanotransduction, nitric oxide and vascular inflammation. *Journal of internal medicine* 259: 351-363, 2006.

61. **Hecker M, Mulsch A, Bassenge E, Forstermann U, and Busse R.** Subcellular localization and characterization of nitric oxide synthase(s) in endothelial cells: physiological implications. *The Biochemical journal* 299 (Pt 1): 247-252, 1994.

62. **Higashi Y, Sasaki S, Kurisu S, Yoshimizu A, Sasaki N, Matsuura H, Kajiyama G, and Oshima T.** Regular aerobic exercise augments endothelium-dependent vascular relaxation in normotensive as well as hypertensive subjects: role of endothelium-derived nitric oxide. *Circulation* 100: 1194-1202, 1999.

63. **Hink U, Li H, Mollnau H, Oelze M, Matheis E, Hartmann M, Skatchkov M, Thaiss F, Stahl RA, Warnholtz A, Meinertz T, Griendling K, Harrison DG, Forstermann U, and Munzel T.** Mechanisms underlying endothelial dysfunction in diabetes mellitus. *Circulation research* 88: E14-22, 2001.

64. **Hoffmann B, Schwarz M, Mehta A, Keshav S, and Fabry Outcome Survey European I.** Gastrointestinal symptoms in 342 patients with Fabry disease: prevalence and response to enzyme replacement therapy. *Clinical gastroenterology and hepatology : the official clinical practice journal of the American Gastroenterological Association* 5: 1447-1453, 2007.

65. **Hornig B, Maier V, and Drexler H.** Physical training improves endothelial function in patients with chronic heart failure. *Circulation* 93: 210-214, 1996.

66. **Huang PL.** eNOS, metabolic syndrome and cardiovascular disease. *Trends Endocrinol Metab* 20: 295-302, 2009.

67. **Huang PL.** Unraveling the links between diabetes, obesity, and cardiovascular disease. *Circulation research* 96: 1129-1131, 2005.

68. **Huang PL, Huang Z, Mashimo H, Bloch KD, Moskowitz MA, Bevan JA, and Fishman MC.** Hypertension in mice lacking the gene for endothelial nitric oxide synthase. *Nature* 377: 239-242, 1995.

69. **Hwu WL, Chien YH, Lee NC, Chiang SC, Dobrovolny R, Huang AC, Yeh HY, Chao MC, Lin SJ, Kitagawa T, Desnick RJ, and Hsu LW.** Newborn screening for Fabry

disease in Taiwan reveals a high incidence of the later-onset GLA mutation c.936+919G>A (IVS4+919G>A). *Hum Mutat* 30: 1397-1405, 2009.

70. **Inoue N, Ramasamy S, Fukai T, Nerem RM, and Harrison DG.** Shear stress modulates expression of Cu/Zn superoxide dismutase in human aortic endothelial cells. *Circulation research* 79: 32-37, 1996.

71. **Ioannou YA, Zeidner KM, Gordon RE, and Desnick RJ.** Fabry disease: preclinical studies demonstrate the effectiveness of alpha-galactosidase A replacement in enzyme-deficient mice. *Am J Hum Genet* 68: 14-25, 2001.

72. **Ito T, Yamakuchi M, and Lowenstein CJ.** Thioredoxin increases exocytosis by denitrosylating N-ethylmaleimide-sensitive factor. *The Journal of biological chemistry* 286: 11179-11184, 2011.

73. **Jahn R, Lang T, and Sudhof TC.** Membrane fusion. *Cell* 112: 519-533, 2003.

74. **Jahn R and Scheller RH.** SNAREs--engines for membrane fusion. *Nature reviews Molecular cell biology* 7: 631-643, 2006.

75. **Jahn R and Sudhof TC.** Membrane fusion and exocytosis. *Annual review of biochemistry* 68: 863-911, 1999.

76. **Ju H, Zou R, Venema VJ, and Venema RC.** Direct interaction of endothelial nitric-oxide synthase and caveolin-1 inhibits synthase activity. *The Journal of biological chemistry* 272: 18522-18525, 1997.

77. **Judkins CP, Diep H, Broughton BR, Mast AE, Hooker EU, Miller AA, Selemidis S, Dusting GJ, Sobey CG, and Drummond GR.** Direct evidence of a role for Nox2 in superoxide production, reduced nitric oxide bioavailability, and early atherosclerotic plaque formation in ApoE-/- mice. *American journal of physiology Heart and circulatory physiology* 298: H24-32, 2010.

78. **Jung SC, Han IP, Limaye A, Xu R, Gelderman MP, Zerfas P, Tirumalai K, Murray GJ, During MJ, Brady RO, and Qasba P.** Adeno-associated viral vector-mediated gene transfer results in long-term enzymatic and functional correction in multiple organs of Fabry mice. *Proceedings of the National Academy of Sciences of the United States of America* 98: 2676-2681, 2001.

79. **Kietadisorn R, Juni RP, and Moens AL.** Tackling endothelial dysfunction by modulating NOS uncoupling: new insights into its pathogenesis and therapeutic possibilities. *American journal of physiology Endocrinology and metabolism* 302: E481-495, 2012.

80. **Kim F, Gallis B, and Corson MA.** TNF-alpha inhibits flow and insulin signaling leading to NO production in aortic endothelial cells. *American journal of physiology Cell physiology* 280: C1057-1065, 2001.

81. **Kint JA.** Fabry's disease: alpha-galactosidase deficiency. *Science* 167: 1268-1269, 1970.

82. **Kuhlencordt PJ, Gyurko R, Han F, Scherrer-Crosbie M, Aretz TH, Hajjar R, Picard MH, and Huang PL.** Accelerated atherosclerosis, aortic aneurysm formation, and ischemic heart disease in apolipoprotein E/endothelial nitric oxide synthase double-knockout mice. *Circulation* 104: 448-454, 2001.

83. **Landmesser U, Engberding N, Bahlmann FH, Schaefer A, Wiencke A, Heineke A, Spiekermann S, Hilfiker-Kleiner D, Templin C, Kotlarz D, Mueller M, Fuchs M, Hornig B, Haller H, and Drexler H.** Statin-induced improvement of endothelial progenitor cell mobilization, myocardial neovascularization, left ventricular function, and survival after experimental myocardial infarction requires endothelial nitric oxide synthase. *Circulation* 110: 1933-1939, 2004.

84. **Lassegue B, Sorescu D, Szocs K, Yin Q, Akers M, Zhang Y, Grant SL, Lambeth JD, and Griendling KK.** Novel gp91(phox) homologues in vascular smooth muscle cells : nox1 mediates angiotensin II-induced superoxide formation and redox-sensitive signaling pathways. *Circulation research* 88: 888-894, 2001.

85. **Laughlin MH, Newcomer SC, and Bender SB.** Importance of hemodynamic forces as signals for exercise-induced changes in endothelial cell phenotype. *Journal of applied physiology* 104: 588-600, 2008.

86. **Laughlin MH, Pollock JS, Amann JF, Hollis ML, Woodman CR, and Price EM.** Training induces nonuniform increases in eNOS content along the coronary arterial tree. *Journal of applied physiology* 90: 501-510, 2001.

87. **Laughlin MH, Welshons WV, Sturek M, Rush JW, Turk JR, Taylor JA, Judy BM, Henderson KK, and Ganjam VK.** Gender, exercise training, and eNOS expression in porcine skeletal muscle arteries. *Journal of applied physiology* 95: 250-264, 2003.

88. **Laursen JB, Somers M, Kurz S, McCann L, Warnholtz A, Freeman BA, Tarpey M, Fukai T, and Harrison DG.** Endothelial regulation of vasomotion in apoE-deficient mice: implications for interactions between peroxynitrite and tetrahydrobiopterin. *Circulation* 103: 1282-1288, 2001.

89. **Lefer DJ, Jones SP, Girod WG, Baines A, Grisham MB, Cockrell AS, Huang PL, and Scalia R.** Leukocyte-endothelial cell interactions in nitric oxide synthase-deficient mice. *The American journal of physiology* 276: H1943-1950, 1999.

90. **Lerman A and Zeiher AM.** Endothelial function: cardiac events. *Circulation* 111: 363-368, 2005.

91. **Li H, Horke S, and Forstermann U.** Vascular oxidative stress, nitric oxide and atherosclerosis. *Atherosclerosis* 237: 208-219, 2014.

92. **Linhart A and Elliott PM.** The heart in Anderson-Fabry disease and other lysosomal storage disorders. *Heart* 93: 528-535, 2007.

93. **Lisanti MP, Scherer PE, Tang Z, and Sargiacomo M.** Caveolae, caveolin and caveolin-rich membrane domains: a signalling hypothesis. *Trends in cell biology* 4: 231-235, 1994.

94. **Lowenstein CJ.** Nitric oxide regulation of protein trafficking in the cardiovascular system. *Cardiovascular research* 75: 240-246, 2007.

95. **Luo S, Lei H, Qin H, and Xia Y.** Molecular mechanisms of endothelial NO synthase uncoupling. *Current pharmaceutical design* 20: 3548-3553, 2014.

96. **MacDermot KD, Holmes A, and Miners AH.** Anderson-Fabry disease: clinical manifestations and impact of disease in a cohort of 60 obligate carrier females. *Journal of medical genetics* 38: 769-775, 2001.

97. **Malhotra V, Orci L, Glick BS, Block MR, and Rothman JE.** Role of an N-ethylmaleimide-sensitive transport component in promoting fusion of transport vesicles with cisternae of the Golgi stack. *Cell* 54: 221-227, 1988.

98. **Matsubara M, Titani K, and Taniguchi H.** Interaction of calmodulin-binding domain peptides of nitric oxide synthase with membrane phospholipids: regulation by protein phosphorylation and Ca(2+)-calmodulin. *Biochemistry* 35: 14651-14658, 1996.

99. **Matsushita K, Morrell CN, Cambien B, Yang SX, Yamakuchi M, Bao C, Hara MR, Quick RA, Cao W, O'Rourke B, Lowenstein JM, Pevsner J, Wagner DD, and Lowenstein CJ.** Nitric oxide regulates exocytosis by S-nitrosylation of N-ethylmaleimide-sensitive factor. *Cell* 115: 139-150, 2003.

100. **Matsushita K, Morrell CN, Mason RJ, Yamakuchi M, Khanday FA, Irani K, and Lowenstein CJ.** Hydrogen peroxide regulation of endothelial exocytosis by inhibition of N-ethylmaleimide sensitive factor. *The Journal of cell biology* 170: 73-79, 2005.

101. **May AP, Whiteheart SW, and Weis WI.** Unraveling the mechanism of the vesicle transport ATPase NSF, the N-ethylmaleimide-sensitive factor. *The Journal of biological chemistry* 276: 21991-21994, 2001.

102. **Mayadas TN, Johnson RC, Rayburn H, Hynes RO, and Wagner DD.** Leukocyte rolling and extravasation are severely compromised in P selectin-deficient mice. *Cell* 74: 541-554, 1993.

103. **McCabe TJ, Fulton D, Roman LJ, and Sessa WC.** Enhanced electron flux and reduced calmodulin dissociation may explain "calcium-independent" eNOS activation by phosphorylation. *The Journal of biological chemistry* 275: 6123-6128, 2000.

104. **McEver RP, Beckstead JH, Moore KL, Marshall-Carlson L, and Bainton DF.** GMP-140, a platelet alpha-granule membrane protein, is also synthesized by vascular endothelial cells and is localized in Weibel-Palade bodies. *The Journal of clinical investigation* 84: 92-99, 1989.

105. **Mehta A, Clarke JT, Giugliani R, Elliott P, Linhart A, Beck M, Sunder-Plassmann G, and Investigators FOS.** Natural course of Fabry disease: changing pattern of causes of death in FOS - Fabry Outcome Survey. *Journal of medical genetics* 46: 548-552, 2009.

106. **Meikle PJ, Hopwood JJ, Clague AE, and Carey WF.** Prevalence of lysosomal storage disorders. *Jama* 281: 249-254, 1999.

107. **Mellman I and Warren G.** The road taken: past and future foundations of membrane traffic. *Cell* 100: 99-112, 2000.

108. **Michel T and Vanhoutte PM.** Cellular signaling and NO production. *Pflugers Archiv : European journal of physiology* 459: 807-816, 2010.

109. **Michell BJ, Chen Z, Tiganis T, Stapleton D, Katsis F, Power DA, Sim AT, and Kemp BE.** Coordinated control of endothelial nitric-oxide synthase phosphorylation by protein kinase C and the cAMP-dependent protein kinase. *The Journal of biological chemistry* 276: 17625-17628, 2001.

110. **Moens AL, Champion HC, Claeys MJ, Tavazzi B, Kaminski PM, Wolin MS, Borgonjon DJ, Van Nassauw L, Haile A, Zviman M, Bedja D, Wuyts FL, Elsaesser RS, Cos P, Gabrielson KL, Lazzarino G, Paolocci N, Timmermans JP, Vrints CJ, and Kass DA.** High-dose folic acid pretreatment blunts cardiac dysfunction during ischemia coupled to maintenance of high-energy phosphates and reduces postreperfusion injury. *Circulation* 117: 1810-1819, 2008.

111. **Moens AL, Goovaerts I, Claeys MJ, and Vrints CJ.** Flow-mediated vasodilation: a diagnostic instrument, or an experimental tool? *Chest* 127: 2254-2263, 2005.

112. **Mollnau H, Wendt M, Szocs K, Lassegue B, Schulz E, Oelze M, Li H, Bodenschatz M, August M, Kleschyov AL, Tsilimingas N, Walter U, Forstermann U, Meinertz T, Griendling K, and Munzel T.** Effects of angiotensin II infusion on the expression and function of NAD(P)H oxidase and components of nitric oxide/cGMP signaling. *Circulation research* 90: E58-65, 2002.

113. **Moore DF, Scott LT, Gladwin MT, Altarescu G, Kaneski C, Suzuki K, Pease-Fye M, Ferri R, Brady RO, Herscovitch P, and Schiffmann R.** Regional cerebral hyperperfusion and nitric oxide pathway dysregulation in Fabry disease: reversal by enzyme replacement therapy. *Circulation* 104: 1506-1512, 2001.

114. **Moroi M, Zhang L, Yasuda T, Virmani R, Gold HK, Fishman MC, and Huang PL.** Interaction of genetic deficiency of endothelial nitric oxide, gender, and pregnancy in

vascular response to injury in mice. *The Journal of clinical investigation* 101: 1225-1232, 1998.

115. **Mozaffarian D, Benjamin EJ, Go AS, Arnett DK, Blaha MJ, Cushman M, de Ferranti S, Despres JP, Fullerton HJ, Howard VJ, Huffman MD, Judd SE, Kissela BM, Lackland DT, Lichtman JH, Lisabeth LD, Liu S, Mackey RH, Matchar DB, McGuire DK, Mohler ER, 3rd, Moy CS, Muntner P, Mussolino ME, Nasir K, Neumar RW, Nichol G, Palaniappan L, Pandey DK, Reeves MJ, Rodriguez CJ, Sorlie PD, Stein J, Towfighi A, Turan TN, Virani SS, Willey JZ, Woo D, Yeh RW, Turner MB, American Heart Association Statistics C, and Stroke Statistics S.** Heart disease and stroke statistics--2015 update: a report from the American Heart Association. *Circulation* 131: e29-322, 2015.

116. **Mukhin DN, Chao FF, and Kruth HS.** Glycosphingolipid accumulation in the aortic wall is another feature of human atherosclerosis. *Arteriosclerosis, thrombosis, and vascular biology* 15: 1607-1615, 1995.

117. **Naghavi M, Libby P, Falk E, Casscells SW, Litovsky S, Rumberger J, Badimon JJ, Stefanadis C, Moreno P, Pasterkamp G, Fayad Z, Stone PH, Waxman S, Raggi P, Madjid M, Zarrabi A, Burke A, Yuan C, Fitzgerald PJ, Siscovick DS, de Korte CL, Aikawa M, Juhani Airaksinen KE, Assmann G, Becker CR, Chesebro JH, Farb A, Galis ZS, Jackson C, Jang IK, Koenig W, Lodder RA, March K, Demirovic J, Navab M, Priori SG, Rekhter MD, Bahr R, Grundy SM, Mehran R, Colombo A, Boerwinkle E, Ballantyne C, Insull W, Jr., Schwartz RS, Vogel R, Serruys PW, Hansson GK, Faxon DP, Kaul S, Drexler H, Greenland P, Muller JE, Virmani R, Ridker PM, Zipes DP, Shah PK, and Willerson JT.** From vulnerable plaque to vulnerable patient: a call for new definitions and risk assessment strategies: Part I. *Circulation* 108: 1664-1672, 2003.

118. **Nakazono K, Watanabe N, Matsuno K, Sasaki J, Sato T, and Inoue M.** Does superoxide underlie the pathogenesis of hypertension? *Proceedings of the National Academy of Sciences of the United States of America* 88: 10045-10048, 1991.

119. **Niebauer J, Maxwell AJ, Lin PS, Tsao PS, Kosek J, Bernstein D, and Cooke JP.** Impaired aerobic capacity in hypercholesterolemic mice: partial reversal by exercise training. *The American journal of physiology* 276: H1346-1354, 1999.

120. **Ohara Y, Peterson TE, and Harrison DG.** Hypercholesterolemia increases endothelial superoxide anion production. *The Journal of clinical investigation* 91: 2546-2551, 1993.

121. **Ohshima T, Murray GJ, Swaim WD, Longenecker G, Quirk JM, Cardarelli CO, Sugimoto Y, Pastan I, Gottesman MM, Brady RO, and Kulkarni AB.** alpha-Galactosidase A deficient mice: a model of Fabry disease. *Proceedings of the National Academy of Sciences of the United States of America* 94: 2540-2544, 1997.

122. **Ohshima T, Schiffmann R, Murray GJ, Kopp J, Quirk JM, Stahl S, Chan CC, Zerfas P, Tao-Cheng JH, Ward JM, Brady RO, and Kulkarni AB.** Aging accentuates and bone

marrow transplantation ameliorates metabolic defects in Fabry disease mice. *Proceedings of the National Academy of Sciences of the United States of America* 96: 6423-6427, 1999.

123. **Pacher P, Beckman JS, and Liaudet L.** Nitric oxide and peroxynitrite in health and disease. *Physiological reviews* 87: 315-424, 2007.

124. **Park JL, Whitesall SE, D'Alecy LG, Shu L, and Shayman JA.** Vascular dysfunction in the alpha-galactosidase A-knockout mouse is an endothelial cell-, plasma membrane-based defect. *Clin Exp Pharmacol Physiol* 35: 1156-1163, 2008.

125. **Pompen AW, Ruiter M, and Wyers HJ.** Angiokeratoma corporis diffusum (universale) Fabry, as a sign of an unknown internal disease; two autopsy reports. *Acta Med Scand* 128: 234-255, 1947.

126. **Pynn M, Schafer K, Konstantinides S, and Halle M.** Exercise training reduces neointimal growth and stabilizes vascular lesions developing after injury in apolipoprotein e-deficient mice. *Circulation* 109: 386-392, 2004.

127. **Qian J, Zhang Q, Church JE, Stepp DW, Rudic RD, and Fulton DJ.** Role of local production of endothelium-derived nitric oxide on cGMP signaling and S-nitrosylation. *American journal of physiology Heart and circulatory physiology* 298: H112-118, 2010.

128. **Rajagopalan S, Kurz S, Munzel T, Tarpey M, Freeman BA, Griendling KK, and Harrison DG.** Angiotensin II-mediated hypertension in the rat increases vascular superoxide production via membrane NADH/NADPH oxidase activation. Contribution to alterations of vasomotor tone. *The Journal of clinical investigation* 97: 1916-1923, 1996.

129. **Rask-Madsen C, Ihlemann N, Krarup T, Christiansen E, Kober L, Nervil Kistorp C, and Torp-Pedersen C.** Insulin therapy improves insulin-stimulated endothelial function in patients with type 2 diabetes and ischemic heart disease. *Diabetes* 50: 2611-2618, 2001.

130. **Rombach SM, Smid BE, Bouwman MG, Linthorst GE, Dijkgraaf MG, and Hollak CE.** Long term enzyme replacement therapy for Fabry disease: effectiveness on kidney, heart and brain. *Orphanet journal of rare diseases* 8: 47, 2013.

131. **Rombach SM, Smid BE, Bouwman MG, Linthorst GE, Dijkgraaf MGW, and Hollak CEM.** Long term enzyme replacement therapy for Fabry disease: effectiveness on kidney, heart and brain. *Orphanet journal of rare diseases* 8: 47, 2013.

132. **Rombach SM, Twickler TB, Aerts JM, Linthorst GE, Wijburg FA, and Hollak CE.** Vasculopathy in patients with Fabry disease: current controversies and research directions. *Molecular genetics and metabolism* 99: 99-108, 2010.

133. **Ross R.** Atherosclerosis--an inflammatory disease. *N Engl J Med* 340: 115-126, 1999.

134. **Ross R.** Atherosclerosis is an inflammatory disease. *Am Heart J* 138: S419-420, 1999.

135. **Ruggeri ZM.** von Willebrand factor. *The Journal of clinical investigation* 100: S41-46, 1997.

136. **Rush JW, Laughlin MH, Woodman CR, and Price EM.** SOD-1 expression in pig coronary arterioles is increased by exercise training. *American journal of physiology Heart and circulatory physiology* 279: H2068-2076, 2000.

137. **Rush JW, Turk JR, and Laughlin MH.** Exercise training regulates SOD-1 and oxidative stress in porcine aortic endothelium. *American journal of physiology Heart and circulatory physiology* 284: H1378-1387, 2003.

138. **Sakamoto S, Minami K, Niwa Y, Ohnaka M, Nakaya Y, Mizuno A, Kuwajima M, and Shima K.** Effect of exercise training and food restriction on endothelium-dependent relaxation in the Otsuka Long-Evans Tokushima Fatty rat, a model of spontaneous NIDDM. *Diabetes* 47: 82-86, 1998.

139. **Sakuraba H, Oshima A, Fukuhara Y, Shimmoto M, Nagao Y, Bishop DF, Desnick RJ, and Suzuki Y.** Identification of point mutations in the alpha-galactosidase A gene in classical and atypical hemizygotes with Fabry disease. *Am J Hum Genet* 47: 784-789, 1990.

140. **Schiffmann R, Warnock DG, Banikazemi M, Bultas J, Linthorst GE, Packman S, Sorensen SA, Wilcox WR, and Desnick RJ.** Fabry disease: progression of nephropathy, and prevalence of cardiac and cerebrovascular events before enzyme replacement therapy. *Nephrology, dialysis, transplantation : official publication of the European Dialysis and Transplant Association - European Renal Association* 24: 2102-2111, 2009.

141. **Seals DR, Desouza CA, Donato AJ, and Tanaka H.** Habitual exercise and arterial aging. *Journal of applied physiology* 105: 1323-1332, 2008.

142. **Sessa WC, Harrison JK, Barber CM, Zeng D, Durieux ME, D'Angelo DD, Lynch KR, and Peach MJ.** Molecular cloning and expression of a cDNA encoding endothelial cell nitric oxide synthase. *The Journal of biological chemistry* 267: 15274-15276, 1992.

143. **Shaul PW.** Regulation of endothelial nitric oxide synthase: location, location, location. *Annual review of physiology* 64: 749-774, 2002.

144. **Shaul PW, Smart EJ, Robinson LJ, German Z, Yuhanna IS, Ying Y, Anderson RG, and Michel T.** Acylation targets endothelial nitric-oxide synthase to plasmalemmal caveolae. *The Journal of biological chemistry* 271: 6518-6522, 1996.

145. **Shen J, Tareste DC, Paumet F, Rothman JE, and Melia TJ.** Selective activation of cognate SNAREpins by Sec1/Munc18 proteins. *Cell* 128: 183-195, 2007.

146. **Shen JS, Meng XL, Moore DF, Quirk JM, Shayman JA, Schiffmann R, and Kaneski CR.** Globotriaosylceramide induces oxidative stress and up-regulates cell adhesion

molecule expression in Fabry disease endothelial cells. *Molecular genetics and metabolism* 95: 163-168, 2008.

147. **Sheth KJ, Werlin SL, Freeman ME, and Hodach AE.** Gastrointestinal structure and function in Fabry's disease. *The American journal of gastroenterology* 76: 246-251, 1981.

148. **Shu L, Murphy HS, Cooling L, and Shayman JA.** An in vitro model of Fabry disease. *J Am Soc Nephrol* 16: 2636-2645, 2005.

149. **Shu L and Shayman JA.** Caveolin-associated accumulation of globotriaosylceramide in the vascular endothelium of alpha-galactosidase A null mice. *The Journal of biological chemistry* 282: 20960-20967, 2007.

150. **Shu L and Shayman JA.** Glycosphingolipid Mediated Caveolin-1 Oligomerization. *J Glycomics Lipidomics* Suppl 2: 1-6, 2012.

151. **Shu L, Vivekanandan-Giri A, Pennathur S, Smid BE, Aerts JM, Hollak CE, and Shayman JA.** Establishing 3-nitrotyrosine as a biomarker for the vasculopathy of Fabry disease. *Kidney Int* 86: 58-66, 2014.

152. **Spada M, Pagliardini S, Yasuda M, Tukel T, Thiagarajan G, Sakuraba H, Ponzone A, and Desnick RJ.** High incidence of later-onset fabry disease revealed by newborn screening. *Am J Hum Genet* 79: 31-40, 2006.

153. **Stamler JS, Lamas S, and Fang FC.** Nitrosylation. the prototypic redox-based signaling mechanism. *Cell* 106: 675-683, 2001.

154. **Stary HC, Chandler AB, Glagov S, Guyton JR, Insull W, Jr., Rosenfeld ME, Schaffer SA, Schwartz CJ, Wagner WD, and Wissler RW.** A definition of initial, fatty streak, and intermediate lesions of atherosclerosis. A report from the Committee on Vascular Lesions of the Council on Arteriosclerosis, American Heart Association. *Circulation* 89: 2462-2478, 1994.

155. **Steinberg D.** The pathogenesis of atherosclerosis. An interpretive history of the cholesterol controversy, part IV: the 1984 coronary primary prevention trial ends it--almost. *J Lipid Res* 47: 1-14, 2006.

156. **Sudhof TC.** The synaptic vesicle cycle. *Annual review of neuroscience* 27: 509-547, 2004.

157. **Sweeley CC and Klionsky B.** Fabry's Disease: Classification as a Sphingolipidosis and Partial Characterization of a Novel Glycolipid. *The Journal of biological chemistry* 238: 3148-3150, 1963.

158. **Taddei S, Galetta F, Virdis A, Ghiadoni L, Salvetti G, Franzoni F, Giusti C, and Salvetti A.** Physical activity prevents age-related impairment in nitric oxide availability in elderly athletes. *Circulation* 101: 2896-2901, 2000.

159. **Taddei S, Virdis A, Ghiadoni L, Salvetti G, Bernini G, Magagna A, and Salvetti A.** Age-related reduction of NO availability and oxidative stress in humans. *Hypertension* 38: 274-279, 2001.

160. **Takimoto E, Champion HC, Li M, Ren S, Rodriguez ER, Tavazzi B, Lazzarino G, Paolocci N, Gabrielson KL, Wang Y, and Kass DA.** Oxidant stress from nitric oxide synthase-3 uncoupling stimulates cardiac pathologic remodeling from chronic pressure load. *The Journal of clinical investigation* 115: 1221-1231, 2005.

161. **Terryn W, Cochat P, Froissart R, Ortiz A, Pirson Y, Poppe B, Serra A, Van Biesen W, Vanholder R, and Wanner C.** Fabry nephropathy: indications for screening and guidance for diagnosis and treatment by the European Renal Best Practice. *Nephrology, dialysis, transplantation : official publication of the European Dialysis and Transplant Association - European Renal Association* 28: 505-517, 2013.

162. **Vedder AC, Biro E, Aerts JM, Nieuwland R, Sturk G, and Hollak CE.** Plasma markers of coagulation and endothelial activation in Fabry disease: impact of renal impairment. *Nephrology, dialysis, transplantation : official publication of the European Dialysis and Transplant Association - European Renal Association* 24: 3074-3081, 2009.

163. **Venema RC, Sayegh HS, Arnal JF, and Harrison DG.** Role of the enzyme calmodulin-binding domain in membrane association and phospholipid inhibition of endothelial nitric oxide synthase. *The Journal of biological chemistry* 270: 14705-14711, 1995.

164. **Wagner DD.** The Weibel-Palade body: the storage granule for von Willebrand factor and P-selectin. *Thrombosis and haemostasis* 70: 105-110, 1993.

165. **Waldek S, Patel MR, Banikazemi M, Lemay R, and Lee P.** Life expectancy and cause of death in males and females with Fabry disease: findings from the Fabry Registry. *Genetics in medicine : official journal of the American College of Medical Genetics* 11: 790-796, 2009.

166. **Warnholtz A, Nickenig G, Schulz E, Macharzina R, Brasen JH, Skatchkov M, Heitzer T, Stasch JP, Griendling KK, Harrison DG, Bohm M, Meinertz T, and Munzel T.** Increased NADH-oxidase-mediated superoxide production in the early stages of atherosclerosis: evidence for involvement of the renin-angiotensin system. *Circulation* 99: 2027-2033, 1999.

167. **Weibel ER and Palade GE.** New Cytoplasmic Components in Arterial Endothelia. *The Journal of cell biology* 23: 101-112, 1964.

168. **Weidemann F, Niemann M, Stork S, Breunig F, Beer M, Sommer C, Herrmann S, Ertl G, and Wanner C.** Long-term outcome of enzyme-replacement therapy in advanced Fabry disease: evidence for disease progression towards serious complications. *Journal of internal medicine* 274: 331-341, 2013.

169. **White CR and Frangos JA.** The shear stress of it all: the cell membrane and mechanochemical transduction. *Philos Trans R Soc Lond B Biol Sci* 362: 1459-1467, 2007.

170. **Whybra C, Kampmann C, Willers I, Davies J, Winchester B, Kriegsmann J, Bruhl K, Gal A, Bunge S, and Beck M.** Anderson-Fabry disease: clinical manifestations of disease in female heterozygotes. *Journal of inherited metabolic disease* 24: 715-724, 2001.

171. **Widlansky ME, Gokce N, Keaney JF, Jr., and Vita JA.** The clinical implications of endothelial dysfunction. *Journal of the American College of Cardiology* 42: 1149-1160, 2003.

172. **Wilcox JN, Subramanian RR, Sundell CL, Tracey WR, Pollock JS, Harrison DG, and Marsden PA.** Expression of multiple isoforms of nitric oxide synthase in normal and atherosclerotic vessels. *Arteriosclerosis, thrombosis, and vascular biology* 17: 2479-2488, 1997.

173. **Wilcox WR, Banikazemi M, Guffon N, Waldek S, Lee P, Linthorst GE, Desnick RJ, and Germain DP.** Long-term safety and efficacy of enzyme replacement therapy for Fabry disease. *Am J Hum Genet* 75: 65-74, 2004.

174. **Wilcox WR, Oliveira JP, Hopkin RJ, Ortiz A, Banikazemi M, Feldt-Rasmussen U, Sims K, Waldek S, Pastores GM, Lee P, Eng CM, Marodi L, Stanford KE, Breunig F, Wanner C, Warnock DG, Lemay RM, Germain DP, and Fabry R.** Females with Fabry disease frequently have major organ involvement: lessons from the Fabry Registry. *Molecular genetics and metabolism* 93: 112-128, 2008.

175. **Wise D, Wallace HJ, and Jellinek EH.** Angiokeratoma corporis diffusum. A clinical study of eight affected families. *The Quarterly journal of medicine* 31: 177-206, 1962.

176. **Woodman CR, Muller JM, Laughlin MH, and Price EM.** Induction of nitric oxide synthase mRNA in coronary resistance arteries isolated from exercise-trained pigs. *The American journal of physiology* 273: H2575-2579, 1997.

177. **Xiang Y and Hwa J.** Regulation of VWF expression, and secretion in health and disease. *Current opinion in hematology* 23: 288-293, 2016.

178. **Yang AL and Chen HI.** Chronic exercise reduces adhesion molecules/iNOS expression and partially reverses vascular responsiveness in hypercholesterolemic rabbit aortae. *Atherosclerosis* 169: 11-17, 2003.

179. **Zerial M and McBride H.** Rab proteins as membrane organizers. *Nature reviews Molecular cell biology* 2: 107-117, 2001.

180. **Zou MH, Shi C, and Cohen RA.** Oxidation of the zinc-thiolate complex and uncoupling of endothelial nitric oxide synthase by peroxynitrite. *The Journal of clinical investigation* 109: 817-826, 2002.

CHAPTER 3

Endothelial nitric oxide synthase uncoupling and microvascular dysfunction in the mesentery of mice deficient in a α-Galactosidase A

Abstract

A defect in the gene for the lysosomal enzyme α-galactosidase A (GLA) results in globotriaosylceramide (Gb3) accumulation in Fabry disease and leads to premature death from cardiac and cerebrovascular events. However, gastrointestinal symptoms are often first observed during childhood in these patients and are not well understood. In this study, we demonstrate an age-dependent microvasculopathy of the mesenteric artery (MA) in a murine model of Fabry disease (Gla-knockout mice) resulting from dysregulation of the vascular homeostatic enzyme endothelial nitric oxide synthase (eNOS). The progressive accumulation of Gb3 in the MA was confirmed by thin-layer chromatographic analysis. A total absence of endothelium-dependent dilation was observed in MAs from mice at 8 mo of age, while suppression of ACh-mediated vasodilation was evident from 2 mo of age. Endothelium-independent dilation with sodium nitroprusside was normal compared with age-matched wild-type mice. The microvascular defect in MAs from Fabry mice was endothelium-dependent and associated with suppression of the active homodimer of eNOS. Phosphorylation of eNOS at the major activation site (Ser1179) was significantly downregulated, while phosphorylation at the major inhibitory site (Thr495) was

remarkably enhanced in MAs from aged Fabry mice. These profound alterations in eNOS bioavailability at 8 mo of age were observed in parallel with high levels of 3-nitrotyrosine, suggesting increased reactive oxygen species along with eNOS uncoupling in this vascular bed. Overall, the mesenteric microvessels in the setting of Fabry disease were observed to have an early and profound endothelial dysfunction associated with elevated reactive nitrogen species and decreased nitric oxide bioavailability.

Introduction

Fabry disease is an X-linked glycosphingolipid disorder caused by deficient or absent activity in the lysosomal enzyme, α-galactosidase A (Gla) (3, 13). The loss of Gla leads to the progressive accumulation of neutral glycosphingolipids with terminal Gal-α1-4Gal linkages, including globotriaosylceramide (Gb3), galabiosylceramide, and globotriaosylsphingosine. A primary site of glycosphingolipid accumulation is the vascular endothelium, although accumulation occurs in various other organ systems throughout the body (6, 24). Premature life-threatening complications arise from involvement of the brain, heart, and kidneys and include cerebrovascular accidents, myocardial infarction, and progressive renal insufficiency (7). Affected hemizygous males and female carriers suffer from Fabry-related complications (15, 26).

The vascular complications of Gla deficiency have been the primary focus of clinical and mechanistic studies of this rare disease. However, the earliest and most common symptoms of Fabry disease are gastrointestinal and include abdominal pain, constipation, diarrhea, and nausea (7, 21). Because these symptoms are common, the diagnosis of Fabry disease is often delayed (21).

Both clinical and experimental studies have focused on the hypothesis that endothelial dysfunction may underlie both the macrovascular and microvascular complications associated with Fabry

disease. The Gla knockout mouse can be used to characterize and study inducible models of vasculopathy. Robust vascular phenotypes in these mice have been reported, including accelerated atherogenesis and thrombus formation following photochemical injury (2, 5). In isolated aortic rings, Gb3 accumulation in endothelium is linked to a defect in endothelial nitric oxide (NO) mediated vasodilation (18). These and other findings are consistent with a Gb3 dependent loss of NO bioavailability as a common mechanism linking atherogenesis, thrombosis, and impaired vasorelaxation.

The purpose of this study was to determine whether the vascular phenotype in the Gla knockout mouse extends beyond the aorta and carotid vasculature. Specifically, an age-dependent mesenteric artery phenotype was characterized in Gla null mice. Gla deficient mice were observed to have age-dependent Gb3 accumulation in their mesenteric arteries in conjunction with a profound loss of microvascular reactivity and increased endothelium nitric oxide synthase (eNOS) uncoupling.

Methods

Mice

A breeding colony of Gla null mice was established from mice provided by Ashok Kulkarni at the NIH. The knockout mice (129/SvJXC57BL/6) were originally generated by replacement of α-galactosidase A (*Gla*) gene with a neomycin resistance (neo) sequence within a portion of exon 3 and intron 4 region (17). These mice were back-crossed a minimum of six generations to the C57BL6/J strain. The Gla null and wild-type (WT) C57BL/6 mice were maintained in University of Michigan animal facility under standard conditions. All animal experiments were performed

according to the protocol of the University of Michigan Committee on the Use and Care of Laboratory Animals.

Vascular reactivity experiments

Two to nine month old mice were euthanized with intraperitoneal pentobarbital (66.5 mg/kg). A segment of small intestine was removed and placed in a dissection Petri dish filled with cold physiological salt solution (mmol/L: NaCl 130, KCl 4.7, $KHPO_4$ 1.18, $MgSO_4$ 1.17, CaCl2 1.6, $NaHCO_3$ 14.9, dextrose 5.5, $CaNa_2$ EDTA 0.03). The second order mesenteric arteries (2-3 mm in length) were carefully dissected and connective tissue surrounding the arteries was removed. The individual vessel segment was mounted on glass cannulas in a pressure myograph system (110P, Danish Myo Technology A/S, Aarhus, Denmark). The vessel diameter was monitored and analyzed digitally in real time (DMT Vessel Acqusition Suite 6.2, Danish Myo Technology A/S, Aarhus, Denmark). In studies to determine acetylcholine (Ach)-mediated relaxation without endothelium, the endothelium was denuded during the mounting procedure by exposing endothelial cells to an air bubble for 30 seconds. Mounted mesenteric arteries were bathed with warmed (37˚C) and aerated (95% O_2 and 5% CO_2) physiological salt solution. Mesenteric arteries were pressurized at 20 mmHg, and the pressure was increased 10 mmHg every 5 minutes until reaching 60 mmHg. The vessels were then equilibrated for 60 minutes. Prior to Ach- and sodium nitroprusside (SNP)-mediated vascular reactivity studies, the vessels were subjected to osmotically balanced high potassium-containing physiological salt solution (mmol/L: NaCl 14.7, KCl 100, $KHPO_4$ 1.18, $MgSO_4$ 1.17, $CaCl_2$ 1.6, $NaHCO_3$ 14.9, dextrose 5.5, $CaNa_2$ EDTA 0.03) and various concentrations of norepinephrine (NE, 10^{-9} to 10^{-4} mol/L) with washes in between each contraction. Pre-constriction of the vessel was performed with NE (10^{-5} mol/L). Subsequently, Ach (10^{-9} to 10^{-}

^{4} mol/L) or SNP (10^{-8} to 10^{-3} mol/L) was added cumulatively to the bath to examine endothelium-dependent (Ach) or endothelium-independent (SNP) relaxation. All chemicals used in the vascular reactivity study were purchased from Sigma Chemical Company (St. Louis, MO).

Reagents

Globotriaosylceramide (Gb3), was purchased from Matreya (Pleasant Gap, PA). Three phosphatase/protease inhibitors; P2714, P0044 and P5726, were obtained from Sigma-Aldrich (St. Louis, MO). Mouse anti-human eNOS monoclonal and mouse anti-human 3-nitrotyrosine monoclonal antibodies were purchased from Abcam (Cambridge, MA). Rabbit anti-human phospho-eNOS Thr495 polyclonal antibody was acquired from Cell Signaling Technology (Danvers, MA). Rabbit anti-bovine phospho-eNOS Ser1179 polyclonal antibody was from Life Technologies (Grand Island, NY). The ECL-plus system was from PerkinElmer Life Sciences (Waltham, MA).

Tissue Lipid Extraction and Gb3 Analysis

Frozen mesenteric artery (MA) tissues, dissected from WT and Gla null mice at ages between 1 and 12 months, were thawed in 0.8 ml/sample of ice-cold sucrose buffer (250 mM sucrose, pH 7.4, 10 mM Hepes and 1 mM EDTA) and homogenized with a Tri-R homogenizer at 10% output. Total and neutral lipid extraction, separation by high performance thin layer chromatography, and quantification were performed as previously described (24).

Western blotting

For immunoblot analysis, frozen MA tissues were thawed in ice-cold lysate buffer formulated with 25 mM Tris-HCl (pH 7.4), 137 mM NaCl, 2 mM EDTA, 2 mM Na_3VO_4, 20 mM NaF, 1% Triton X-100, 10% glycerol and 1X mixture of phosphatase/protease inhibitors composed of P2714, P0044, and P5726. Unfrozen samples were homogenized with a Tri-R homogenizer for 20 seconds at 5% output at 4°C, and then sonicated with a probe sonicator for 1 second 5 times at 50% output at 4°C. The cell debris was removed by centrifugation at 10,000 × g for 10 minutes at 4°C.

Quantification of total protein in each MA sample was performed by using bicinchoninic acid assay with bovine serum albumin as a standard. To determine total eNOS expression in MA of wild type and Gla null mice, 40 µg of MA lysate protein, either denatured with 1% 2-mercaptoethanol or non-denatured, were separated by SDS-PAGE using a 6-12% gradient. Monomeric and homodimeric eNOS in WT and Gla null mouse MA were detected with a mouse anti-human eNOS monoclonal antibody at a concentration of 0.5 µg/ml. MA samples for determination of protein-bound 3-nitrotyrosine levels were dissected from WT and Fabry mouse in antioxidant buffer containing 100 µM diethylene tetraamino pentaacetic acid, 50 µM butylated hydroxytoluene, 10 µL/mL protease inhibitor (Pierce, Rockford, IL). Expression of 3-nitrotyrosine in MA samples were evaluated using a mouse anti-human 3-nitrotyrosine antibody (0.4 µg/ml) diluted in blotting buffer (TBS) consisting of 20 mM Tris-HCl (pH, 7.6), 150 mM NaCl and 2.5% fat-free dry milk. Primary antibodies against human p-eNOS Thr495 (0.5 µg/ml) and bovine p-eNOS Ser1179 (1.0 µg/ml) residues were selected to measure phosphorylation of eNOS in wild type and Gla null mouse MA. Both antibodies were diluted in 1% milk-TBS. Based on amino acid sequence homology, all of the eNOS specific antibodies cross-react with indicated proteins in mouse MA. The immunoreactive bands were stained with the ECL-plus system and quantified by densitometric scanning using ImageJ software.

Statistical analysis

GraphPad Prism software was used for statistical analysis. The data are presented as mean ± standard error of the mean. Results were analyzed using unpaired t-test for comparison of two groups. For multiple comparisons, data were analyzed using two-way ANOVA, followed by Bonferroni post-hoc analysis. Statistical significance was set at $p<0.05$.

Results

Age-dependent Gb3 accumulation in the mesenteric arteries of Gla null mice.

MAs from 2 and 9 month old wild type mice on a C57BL/6 background had no detectable Gb3. However, in Gla-deficient mouse MA, Gb3 levels were readily detected at 2 months of age and were markedly elevated in the 9 month old MA (Figure 3 - 1A). The Gb3 levels from 9 month old Gla null mouse MAs were 5 fold higher than that observed in 2 month old knockout MA (Figure 3 - 1B) and continued to increase through 12 months of age (Figure 3 - 1C). These data indicate that the Gb3 accumulation in the Gla null mouse MAs is progressive as a function of age.

Acetylcholine (Ach) mediated relaxation in endothelium-intact mesenteric arteries

The endothelium-dependent relaxation to Ach was examined in isolated MAs from wild type and Gla null mice that were pre-contracted with norepinephrine (NE) (10^{-5} mol/L). The MAs from 2 month-old Gla knockout mice dilated significantly less (15.9 ± 5.8%, $p<0.001$) when compared to vessels from age matched wild type mice (53.4 ± 9.2%) in response to the highest dose of Ach (10^{-4} mol/L) (Figure 3 - 2A). The MAs from 8 month-old wild type mice relaxed in a concentration-

dependent manner following exposure to Ach. In the wild type MAs the relaxation to the highest concentration of Ach (59.2 ± 5.6%) was comparable to that observed in the 2 month old mice. By contrast, the vessels from age-matched Gla null mice were nearly devoid of Ach-mediated dilatation (1.5 ± 5.8%, $p<0.001$) (Figure 3 - 2B).

Sodium nitroprusside (SNP) -mediated relaxation in endothelium intact mesenteric arteries.

The difference in Ach dependent relaxation could be secondary to a functional defect in either the endothelium or smooth muscle cells. To determine whether the responsiveness of the smooth muscle layer to nitric oxide is different between the wild type and Gla null vessels, sodium nitroprusside (SNP), a nitric oxide donor, was added at increasing concentrations. SNP induced an endothelium-independent vasodilatation in both wild type and knockout MAs. In 2 month old arteries, the maximum relaxation to SNP in wild type mouse MA (78.2 ± 2.2%) was not statistically different from Gla null mouse MA (84.2 ± 5.4%) (Figure 3 - 3A). The maximum relaxation observed in 8 month old MA was also no different between wild type (80.5 ± 5.0%) and Gla null (69.6 ± 4.3%) mice. However, the observed SNP responsiveness in vessels from the 8 month old mice revealed a greater sensitivity at lower concentrations of SNP (10^{-7} to 10^{-6} mol/L) in wild type compared to null background (Figure 3 - 3B).

Acetylcholine- and sodium nitroprusside- mediated dilation in endothelium-denuded mesenteric arteries.

It was next determined whether the attenuation in Ach-mediated relaxation observed in the Gla null mice was endothelium-dependent. The endothelium of the MA vessels was removed before

determining the Ach and SNP dose responses. As expected, denuding the MA endothelium inhibited any measurable vasodilatation in response to Ach in vessels from either wild type or Gla null mice (Figure 3 - 4A). SNP induced a concentration-dependent vasodilatation in both groups, and the maximum relaxation did not differ between wild type (75.9 ± 3.2%) and null (74.4 ± 5.7%) mice (Figure 3 - 4B).

Decreased eNOS homodimers and monomers in the mesenteric arteries from Gla null mice.

The basis for the decrease in NO bioavailability was next evaluated. The dimerization of eNOS is required for catalytic activity and NO production (28). Two forms of eNOS, monomers and homodimers, can be measured by polyacrylamide gel electrophoresis under reducing or non-reducing conditions. A decrease in both eNOS dimers and monomers was observed in the null MAs compared to the wild type MAs from 8 month old mice (Figure 3 - 5A). This difference was confirmed with repeated measurements (Figure 3 - 5B). The observed 53% decrease in homodimer expression from the knockout mouse MA compared to wild type MA (eNOS to actin ratios of 1.39 ± 0.08 versus 0.66 ± 0.12 in wild type versus Gla knockout) was statistically significant.

Serine1179 and threonine495 phosphorylation in the mesenteric arteries

eNOS phosphorylation at Ser-1179 in MA was evaluated with an anti-bovine Ser-1179 antibody reacting crossly with mouse eNOS phospho-Ser-1179. Phosphorylation of eNOS-Ser-1179 was not observed in wild type or null MA extracts from 2 month old mice. However, phospho-Ser-1179 was readily observed in 8 month old wild type and Gla knockout mouse MA (Figure 3 - 6A). A modest decrement in phospho-Ser-1179 was observed in the Gla null compared to the wild type

MAs (-21 ± 0.67%, p=0.0343) consistent with the down-regulation of eNOS activity (Figure 3 - 6B). In contrast to this modest difference, the phosphorylation of eNOS at Thr-495 was markedly enhanced in aged Gla null MA (Figure 3 - 7A). A 16 fold increase in eNOS phosho-Thr-495 was observed in 8 month old Gla null MA compared to wild type MA. The marked increase in Thr-495 phosphorylation is consistent with a suppression of eNOS activity (Figure 3 - 7B).

Increased reactive nitrogen species in the mesenteric artery from Gla null mice

Protein modification by nitration of tyrosine to 3-nitrotyrosine has been correlated with elevated oxidative stress and is specifically formed in the setting of eNOS uncoupling. The levels of protein-bound 3-nitrotyrosine in both wild type and Gla null mouse MAs were measured using a specific antibody for protein-bound 3-nitrotyrosine. 3-Nitrotyrosine levels increased in both mouse lines as a function of age (Figure 3 - 8A). However, protein-bound 3-nitrotyrosine content was significantly higher (~4 fold) in Gla null MAs compared to wild type MAs at each age studied (Figure 3 - 8B). These findings suggest that the Gla null phenotype not only results in lower NO formation but also induces eNOS uncoupling and increased reactive nitrogen species formation in MAs.

Discussion

Consistent with previous findings in other vascular beds (5, 23), we observed an age-dependent accumulation of Gb3 in the mesenteric arteries of Gla null but not wild type mice. We also measured a significant reduction in the vasodilatory capacity of MA in Gla deficient mice. These data suggest that the endothelial dysfunction associated with Gb3 accumulation is widespread

within the vasculature and includes the gastrointestinal microvessels. Similar to the previous findings in aortic rings (18), an age- and endothelial cell-dependent dysfunction in the MA of Gla null mice was observed as manifest by a loss of acetylcholine stimulated vasodilation. The ability of sodium nitroprusside to restore the vasodilation was consistent with a primary defect in nitric oxide bioavailability. However, despite the profound nature of this defect, no spontaneous GI phenotype was observed in Gla null mice of any age. Surprisingly, the age of onset of the MA abnormality was earlier, and the magnitude of the endothelial dysfunction appeared greater compared to previously studied macrovessels that included the aorta and carotid arteries.

eNOS dysfunction may result from either a decrease in nitric oxide bioavailability or uncoupling resulting in the formation of reactive nitrogen species. The active and functional form of eNOS is a dimer (20). We therefore measured the dimerization and expression of eNOS in the MA in Gla deficient and WT mice. In the older mice, both total eNOS expression and eNOS dimerization were decreased significantly, suggesting that uncoupling of eNOS in the mesenteric artery may, in part, contribute to the endothelial dysfunction. However, the measurement of eNOS monomers was also lower in Gla deficient mice and no difference in the eNOS monomer to homodimer ratio was evident between WT and Gla deficient mice at 2 or 8 months of age. In previous studies examining the effect of age on endothelial function in C57BL/6J mice, a significant increase in the eNOS monomer to dimer ratio in 24 months versus 3 months old mesenteric arteries was observed with no significant difference in total eNOS protein levels (27). Therefore, the observed reduction in eNOS protein and monomers in Gla deficient mice does not appear to represent a simple acceleration of normal age-related changes. Rather, the observed changes likely represent a specific consequence of Gla-deficiency such as the accumulation of endothelial cell globo series glycosphingolipids.

Nitric oxide production can lead to the formation of peroxynitrite ($ONOO^-$) in the setting of increased superoxide generation (9). Peroxynitrite is both an oxidant and nitrative agent that has been shown to induce cellular dysfunction and apoptosis (20). Possibly, the increased levels of this oxidant during sustained periods of oxidative stress or resulting from eNOS uncoupling caused a decrease in the expression of functional eNOS. To explore the possibility that some of the observed abnormalities were peroxynitrite mediated, the levels of 3-nitrotyrosine, an NO-dependent nitrosative stress marker in the MA was measured. 3-Nitrotyrosine was significantly elevated in the mesenteric artery from Gla knockout mice at 2 months of age, and the levels of 3-nitrotyrosine were further elevated in the older Gla null mice, consistent with the early onset and a progressive increase in eNOS uncoupling in the Fabry mesenteric arteries.

To further characterize the altered eNOS regulation in Gla-deficient mice, post-transcriptional modifications to the eNOS protein were also evaluated. The phosphorylation of eNOS at the Ser-1179 and Thr-495 residues was studied. In general, phosphorylated Ser-1179 activates eNOS, and phosphorylated Thr-495 inhibits eNOS catalytic activity (1, 25), and at least four protein kinases, Akt, PKA, PKC, and AMPK, are known to target eNOS (16). Phosphorylation or dephosphorylation of Ser-1179 and Thr-495 potentially could be regulated reciprocally or independently by those kinases**.** PKC signaling is reported to result in the simultaneous phosphorylation and dephosphorylation of eNOS Ser-1179 and Thr-495 respectively (16). In addition, the phosphorylation state of Thr-495 is inversely associated with eNOS activation and NO production (8, 11, 16). Previous studies examining the function of mutant Thr-495 and Ser-1179 cells have suggested that the ratio of phosphorylated to dephosphorylated Thr-495 may act as an intrinsic switch for determining whether eNOS generates nitric oxide or superoxide anion

(14). Therefore, we measured phosphorylation of eNOS at Thr-495 in the mesenteric artery to evaluate whether this site may be specifically altered in Gla null mice.

Compared to age-matched WT mice, eNOS phosphorylation of Thr-495 was highly increased in Gla deficient mice in the older group, suggesting that phosphorylated Thr-495 may promote eNOS dysregulation in older Gla null mice. Although we did not observe elevated phosphorylation of Thr-495 at 2 months of age, we did observe evidence of elevated 3-nitrotyrosine at this younger age. These data are consistent with the interpretation that the modest early onset phenotype of endothelial dysfunction is linked to nitric oxide uncoupling through a mechanism that is independent of Thr-495 phosphorylation. It is possible, therefore, that the more profound endothelial dysfunction present at 8 months is the result of the additional activation of the inhibitory eNOS Thr-495 site.

In addition to alterations in nitric oxide, EDHF is also an Ach-mediated and endothelium produced factor, and we cannot rule out the possibility of an EDHF defect in the setting of Gla deficiency. A recent study reported that Gb3 incubation of mouse aortae partially inhibited Ach-mediated dilatation (19). In this paper, a significant decrease in K_{Ca}^{2+} channel current, mRNA and protein expression was observed in both mouse aortic endothelial cells from Gla knockout mice and WT mouse aortic endothelial cells treated with Gb3. This study provided evidence that Gb3 accumulation may contribute to vasculopathy through direct effects on intermediate-conductance K_{Ca}^{2+} channel activity (19).

A growing body of evidence also suggests that the contribution of EDHF is at least as important as NO in terms of endothelium-dependent vascular relaxation in the microvasculature (4, 22). One could propose that a decrease in EDHF through K_{Ca}^{2+} channel blockade may contribute to the earlier onset and profound endothelial dysfunction observed in the MA in the present study. In

addition, pharmacologic blockade of the small and intermediate K_{Ca}^{2+} channels has been demonstrated to increase superoxide formation and enhance phospho-eNOS at Thr-495 without changes in the total eNOS protein levels (10). Thus, Gb3 accumulation may lead to an endothelial plasma membrane defect, which results in impaired or altered signaling of multiple endothelium-dependent relaxing factors including NO and EDHF. Further studies designed to identify the underlying molecular mechanisms responsible for the microvascular phenotype in this mouse model of Fabry disease will be necessary.

Acknowledgements

This manuscript was published in American Journal of Physiology – Gastrointestinal and Liver Physiology (12). This research was supported by National Institutes of Health grant 5R01DK055823-13 (to J.A.S.).

Figures

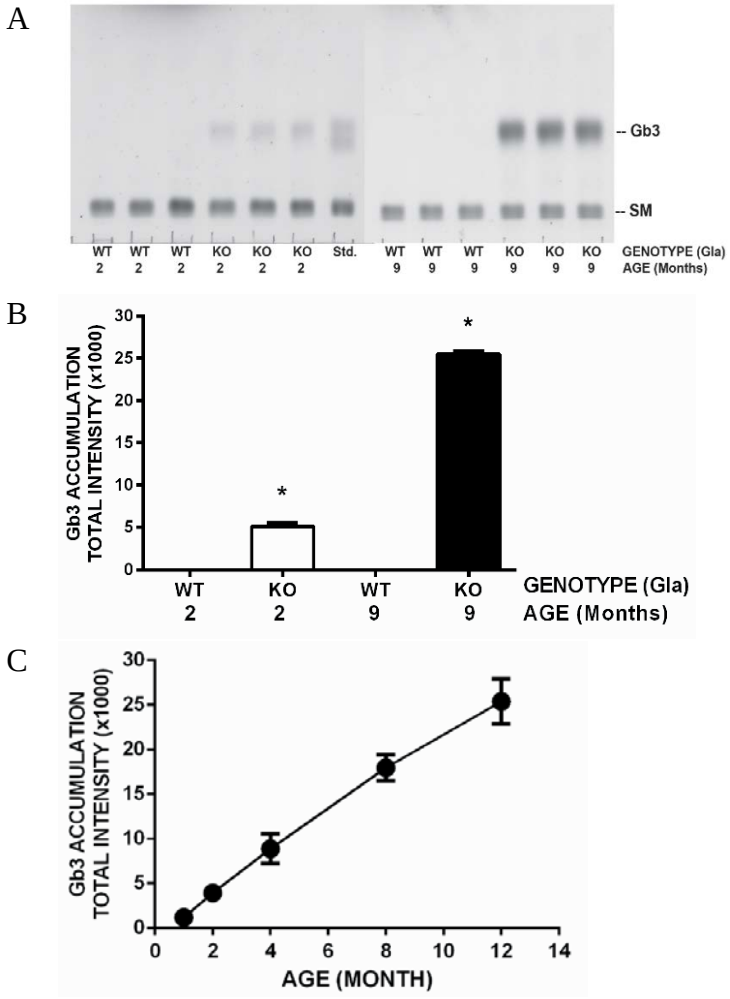

Figure 3 - 1. Age-dependent accumulation of Gb3 in the mesenteric arteries of WT and Gla knockout mice

Neutral glycosphingolipids were extracted and purified from MAs of 2 and 9 month old WT and Gla null mice. The neutral lipids, normalized to 50 nmol of total lipid phosphate, were spotted on high performance thin layer chromatography plates, and the bands were visualized by charring with 8 % cupric acetate in 8 % phosphoric acid solution. **A.** Representative separation of MA extracts from three separate mice per group. **B.** The combined densitometric analyses of the Gb3 levels from all mice. The data are pooled from three individual experiments with three mice per group (n=9 per group). **C.** Deposition of Gb3 in Fabry mouse MAs progressively accumulated from 1 to 12 months of age. Following lipid extraction, each sample containing 40 nmol of total phospholipid phosphate was spotted onto a high performance thin layer chromatography plate. Each data point represents age (months) and average of triplicate samples (n=3). Abbreviations include: Gb3, globotriaosylceramide; SM, sphingomyelin; and Std, internal standard. $P < 0.0001$.

A

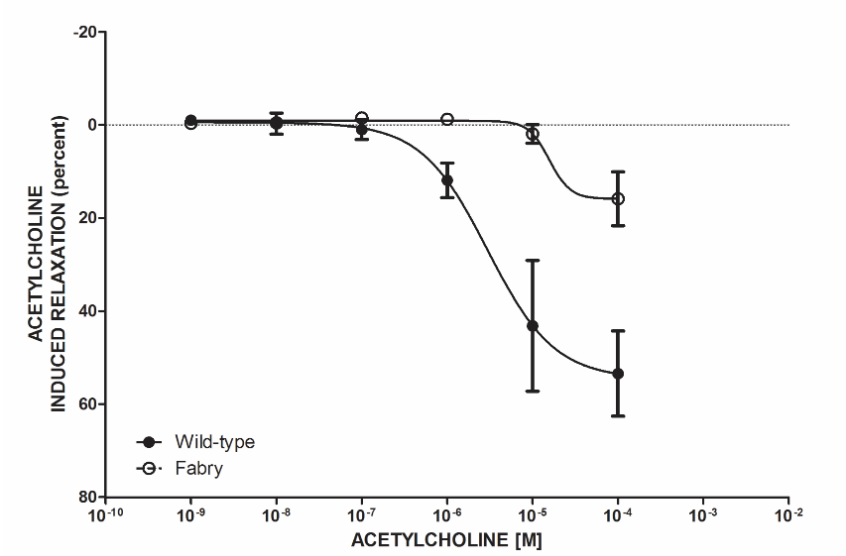

B

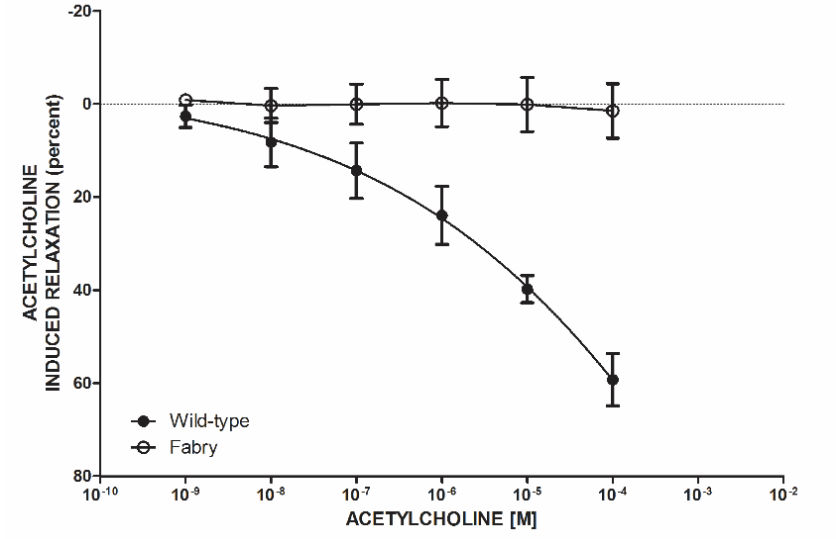

Figure 3 - 2. Acetylcholine (Ach)-mediated endothelium-dependent vasodilatation in the mesenteric arteries from WT and Gla knockout mice

All vessels (n=4 per group) were pre-contracted with 10^{-5} M of NE. **A.** Percent relaxation in endothelium-intact mesenteric artery from 2 month old mice. **B.** Percent relaxation in endothelium-intact mesenteric artery from 8 month old mice. The data are expressed as the percentage of changes in lumen diameter relative to baseline. ** = $p<0.01$, and *** = $p<0.001$ compared to WT mice by two-way ANOVA followed by Bonferroni post-hoc analysis.

A

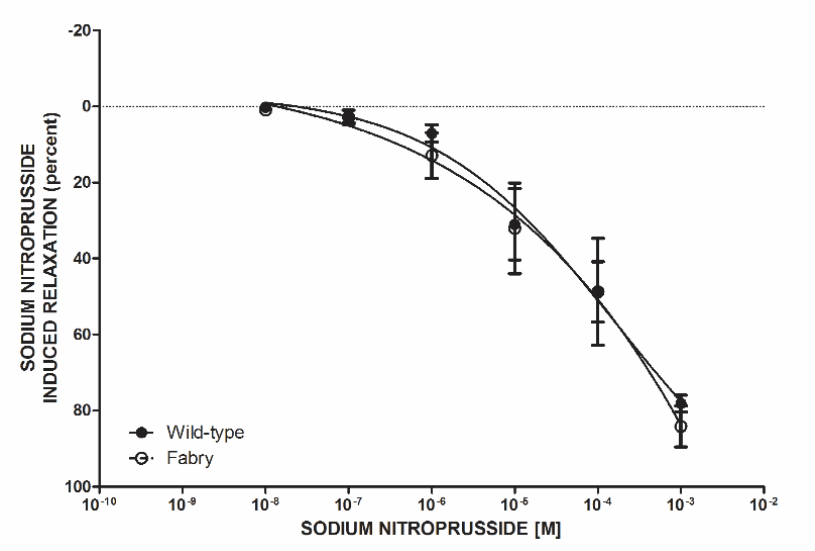

B

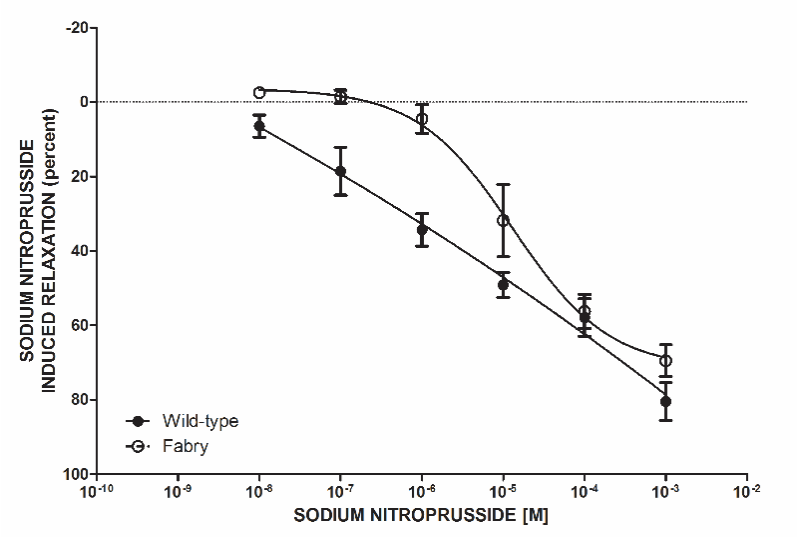

Figure 3 - 3. Sodium nitroprusside (SNP)-mediated, endothelium-independent vasodilatation in the mesenteric arteries from WT and Gla knockout mice

All vessels (n=4 per group) were pre-contracted with 10^{-5} M of NE. **A.** Percent relaxation to SNP in endothelium-intact mesenteric arteries from 2 month old mice. **B.** Percent relaxation to SNP in endothelium-intact mesenteric arteries from 8 month old mice. The data are expressed as the percent change in lumen diameter relative to baseline. * = $p<0.05$, and *** = $p<0.001$ compared to WT artery by two-way ANOVA followed by Bonferroni post-hoc analysis.

A

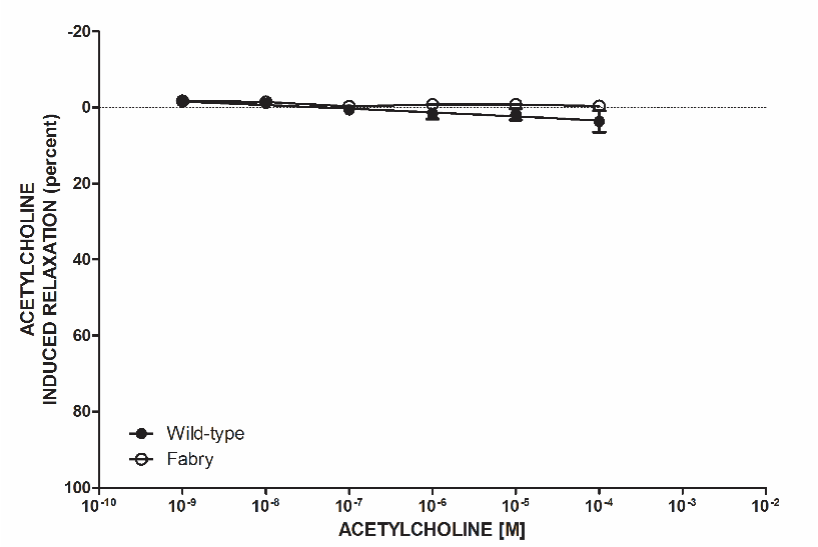

B

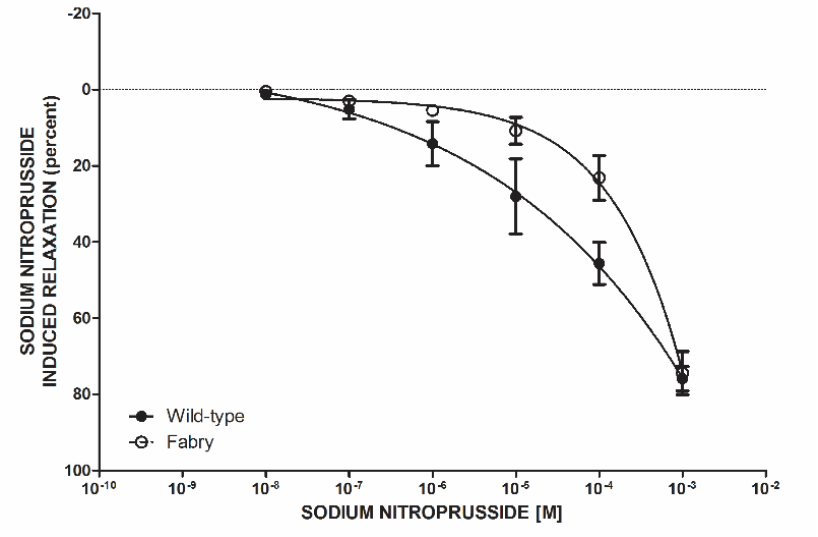

Figure 3 - 4. Acetylcholine (Ach)- and sodium nitroprusside (SNP)-mediated vasodilatation in endothelium-denuded mesenteric arteries from WT and Gla knockout mice

All vessels (n=4 per group) were pre-contracted with 10^{-5} M of NE. **A.** Relaxation response as a function of Ach concentration in endothelium-denuded mesenteric arteries from 8 month old mice. **B.** Relaxation response as a function of SNP concentration in endothelium-denuded mesenteric arteries from 8 month old mice. The data are expressed as the percentage change in lumen diameter relative to baseline. ** = $p<0.01$ compared to WT by two-way ANOVA followed by Bonferroni post-hoc analysis.

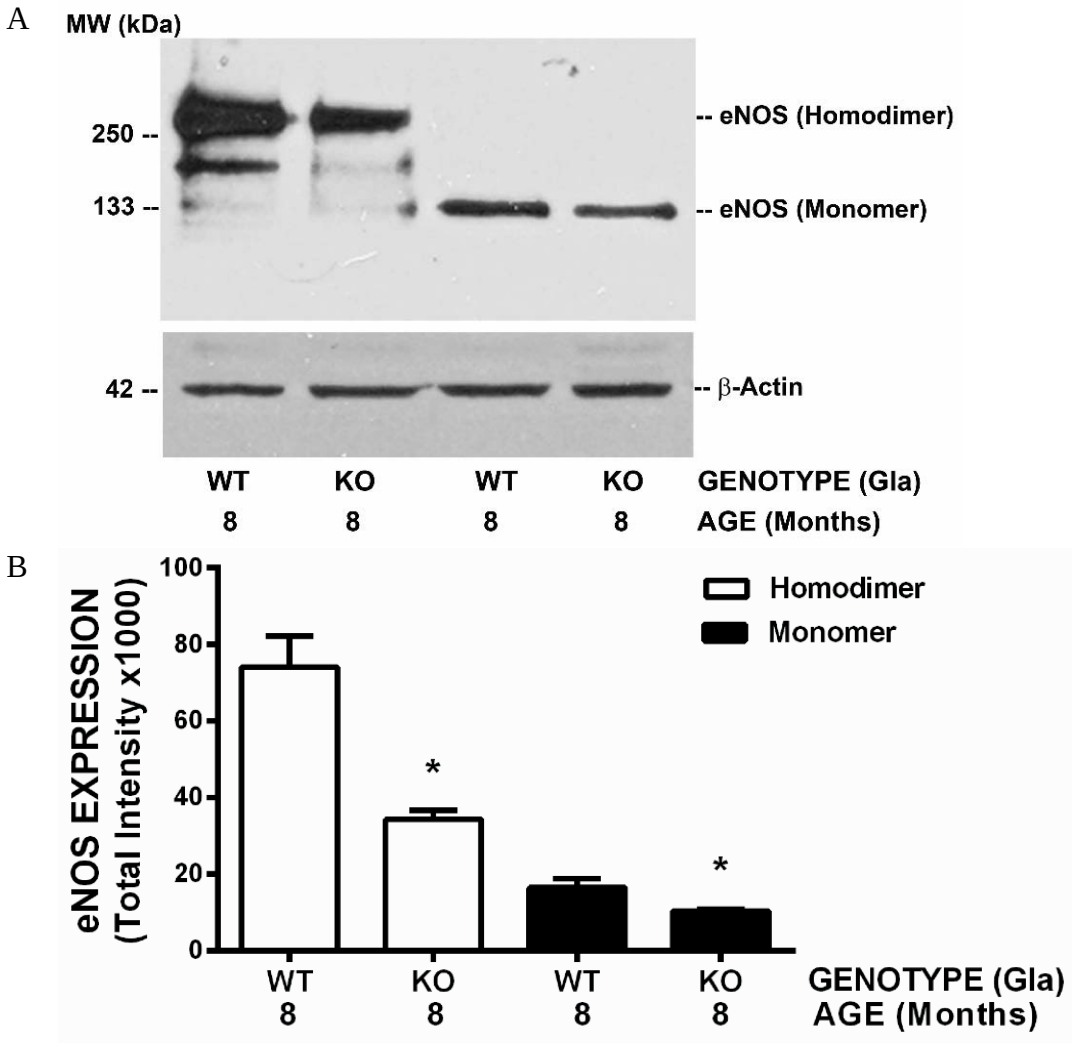

Figure 3 - 5. eNOS levels in the mesenteric arteries of 8 month old WT and Gla null mice

Mouse MA lysates equivalent to 50 µg of total lysate protein were analyzed by Western blot using a mouse anti-human eNOS antibody as an immuno-probe. **A.** A representative immunoblot for comparison of eNOS expression in the MAs of wild type (WT) and Gla knockout (KO) mice at 8 months of age (upper panel). The eNOS homodimer was only detected under non-reducing condition (lanes 1 and 2). Monomeric eNOS was probed under denaturing conditions using 1% 2-mercaptoethanol (lanes 3 and 4). β-actin was also probed an internal loading control (lower panel). **B.** Quantification of the MA monomeric and dimeric eNOS from 8 month old WT and Gla null mice (n = 3 per group). The densitometric values represent the mean ± SE. $P < 0.05$.

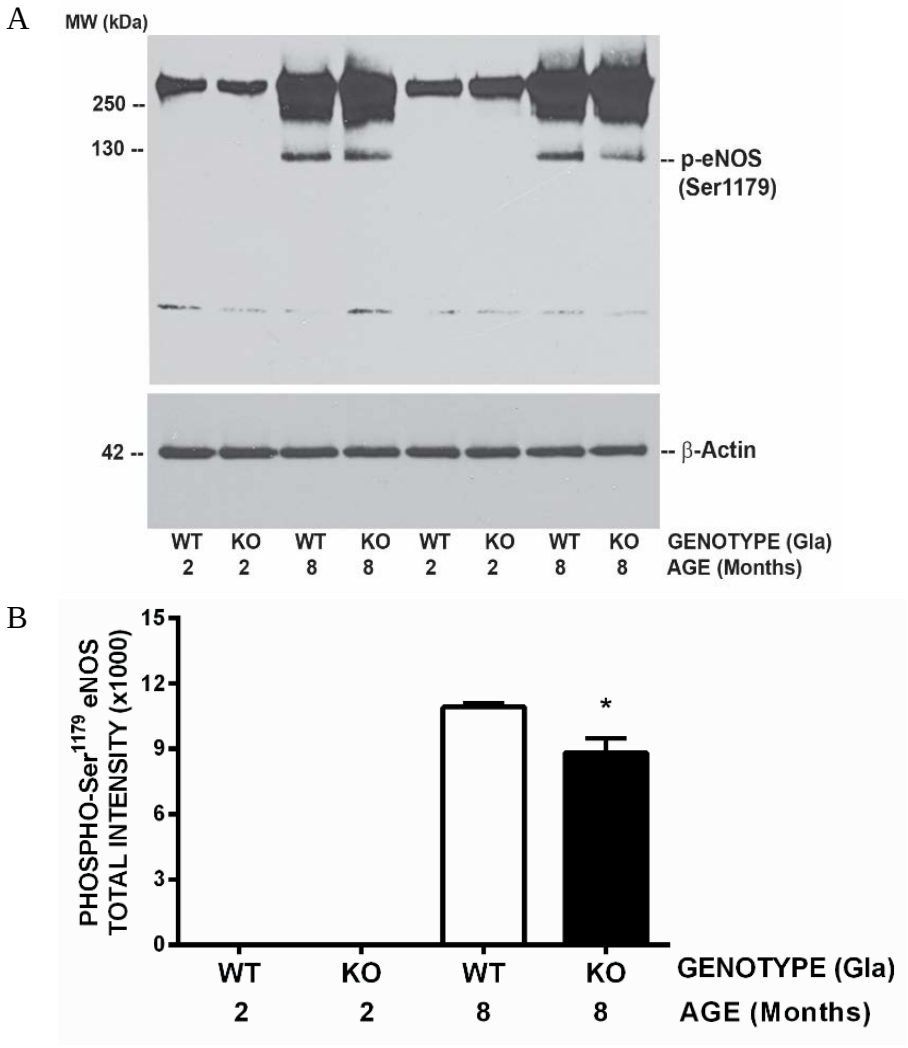

Figure 3 - 6. eNOS Ser-1179 phosphorylation in mesenteric arteries of 8 month old mice

Total MA lysates equal to 80 µg of total lysate protein were subjected to a gradient SDS-PAGE (6-12%) separation and immunoblotting. The phosphorylation of eNOS Ser-1179 in WT and Gla null mouse MA was determined with a rabbit anti-bovine eNOS-S1179 antibody under non-reducing conditions. **A.** Western blots from two sets of MAs dissected from WT and Gla null mice at the indicated ages (upper panel). β-actin was served as a loading control (lower panel). **B.** The combined densitometric data from four groups with 3 mice per group. The data were expressed as the mean ± SE. $P < 0.05$.

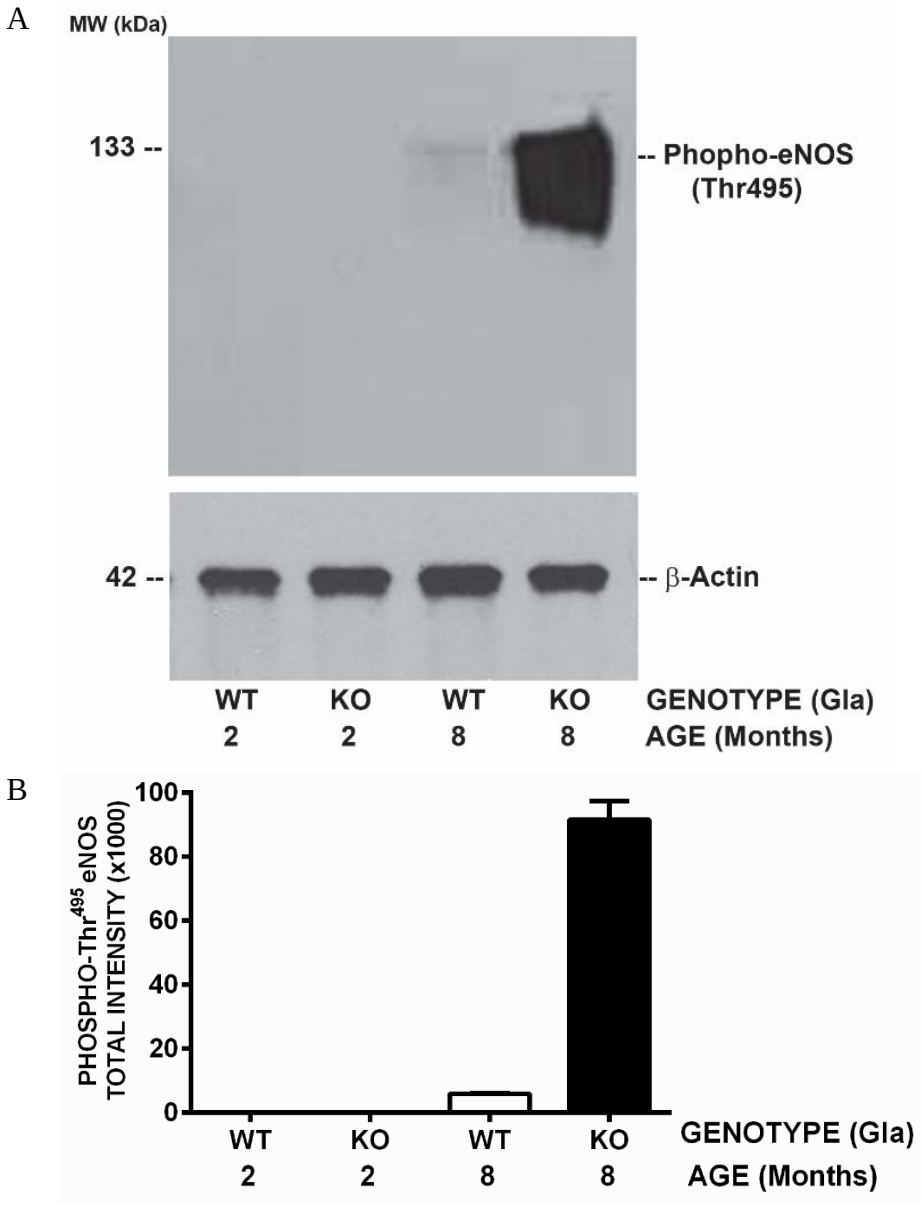

Figure 3 - 7. eNOS Thr-495 phosphorylation in the mesenteric arteries of WT and Gla knockout mice

A total of 60 μg lysate protein from each sample was used for immunoblotting of eNOS Thr-495 phosphorylation was measured under non-reducing conditions. **A.** A representative Western blot of phospho- Thr-495 (upper panel). β-actin was immunoblotted as an internal loading control (lower panel). **B.** Quantification of the immuno-signals of eNOS Thr-495 was performed by using ImageJ software. In the plotted graphic, each point represents the average value of three independent experiments. Data were shown as mean ± S.E. $p < 0.0001$.

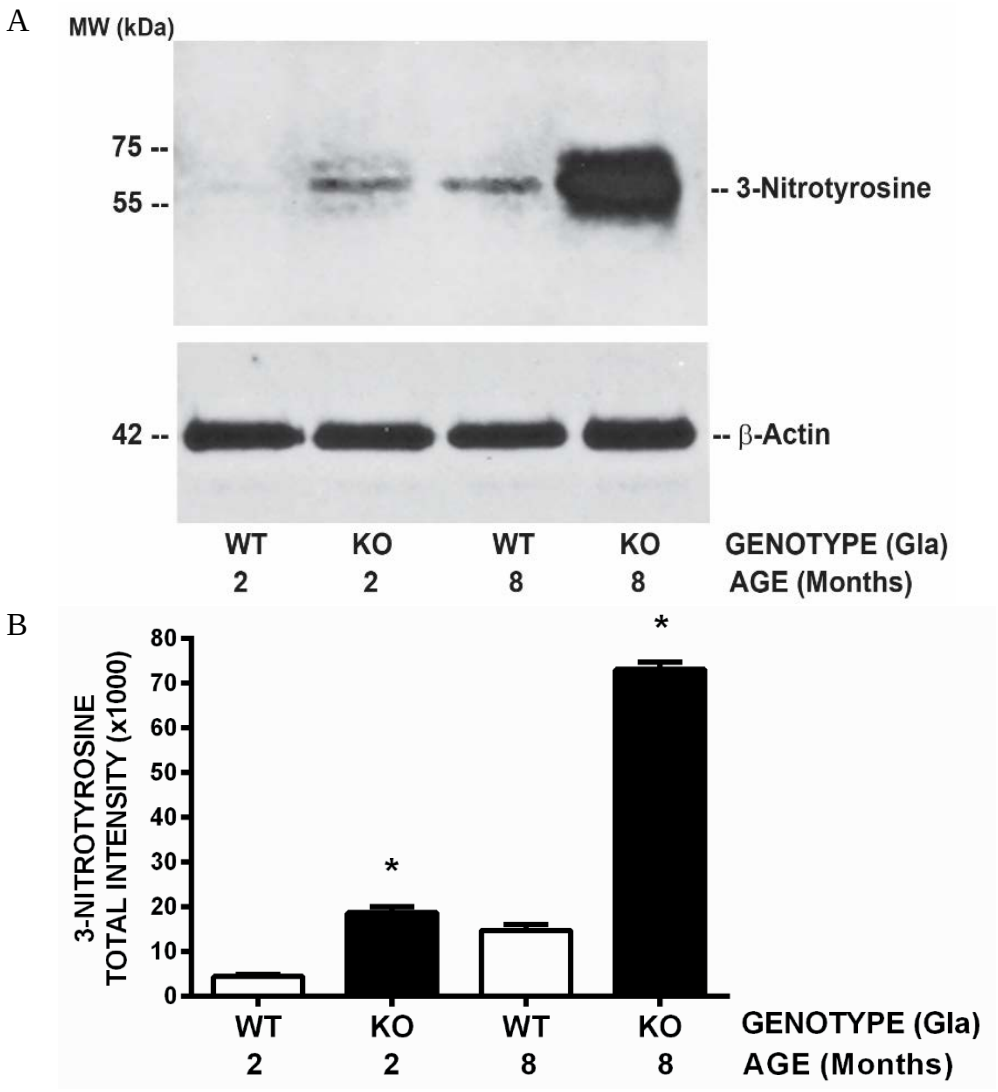

Figure 3 - 8. Expression of protein-bound 3-nitrotyrosine in the mesenteric arteries of WT and Gla null mice

A. Fifty µg of Triton X-100 soluble MA lysate protein was immunoblotted using a protein-bound nitrotyrosine specific monoclonal antibody. Reducing conditions with 1% 2-mercaptoethanol were employed. **B.** Densitometric comparison of WT and Gla null protein-bound 3-nitrotyrosine levels in the MAs in 2 and 8 month old mice. In the plotted graphic, each point represents the average value of three independent experiments. The data represent the mean ± SE. $p < 0.001$.

References

1. **Atochin DN and Huang PL.** Endothelial nitric oxide synthase transgenic models of endothelial dysfunction. *Pflugers Archiv : European journal of physiology* 460: 965-974, 2010.

2. **Bodary PF, Shen Y, Vargas FB, Bi X, Ostenso KA, Gu S, Shayman JA, and Eitzman DT.** Alpha-galactosidase A deficiency accelerates atherosclerosis in mice with apolipoprotein E deficiency. *Circulation* 111: 629-632, 2005.

3. **Brady RO, Gal AE, Bradley RM, Martensson E, Warshaw AL, and Laster L.** Enzymatic defect in Fabry's disease. Ceramide trihexosidase deficiency. *N Engl J Med* 276: 1163-1167, 1967.

4. **Brandes RP, Schmitz-Winnenthal FH, Feletou M, Godecke A, Huang PL, Vanhoutte PM, Fleming I, and Busse R.** An endothelium-derived hyperpolarizing factor distinct from NO and prostacyclin is a major endothelium-dependent vasodilator in resistance vessels of wild-type and endothelial NO synthase knockout mice. *Proceedings of the National Academy of Sciences of the United States of America* 97: 9747-9752, 2000.

5. **Eitzman DT, Bodary PF, Shen Y, Khairallah CG, Wild SR, Abe A, Shaffer-Hartman J, and Shayman JA.** Fabry disease in mice is associated with age-dependent susceptibility to vascular thrombosis. *J Am Soc Nephrol* 14: 298-302, 2003.

6. **Eng CM and Desnick RJ.** Molecular basis of Fabry disease: mutations and polymorphisms in the human alpha-galactosidase A gene. *Hum Mutat* 3: 103-111, 1994.

7. **Eng CM, Fletcher J, Wilcox WR, Waldek S, Scott CR, Sillence DO, Breunig F, Charrow J, Germain DP, Nicholls K, and Banikazemi M.** Fabry disease: baseline medical characteristics of a cohort of 1765 males and females in the Fabry Registry. *Journal of inherited metabolic disease* 30: 184-192, 2007.

8. **Fleming I, Fisslthaler B, Dimmeler S, Kemp BE, and Busse R.** Phosphorylation of Thr(495) regulates Ca(2+)/calmodulin-dependent endothelial nitric oxide synthase activity. *Circulation research* 88: E68-75, 2001.

9. **Forstermann U and Munzel T.** Endothelial nitric oxide synthase in vascular disease: from marvel to menace. *Circulation* 113: 1708-1714, 2006.

10. **Gaete PS, Lillo MA, Ardiles NM, Perez FR, and Figueroa XF.** Ca2+-activated K+ channels of small and intermediate conductance control eNOS activation through NAD(P)H oxidase. *Free radical biology & medicine* 52: 860-870, 2012.

11. **Harris MB, Ju H, Venema VJ, Liang H, Zou R, Michell BJ, Chen ZP, Kemp BE, and Venema RC.** Reciprocal phosphorylation and regulation of endothelial nitric-oxide

synthase in response to bradykinin stimulation. *The Journal of biological chemistry* 276: 16587-16591, 2001.

12. **Kang JJ, Shu L, Park JL, Shayman JA, and Bodary PF.** Endothelial nitric oxide synthase uncoupling and microvascular dysfunction in the mesentery of mice deficient in alpha-galactosidase A. *American journal of physiology Gastrointestinal and liver physiology* 306: G140-146, 2014.

13. **Kint JA.** Fabry's disease: alpha-galactosidase deficiency. *Science* 167: 1268-1269, 1970.

14. **Lin MI, Fulton D, Babbitt R, Fleming I, Busse R, Pritchard KA, Jr., and Sessa WC.** Phosphorylation of threonine 497 in endothelial nitric-oxide synthase coordinates the coupling of L-arginine metabolism to efficient nitric oxide production. *The Journal of biological chemistry* 278: 44719-44726, 2003.

15. **MacDermot KD, Holmes A, and Miners AH.** Anderson-Fabry disease: clinical manifestations and impact of disease in a cohort of 60 obligate carrier females. *Journal of medical genetics* 38: 769-775, 2001.

16. **Michell BJ, Chen Z, Tiganis T, Stapleton D, Katsis F, Power DA, Sim AT, and Kemp BE.** Coordinated control of endothelial nitric-oxide synthase phosphorylation by protein kinase C and the cAMP-dependent protein kinase. *The Journal of biological chemistry* 276: 17625-17628, 2001.

17. **Ohshima T, Murray GJ, Swaim WD, Longenecker G, Quirk JM, Cardarelli CO, Sugimoto Y, Pastan I, Gottesman MM, Brady RO, and Kulkarni AB.** alpha-Galactosidase A deficient mice: a model of Fabry disease. *Proceedings of the National Academy of Sciences of the United States of America* 94: 2540-2544, 1997.

18. **Park JL, Whitesall SE, D'Alecy LG, Shu L, and Shayman JA.** Vascular dysfunction in the alpha-galactosidase A-knockout mouse is an endothelial cell-, plasma membrane-based defect. *Clin Exp Pharmacol Physiol* 35: 1156-1163, 2008.

19. **Park S, Kim JA, Joo KY, Choi S, Choi EN, Shin JA, Han KH, Jung SC, and Suh SH.** Globotriaosylceramide leads to K(Ca)3.1 channel dysfunction: a new insight into endothelial dysfunction in Fabry disease. *Cardiovascular research* 89: 290-299, 2011.

20. **Rafikov R, Fonseca FV, Kumar S, Pardo D, Darragh C, Elms S, Fulton D, and Black SM.** eNOS activation and NO function: structural motifs responsible for the posttranslational control of endothelial nitric oxide synthase activity. *J Endocrinol* 210: 271-284, 2011.

21. **Ramaswami U, Whybra C, Parini R, Pintos-Morell G, Mehta A, Sunder-Plassmann G, Widmer U, and Beck M.** Clinical manifestations of Fabry disease in children: data from the Fabry Outcome Survey. *Acta Paediatr* 95: 86-92, 2006.

22. **Shimokawa H, Yasutake H, Fujii K, Owada MK, Nakaike R, Fukumoto Y, Takayanagi T, Nagao T, Egashira K, Fujishima M, and Takeshita A.** The importance of the hyperpolarizing mechanism increases as the vessel size decreases in endothelium-dependent relaxations in rat mesenteric circulation. *J Cardiovasc Pharmacol* 28: 703-711, 1996.

23. **Shu L, Park JL, Byun J, Pennathur S, Kollmeyer J, and Shayman JA.** Decreased nitric oxide bioavailability in a mouse model of Fabry disease. *J Am Soc Nephrol* 20: 1975-1985, 2009.

24. **Shu L and Shayman JA.** Caveolin-associated accumulation of globotriaosylceramide in the vascular endothelium of alpha-galactosidase A null mice. *The Journal of biological chemistry* 282: 20960-20967, 2007.

25. **Singh U, Devaraj S, Vasquez-Vivar J, and Jialal I.** C-reactive protein decreases endothelial nitric oxide synthase activity via uncoupling. *Journal of molecular and cellular cardiology* 43: 780-791, 2007.

26. **Whybra C, Kampmann C, Willers I, Davies J, Winchester B, Kriegsmann J, Bruhl K, Gal A, Bunge S, and Beck M.** Anderson-Fabry disease: clinical manifestations of disease in female heterozygotes. *Journal of inherited metabolic disease* 24: 715-724, 2001.

27. **Yang YM, Huang A, Kaley G, and Sun D.** eNOS uncoupling and endothelial dysfunction in aged vessels. *American journal of physiology Heart and circulatory physiology* 297: H1829-1836, 2009.

28. **Zou MH, Shi C, and Cohen RA.** Oxidation of the zinc-thiolate complex and uncoupling of endothelial nitric oxide synthase by peroxynitrite. *The Journal of clinical investigation* 109: 817-826, 2002.

CHAPTER 4

GLA deficiency promotes endothelial nitric oxide synthase dysregulation and robust VWF secretion from endothelial cells

Abstract

Fabry disease is caused by loss of activity of the lysosomal enzyme α-galactosidase A (GLA), leading to the accumulation of globo-series glycosphingolipids in vascular endothelial cells. However, the mechanism of the vasculopathy remains unclear. In this study the relationship between GLA deficiency and endothelial cell von Willebrand factor (VWF) secretion was explored. Plasma VWF was significantly higher at two months and further elevated with age in Gla-null compared to wild-type mice. The disruption of GLA by siRNA and CRISPR/Cas9 resulted in a three and five fold increase in VWF secretion, respectively, in EA.hy926 human endothelial cells. Decreased endothelial nitric oxide synthase (eNOS) activity was associated with the elevated VWF levels in both *in vitro* models of Fabry disease. Pharmacological approaches that increase NO bioavailability or decreasing reactive oxygen species completely normalized the elevated VWF secretion in GLA deficient cells. However, the abnormality was not readily reversed by recombinant human GLA or by the inhibition of glycosphingolipid synthesis with eliglustat. This study suggests that GLA deficiency may promote robust VWF secretion through eNOS dysregulation.

Introduction

Fabry disease is a rare and often devastating lysosomal disorder caused by mutations in the α-galactosidase A (*GLA*) gene resulting in a partial or complete absence of GLA activity (9). Fabry disease is X-linked, but heterozygous females may also develop clinically significant cardiovascular disease (28, 58). The deficiency in GLA causes a progressive deposition of one of its substrates, globotriaosylceramide (Gb3), primarily in vascular endothelial and smooth muscle cells (14, 44). Increased plasma levels of deacylated Gb3 (lyso-Gb3) are also present (1). The manifestations of Fabry disease occurring in childhood tend to be less severe and include angiokeratomas, neuropathic pain, hypohidrosis, and gastrointestinal symptoms (43). However, adult Fabry patients may develop life-threatening complications including stroke and renal failure (18).

Thrombotic events have been reported in Fabry patients (50, 52). In addition, accelerated clot formation is observed in studies of experimentally induced models of thrombosis in Gla knockout mice (13, 45). Although enzyme replacement therapy (ERT) has been shown to reduce stored Gb3, evidence from clinical studies suggest that cerebral vascular events continue to occur in Fabry patients with advanced disease treated with long-term ERT (2, 40, 57, 59). Endothelial cells are among the most affected cell type in Fabry disease (12), in part secondary to decreased nitric oxide (NO) bioavailability and endothelial nitric oxide synthase (eNOS) uncoupling as noted in Study 1. Thus, factors regulating interactions of platelets and leukocytes at the endothelial level may be affected in the setting of GLA deficiency. von Willebrand factor (VWF), stored in Weibel-Palade bodies (WPB) of endothelial cells, is a large adhesive glycoprotein that plays a pivotal role in platelet adhesion and subsequent thrombus formation, supporting normal hemostasis and

thrombosis (61). High levels of VWF are predictive of an increased risk of thrombotic cardiovascular diseases, including stroke and coronary heart disease (33, 53, 55). Although a prothrombotic profile and increased production of reactive oxygen species (ROS) have been documented in Fabry disease (10, 17, 44, 54), less attention has been paid to the direct effect of GLA deficiency on the endothelium-derived coagulation factor, VWF.

The purpose of this study was to examine the effects of GLA disruption on VWF secretion and its mechanistic link with NO bioavailability in endothelial cells. In addition, the *in vitro* endothelial cell model of GLA deficiency was exploited to evaluate the influence of treatment modalities to suppress the enhanced VWF secretion present in endothelial cells with GLA deficiency.

Methods

Mice

C57BL6/J mice were obtained from the Jackson Laboratory (Bar Harbor, ME). Gla null mice (129/SvJXC57BL/6) used in this study were bred from mice originally developed and provided by Drs. Ashok Kulkarni and Roscoe Brady (National Institutes of Health, Bethesda, MD) by replacement of α-galactosidase A (*Gla*) gene with a neomycin resistance sequence within a portion of the exon 3 and intron 4 region (37). These mice were back-crossed a minimum of six generations to the C57BL6/J strain. All mice were maintained in University of Michigan animal facility under standard specific pathogen-free conditions. All animal experiments were conducted according to the protocol of the Institutional Animal Care and Use Committee of the University of Michigan.

Small Interfering RNA (siRNA) Silencing

The EA.hy926 human endothelial cell line (#CRL-2922) was purchased from ATCC (Manassas, VA). The cells were maintained in complete growth medium consisting of Dulbecco's Modified Eagle Medium/F12, GlutaMAX (#ILT10565018, Life Technologies, Grand Island, NY), 10% fetal bovine serum, 100U/ml penicillin, and 100 µg/ml streptomycin. Anti-human siRNA oligonucleotides were purchased from AMS biotechnology (GLA: #SR301812; SCR: #SR30004, Cambridge, MA). Stock concentrations of the siRNAs were made at 20 µM in RNase-free reconstitution buffer consisting of 100mM potassium acetate and 30 mM HEPES (pH 7.5). Reconstituted siRNAs were heated at 94 ˚C for 2 min, and then cooled down to room temperature before storage at -20 ˚C. Transfection was performed as described before with minor modifications (49). Briefly, approximately 9 x 10^5 cells were seeded in 100 mm petri dishes one day before the transfection. The transfection mixture was prepared immediately before addition. Forty microliter of Lipofectamine RNAiMAX (#13778, Life Technologies) was diluted into 1 mL of Opti-MEM-I. The siRNA duplex, prepared in 1 mL of Opti-MEM-I, was added to diluted RNAiMAX reagent at 1:1 ratio and incubated at room temperature for 20 min to form the siRNA/transfection reagent complex. The culture medium was washed with 6 mL of Opti-MEM-I and replaced with 6 mL of Opti-MEM-I without serum and antibiotics. Two milliliter of the siRNA/transfection reagent complex with the siRNA duplex at a final concentration of 10 nM was then gently added into the cell culture dish. After 8 hours, the media was replaced with 10 mL of DMEM/F-12, GlutaMAX media containing 2% FBS without antibiotics. Two days after the first transfection, the cells were transfected again as described above. Transfected cells were harvested for the biotin switch assay and immunoblotting analyses 3 days after the second transfection. Cell culture supernatants were collected and spun down at 365 x g for 5 min to remove any cell debris. The samples were frozen

in liquid nitrogen and stored in -80 ˚C until analyzed. All the experiments were performed in cells at passage 3 or 4.

CRISPR/Cas9 plasmid generation and delivery

Single-stranded guide RNA was designed to target Exon 1 of *GLA*. Forward and reverse single-stranded oligonucleotides were annealed to generate a double-stranded oligonucleotide. The oligonucleotide was cloned into the GeneArt CRISPR nuclease vector (Thermo Fisher Scientific, Waltham, MA), which expresses the orange florescence protein (OFP) reporter. The vector was transformed into One Shot TOP10 *E. coli* cells (Thermo Fisher Scientific, Waltham, MA). Bacteria were grown on LB agar plates with ampicillin and incubated at 37 °C overnight. Clones were selected and grown in LB broth overnight. Plasmids were purified and sequenced with the U6 forward primer to verify the presence and proper orientation of double-stranded oligonucleotide.
EA.hy926 cells were plated at 600,000 cells per well on 6 well dishes. The following day, the cells were transfected with 2 µg of CRISPR plasmid DNA using Lipofectamine 3000 (Thermo Fisher Scientific, Waltham, MA). Cells were grown in DMEM-F12 GlutaMAX supplemented with 10% FBS and FACS sorted 24 hours after transfection. OFP positive cells were collected and plated onto 150 mm dishes at low density in normal growth conditions. Cells were allowed to grow for several days, and then cloning cylinders were used to isolate individual colonies. Colonies were expanded and DNA was extracted using the DNeasy Blood and Tissue Kit (Qiagen, Germantown, MD). To detect mutations, the region around the CRISPR-targeted region was PCR amplified and the surveyor nuclease assay (Integrated DNA Technologies, Coralville, IA) was performed according to the manufacturer's instructions. From 19 colonies isolated, 14 had a mutation in the CRISPR-targeted region. Western blot confirmed the absence of GLA expression in 4 of these

colonies. One of the GLA-negative cell lines was used for assays in this study. One wild type colony that was negative for a mutation in the surveyor assay was used as a wild type control in all assays.

The primers used were: CRISPR guide RNA primers: forward 5'-GCT AGC TGG CGA ATC CCA TG (GTTTT)-3', reverse 5'-CAT GGG ATT CGC CAG CTA GC (CGGTG)-3'; PCR primers: forward 5'-GCC CCT GAG GTT AAT CTT AAA AGC C-3', reverse: 5'-AGC TCT CCC TCG GGC TCA ACT GTT C-3'. Parentheses denote the sequence complementary to the 3' overhang sequence in the CRISPR nuclease vector.

VWF antigen measurement

Mouse plasma was withdrawn from wild type and GLA null mice at various ages via the retro-orbital sinus using heparinized capillary tubes (#22362566, Fisher Scientific, Pittsburgh, PA). Blood was centrifuged at 2,000 x g for 10 min at room temperature to obtain platelet-poor plasma. The plasma was recovered, immediately frozen in liquid nitrogen, and stored at -80 °C for VWF analysis. CRISPR cells or EA.hy926 cells transfected with control (siSCR) or GLA (siGLA) were incubated in DMEM/F-12, GlutaMAX media containing 2% FBS for 3 days. Cell culture supernatants were collected and centrifuged at 365 x g for 5 min at room temperature to remove cell debris. These supernatants were concentrated using Amicon ultrafiltration units (#UFC903096, Sigma, St. Louis, MO) with 30 kDa molecular weight cutoff membranes at 3,000 x g for 15 minutes. The samples were recovered, immediately frozen in liquid nitrogen, and stored at -80 °C for analysis of VWF. VWF antigen levels in the plasma and cell culture supernatants were determined using either a custom AlphaLISA (Perkin-Elmer) assay or enzyme-linked immunosorbent assay (ELISA) as described previously (11, 63). Briefly, polyclonal anti-human

VWF antibody (#A0082, DAKO, Glostrup, Denmark) was biotinylated using an NHS activated biotynylating reagent (Solulink, San Diego, CA). In addition, another set of antibody was conjugated to Alphalisa acceptor beads with sodium cyanoborohydride (Sigma, St Louis, MO). Plasma from WT and GLA null mice were thawed in 37°C water bath and diluted 1:160 in phosphate buffered saline pH 7.4. Twenty µL of each sample was plated in wells with 16 µL assay buffer containing biotinylated VWF antibody (0.5 nM) and VWF antibody-conjugated Alphalisa acceptor beads (10 µg/mL). After incubating for 60 minutes at room temperature, 24 µL of streptavidin coated donor beads (40 µg/mL) in assay buffer was added and incubated for an additional 30 minutes. The alpha signals were generated and detected on an EnSpire 2300 Multilabel Plate Reader (Perkin Elmer). VWF levels in the plasma were calculated using a dilution series of pooled platelet-poor plasma from 10 C57BL/6J mice as a reference (100%). For ELISA, U-shaped bottom Maxisorp 96-well plates (#449824, Nunc) were coated with 50 µL/well of rabbit-anti VWF (A0082, DAKO) in 50mM bicarbonate/carbonate buffer (1:500 at pH 9.8) at 4°C overnight. Next, the plates were washed 3 times with Tris-buffered saline containing 0.05% tween-20 (TBST) and blocked with 300µL/well of 5% BSA in TBST at room temperature. After washing, 50 µL of the analytes were added into the coated/blocked plates and incubated overnight at 4°C. After washing with TBST, the analytes were probed with horse radish peroxidase-conjugated VWF antibodies (1:4000 in 5% BSA in TBST) for 2 hours, followed by washes with TBST. Wells were developed (50 µL/well) with 3,3',5,5'-Tetramethylbenzidine Stabilized Chromogen solution (#SB02, ThermoFisher, Waltham, MA) to detect HRP activity. The reaction was stopped by adding 2M sulfuric acid (50µL/well). The absorbance of each well was measured at 450nm. VWF levels in the cell culture supernatants were calculated using a dilution series of pooled normal plasma with known VWF antigen levels (FACT, George King Bioscience) as standards. Results,

which were normalized for the number of cells in each sample, were expressed as fold changes with respect to siSCR or CR-WT control condition.

GLA Enzyme Activity Assay

The enzyme activity was measured as described previously with minor modification (3). CRISPR cells were trypsinized, and cell pellet was obtained by centrifugation at 365 x g for 5 min. Pelleted cells were washed twice with cold PBS and homogenized in lysis buffer consisting 3 mg/mL of sodium taurocholate, 28 mM citric acid, and 44 mM Na_2HPO_4. The homogenates were sonicated for 3 min on ice (9 periods of 10 sec each with intervals of 10 sec in between), and centrifuged at 20,000 x g for 30 min at 4°C to remove cell debris. Total protein level in each sample was quantified using bicinchoninic acid assay with bovine serum albumin as a standard. Three µg of protein in 20 µL of lysis buffer was added to 80 µL of assay buffer (5 mM *p*-Nitrophenyl α-D-galactopyranoside (PNPαGal), 28 mM citric acid, 44 mM Na_2HPO_4, and 5 mg/mL BSA with 117 mM *N*-acetyl-*D*-galactosamine) in a 96-well plate. *N*-acetyl-*D*-galactosamine was used as an inhibitor for α-*N*-acetylgalactosaminidase, another lysosomal enzyme that hydrolyses the PNPαGal substrate (32). GLA activity in the cell lysates were calculated using a dilution series of α-galactosidase (#G8507, Sigma) as a reference, which hydrolyzes 1.0 µmol of PNPαGal to p-nitrophenol and D-galactose per minute. The assay plate was incubated at 37°C for 1 hr. Stop solution (100 µL of 200 mM Na_2CO_3) was then added and fluorescence was read on a plate reader (SpectraMax 250, Molecular devices, Sunnyvale, CA, USA) at 400 nm.

eNOS activity measurements

Activity of endothelial nitric oxide synthase (eNOS) in EA.hy926 cell lysates was analyzed by using a NOS activity assay kit (#781001, Cayman Chemical, Ann Arbor, MI) according to the manufacturer's instructions. This assay measures the biochemical conversion of L-arginine to L-citrulline by NOS. Cells were harvested with 0.05% trypsin-EDTA and washed twice with PBS. Cell pellets were lysed in the provided homogenization buffer (final concentration 1 mM EDTA and 1 mM EGTA in 25 mM Tris-HCl (pH 7.4) buffer). After brief sonication, the samples were centrifuged at 21,130 x g for 5 minutes, and the supernatants transferred to new tubes. Cell lysates (5 µL) were incubated at room temperature for 3 hours with 1 µCi ^{3}[H]arginine (PerkinElmer), 100 nM calmodulin, and the provided reaction buffer (final concentration 1 mM NADPH, 600 µM $CaCl_2$, 25 mM Tris-HCl (pH 7.4), 3 µM tetrahydrobiopterin, 1 µM flavin adenine dinucleotide, and 1 µM flavin adenine mononucleotide in 50 µL). The reaction was stopped by adding 400 µL of 5 mM EDTA in 50 mM HEPES (pH 5.5) buffer. The provided kit resin was added to each sample to remove ^{3}[H]arginine. Radioactivity due to ^{3}[H]Citrulline radioactivity was measured as counts per minute (cpm) using a scintillation counter. NOS activity of each sample was calculated by subtracting background cpm from the cpm for each sample, and then normalizing to total protein in each 5 µL sample, determined by the bicinchoninic acid protein assay.

Cell treatments

One day before the second transfection, siRNA-transfected cells were incubated with vehicle (10 mM HEPES) or DETA-NONOate (50µM, #82120 Cayman, Ann Arbor, MI). The following day, the cells were treated with either vehicle or the NO donor in 2% FBS DMEM/F12, GlutaMAX media for 3 days after the second siRNA transfection to investigate the effects of exogenous NO on VWF secretion. CRISPR cells were treated as described above with vehicle (10 mM HEPES)

or DETA-NONOate (100 μM). Because the half-life of DETA-NONOate is 20 hours at 37°C (24), DETA-NONOate was re-added every 20 hours during the treatment for 3 days. For studies on the effects of endogenous NO on VWF secretion, vehicle (0.3% DMSO) or sepiapterin (300 μM) were added to confluent CRISPR cells over 3 days. In separate sets of experiments, 1H-[1,2,4]oxadiazolo[4,3-a]quinoxalin-1-one (ODQ, 5 μM) was added 1 hr before the addition of DETA-NONOate or sepiapterin to inhibit the activation of sGC by NO. For studies on human α-galactosidase A (α-Gal A), cells were seeded, and incubated with either vehicle (25 mM Tris and 150 mM NaCl, pH 7.5) or α-Gal A (10 ug/mL) from the following day for two days. After cell confluency was attained, the media was replaced with 2% serum containing media with one of the treatments or vehicle for additional three days. Either DMEM media as vehicle or eliglustat (200nM) was used and incubated as described above to study the effects of eliglustat on VWF secretion.

S-nitrosylation measurements

Levels of NSF S-nitrosylation were determined using a biotin switch assay as previously described (21). Briefly, EA.hy926 cells were washed with cold Dulbecco's Phosphate-Buffered Saline and lysed with HENS buffer (100 mM HEPES, 1 mM EDTA, 0.1 mM Neocuproine, 1% SDS, pH 8.0; Thermo Fisher, Waltham, MA). The lysates were sonicated using a probe sonicator (Branson sonifier 450) on ice for 30 seconds at output 2. Cell debris was removed by centrifugation at 10,000 x g for 10 min. Positive control samples were incubated with 200 μM of S-nitrosoglutathion (GSNO) for 30 min in dark. Excess GSNO was removed by 7K MWCO Zeba spin desalting column (#89890, Thermo Fisher, Waltham, MA) according to the manufacturer's instructions. Three hundred micrograms of proteins were subjected to the biotin switch assay. Free thiol

residues were first blocked with 20 mM of sulfhydryl-reactive compound S-methyl methanethiosulfonate (#64306, MMTS, Sigma-Aldrich, St. Louis, MO) for 20 min at 50 °C with vortexing every 5 min. Excess MMTS was removed by incubation in 5 mL of pre-chilled acetone at -20 °C for 20 min. The samples were pelleted by centrifugation at 3,000 x g for 10 min at 4 °C, and washed once with pre-chilled 70% acetone. The samples were resuspended in 240 µL of HENS buffer. S-nitrosylated cysteines were then selectively reduced by 1 mM of sodium ascorbate (#11140, Sigma-Aldrich, St. Louis, MO) and labeled with 30 µL of biotin (2.5 mg/mL in DMSO) N-[6-(biotinamido)hexyl]-3´-(2´-pyridyldithio) propionamide (#21341, biotin-HPDP, ThermoFisher, Waltham, MA) in the presence of 1 µM of CuCl (#AC208390250, Fisher Scientific) for two hours in the dark. Excess sodium ascorbate and unlabeled biotin were removed by acetone precipitation at -20 °C for 20 min. The samples were centrifuged at 5,000 x g for 10 min at 4°C, and washed once with pre-chilled 70% acetone. The samples were resuspended in 250 µL of HENS/10 buffer (HENS diluted 10-fold into H_2O containing 1% SDS), and 750 µL of neutralization buffer (25 mM HEPES, 100 mM NaCl, 1 mM EDTA, 0.5% Triton X-100, pH 7.5) was added. Twenty five microliters from each sample was saved for analysis of total protein "input". The residual was transferred to a tube containing 70 µL of pre-washed streptavidin immobilized on agarose beads and incubated overnight at 4°C with gentle rotation. The beads were centrifuged at 200 x g for 5 seconds, washed, and eluted in 30 µL HEN/10 containing 1% β-mercaptoethanol for 20 min for immunoblotting analyses.

Western blotting

The cell lysates were prepared as described above. Quantification of total protein in each sample was performed by a bicinchoninic acid assay with bovine serum albumin as a standard. Thirty µg

of each sample lysate was separated by SDS-PAGE using a 4-12% gradient gel. Proteins were transferred onto nitrocellulose membranes, and blocked in 5% nonfat dry milk in TBST for at least 1 hr. The membranes then were incubated overnight at 4°C with primary antibodies used at 1:1,000 dilution; NSF (#2145, cell signaling, Danvers, MA), GLA (#LS-B8027, LS Bio, Seattle, WA), GAPDH (#MAB374, EMD Millipore, Billerica, MA), eNOS (#ab76198, Abcam, Cambridge, MA), and TRX-1 (#2429, Cell Signaling, Danvers, MA). After washing with TBST, the membrane was incubated with appropriate secondary antibody in 5% milk in TBST. The immunoreactive bands were detected with ECL western blotting substrate (#32106, Thermo Fisher, Waltham, MA), and quantified by densitometric scanning using ImageJ software.

Quantitative RT-PCR

WT and GLA null mice were perfused with 3 mL of cold PBS using a 25-gauge needle, inserted into the left ventricle, at a rate of 1 mL/min. Total RNA was extracted from lung and liver tissues with RNeasy Protect Mini Kit (#74124, Qiagen). Total cellular RNA was isolated using RNeasy Plus Mini Kit (#74134, Qiagen). Reverse transcription was performed using High Capacity cDNA Reverse Transcription Kit (#4368814, Applied Biosystems). Power SYBR Green PCR Master Mix (#4367659, Applied Biosystems) and cDNA were transferred to a 48-well plate, and real-time PCR was performed with a StepOne Real-Time PCR System instrument. Data were normalized to GAPDH or TATA binding protein, and the results were expressed relative to the WT mice or CR-WT. The primers used were: mouse VWF primers: forward 5'-GGG TGA CCA AAG CAT CTC CA-3', reverse 5'-CAT CGA TTC TGG CCG CAA AG-3'; mouse GAPDH primers: forward 5'-GAC CAC AGT CCA TGC CAT CA-3', reverse: 5'-ACT TGG CAG GTT TCT CCA GG-3'; human VWF primers: forward 5'-TTG ACG GGG AGG TGA ATG TG-3', reverse 5'-ATG TCT

GCT TCA GGA CCA CG-3'; human GAPDH: forward 5'-TTG TTG CCA TCA ATG ACC CCT-3', reverse 5'-GAT CTC GCT CCT GGA AGA TGG-3'; human TBP: forward 5'-GCC GCC GGC TGT TTA ACT-3', reverse 5'-ACG CCA AGA AAC AGT GAT GCT-3'.

Statistical analysis

GraphPad Prism software (Graphpad Software Inc., La Jolla, CA) was used for statistical analysis. The data were presented as mean ± SEM. Results were analyzed using the unpaired t-test for comparison of two groups. Statistical significance was set at $p<0.05$.

Results

Endothelial activation in Gla null mice

In previous studies Gla deficiency was demonstrated to accelerate vascular complications in mice including models of atherosclerosis on apoE null background and oxidant-induced arterial thrombosis (8, 13). Soluble vascular cell adhesion molecule-1 (sVCAM-1) and von Willebrand factor (VWF) were measured in plasma to assess whether endothelial inflammation was evident in young Fabry mice without experimental injury or other alteration. The serum levels of sVCAM-1 were not different between WT and Gla null mice at 2 months (Figure 4 - 1A). However, sVCAM-1 was significantly elevated in Gla deficient mice at 12 months compared to the younger age of the same genotype and their age-matched WT mice. Intriguingly, plasma VWF level was significantly higher in 2 month old Gla null mice compared to WT mice (Figure 4 - 1B). Plasma VWF levels from Gla null mice at 5 and 17 months of age, but not WT mice, were significantly elevated in comparison with the same genotype at 2 months. It was previously observed that

microvascular dysfunction and eNOS uncoupling were evident at 2 months and exacerbated with age in these mice (23). These data indicated that Gla deficiency resulted in an age-dependent endothelial dysfunction and elevated VWF secretion into the circulation. Further experiments were next performed to probe the mechanism for the enhanced secretion of VWF in the setting of GLA deficiency.

VWF gene expression

VWF mRNA levels were next measured. In mouse, the lung expresses the highest level of VWF mRNA, and therefore, is the primary organ responsible for the circulating VWF antigen level (62). Lung homogenates from WT and Gla null mice were analyzed for VWF gene expression. No difference in VWF mRNA levels was observed between the Gla deficient mice and the WT mice by qRT-PCR analyses (Figure 4 - 2A, WT vs GLA null; 1.02 ± 0.12 vs 0.97 ± 0.15 arbitrary unit). In addition, VWF mRNA levels did not differ in the liver homogenates between WT and GLA null mice (Figure 4 - 2B, WT vs GLA null; 1.00 ± 0.24 vs 1.08 ± 0.17 arbitrary unit). Thus, these results suggested that the elevated VWF level in Gla deficient mice was not due to increased VWF production from these sites.

Elevated VWF secretion in cells with GLA knockdown

An established *in vitro* model of Fabry disease was employed to explore whether GLA deficiency directly promotes VWF secretion from the endothelial cells (49). We first determined the expression of VWF in the EA.hy926 human endothelial cell line. A positive linear relationship was confirmed between VWF level and the number of cells (r^2 = 0.9242). The effect of GLA

disruption on WPB exocytosis was next characterized by RNA interference in these cells. After GLA siRNA treatment, GLA expression was decreased to a level not detected by western blotting while GAPDH expression was unaffected (Figure 4 - 3A). Cells were then incubated in 2% serum media under control siRNA (siSCR) or GLA siRNA (siGLA) conditions for three days to measure the amount of VWF released into the media. An almost 3-fold increase in the VWF level was observed by ELISA in the supernatants from siGLA compared with that of siSCR (Figure 4 - 3B). These data demonstrate that the loss of GLA directly results in the release of VWF from endothelial cells consistent with the increased plasma VWF levels observed in knockout mice.

Decreased eNOS activity and inhibition of VWF secretion with NO provision in GLA knockdown cells

Because GLA deficiency results in less NO production from this endothelial cell line due to lower eNOS activity (49), studies were performed to assess whether the elevated VWF secretion was associated with decreased NO bioavailability. Consistent with previous reports (47, 49), eNOS activity was significantly lower in siGLA than siSCR (Figure 4 - 4A). Because NO inhibits VWF secretion (27), siRNA-treated cells were incubated in the presence or absence of an exogenous NO donor, DETA-NONOate. In contrast to control conditions, the supplemental provision of NO (50 μM) resulted in a 35% reduction in VWF secretion in siGLA cells (Figure 4 - 4B).

Elevated VWF secretion in a permanent GLA deficient cell line by CRISPR/Cas9

A previous study reported that VWF secretion is dependent on cell density as well as the duration of cell culture (26). Because siRNA treatments do not persist for more than three days, and the

efficiency of the transfection is dependent on cell seeding density (data not shown), a permanent GLA deficient cell line was generated to avoid confounding factors such as confluency and a transient effect of the siRNA interference. GLA activity level was first measured in this cell line. As expected, the enzyme activity was not detectable in CRISPR GLA cells (CR-GLA) as compared to that from CRISPR WT cells (CR-WT) (Figure 4 - 5A). Next, these cells were grown until confluent, and replaced with 2% serum media. VWF levels were measured in the media of CR-WT and CR-GLA over a more extended period of 96 hrs. VWF levels, measured by ELISA, were higher at the 12 hr time point and significantly elevated at the 24 hr time point (Figure 4 - 5B). In additional sets of experiments, an approximately 4.7-fold increase in the level of VWF was observed in the media from CR-GLA compared to CR-WT cells at 48 hr and 72 hr time points (Figure 4 - 5C). It was next tested whether exogenous NO inhibits VWF secretion in CRISPR cells. Compared to the siRNA treated cells, CRISPR cells were viable at higher concentrations of exogenous NO (data not shown). Provision of 100 μM of NO donor for 3 days significantly decreased VWF secretion from both CR-WT and CR-GLA cells (Figure 4 - 5D). Surprisingly, VWF level from CR-GLA was completely normalized to the level seen in CR-WT vehicle treated cells with 100 μM of NO.

VWF mRNA level was slightly, but significantly increased in CR-GLA in comparison with CR-WT by qRT-PCR analysis (Figure 4 - 6A, CR-WT vs CR-GLA; 1.00 ± 0.02 vs 1.23 ± 0.14 arbitrary unit, $p<0.01$). The levels of IL-8, another component of WPBs, were also measured to confirm that elevated VWF secretion in GLA deficiency was due to enhanced WPB exocytosis. The IL-8 concentration was significantly higher in the media of CR-GLA when compared with that of CR-WT (Figure 4 - 6B, CR-WT vs CR-GLA; 544.8 ± 15.2 vs 1086.7 ± 23.5 pg/mL) consistent with increased WPB exocytosis. Together, these data reinforced the prior observations that GLA

deficiency promotes VWF secretion and exogenous NO inhibits the release. Since CRISPR cells were more stable for pharmacologic studies in comparison with the siRNA-treated cells, this cell line was used in subsequent studies.

Sepiapterin treatment in CR-GLA

eNOS protein expression in CR-GLA and CR-WT cells was next analyzed. Consistent with the previous finding in cultured primary aortic endothelial cells from Gla null mice (47), a greater than 50% reduction in the eNOS expression of CR-GLA was observed compared with that of CR-WT (Figure 4 - 7A). Previously, a robust elevation of 3-nitrotyrosine was observed in GLA deficient cells, a marker of reactive nitrogen species produced in the presence of eNOS uncoupling (49). An attempt was made to "recouple" eNOS activity with sepiapterin treatment in CR-GLA cells. The activity of eNOS from CR-WT and CR-GLA was increased with sepiapterin in a dose-dependent manner (Figure 4 - 7B). However, eNOS activity of CR-GLA was approximately 50% lower than that of CR-WT at any given doses of sepiapterin. Nevertheless, eNOS activity of CR-GLA was 2.5-fold higher with 300 μM sepiapterin than that of CR-WT vehicle condition (Figure 4 - 7B). Because exogenous NO treatment inhibited VWF secretion (Figure 4 - 5D), it was next examined whether increased endogenous NO production resulting from activating eNOS with sepiapterin decreases VWF exocytosis. Three days of sepiapterin (300 μM) treatment reduced VWF secretion from CR-GLA to the level of CR-WT control conditions (Figure 4 - 7C), similar to the effect of the exogenous NO donor. Nevertheless, the level of VWF with sepiapterin treatment in CR-GLA remained significantly higher than that of CR-WT, presumably due to the lower level of eNOS activity compared to CR-WT with 300 μM sepiapterin (Figure 4 - 7D). Endothelial-derived NO regulates vascular function, in part, through a soluble guanylate cyclase (sGC) and cyclic

guanosine monophosphate (cGMP) signaling pathway (39). However, the inhibition of sGC by a specific irreversible inhibitor, ODQ, did not modify the effects of the NO donor and sepiapterin on VWF release in CR-WT and CR-GLA cells (Figure 4 - 8). Together, these data indicate that both exogenous and endogenous NO repletion inhibit increased VWF release via a sGC/cGMP-independent signaling pathway in the setting of GLA deficiency.

Changes in SNO-NSF level in siGLA and CR-GLA cells

A previous study from Matsushita and colleagues reported that NO inhibits WPB exocytosis through NSF S-nitrosylation (SNO-NSF) (30). In addition to NO, thioredoxin-1 is known to regulate VWF secretion by denitrosylating SNO-NSF in endothelial cells (19). Having characterized that GLA deficiency resulted in decreased NO production and increased VWF secretion (Figures 4 - 4, 5, and 7), it was next determined whether elevated VWF secretion is associated with decreased level of SNO-NSF in the setting of GLA deficiency. The siRNA-treated and the CRISPR cells were subjected to a biotin switch assay. Immunoblotting analyses of isolated biotin-labeled proteins showed approximately 75% higher level of SNO-NSF in siGLA compared to siSCR cells (Figure 4 - 9A). In addition, a 12% lower level of TRX-1 was associated with increased SNO-NSF in the siGLA compared to siSCR cells (Figure 4 -9B). Consistent with the findings in siRNA-treated cells, CR-GLA had approximately 50% higher and 24% lower levels of SNO-NSF and TRX-1, respectively, than those in CR-WT cells (Figure 4 - 9C and 9D). Together, these data showed that GLA deficiency resulted in increased SNO-NSF level and decreased TRX-1 level in the endothelial cells.

Antioxidant treatments in CR-GLA cells

Decreased eNOS expression, reduced enzymatic activity, and deactivation of NO by reactive oxygen species can decrease NO bioavailability. Based on the previous finding that GLA deficiency elevated reactive oxygen species (44), it was evaluated whether decreasing ROS could lower VWF levels. CR-WT and CR-GLA cells were grown to confluence in the presence of ebselen (10 μM) or TEMPOL (1mM), glutathione peroxidase-1 and superoxide dismutase mimetics, respectively. After cell confluency was attained, the media was replaced with 2% serum containing media with one of the treatments or vehicle. The ebselen treatment for 3 days significantly reduced VWF secretion in both CR-WT and CR-GLA cells compared to their vehicle conditions (Figure 4 - 10A). In addition, the treatment in CR-GLA decreased VWF level below the level of CR-WT vehicle condition. Three days of TEMPOL incubation resulted in decreased VWF level in CR-GLA to a similar level of CR-WT vehicle condition (Figure 4 - 10B). However, the level of VWF in CR-GLA after the treatment remained significantly higher in comparison with CR-WT with TEMPOL incubation. These data are consistent with the interpretation that GLA deficiency elevates VWF secretion, in part, through increased production of ROS.

Recombinant human GLA and eliglustat treatment

Previously it was shown that 2 days of recombinant human GLA (α-Gal A) treatment lowered Gb3 in Gla null mouse aortic endothelial cells (46). When eNOS activity was examined in a subsequent study, the reduction of Gb3 by the potent glucosylceramide synthase inhibitor, eliglustat, failed to restore the decreased eNOS activity significantly in these cells (47). The effects of recombinant α-Gal A and eliglustat were evaluated to examine whether GLA deficiency *per se* or elevated globo-

series glycosphingolipids was the primary cause for the elevated secretion of VWF. The CRISPR cells were pre-treated with α-Gal A (10 μg/mL) or eliglustat (200 nM) for 2 days prior to becoming confluent. After the pre-treatment, fresh low serum media with α-Gal A or eliglustat was used and VWF accumulation in the media measured over 3 days. VWF levels were no different with or without the enzyme treatment in CR-WT cells (Figure 4 - 11A). In CR-GLA, exogenous α-Gal A reduced VWF secretion by 18% on average in CR-GLA compared to vehicle controls, but this did not reach statistical significance ($p=0.13$). On the other hand, eliglustat treatment slightly, but significantly increased VWF secretion from both CR-WT and CR-GLA cells (Figure 4 - 11B).

Discussion

In this study, we report that GLA deficiency decreases eNOS activity and promotes VWF secretion in a mouse model and two *in vitro models*, identifying a potential mechanism for the vascular involvement in Fabry disease. Furthermore, pharmacological approaches that increase NO bioavailability or decrease ROS completely normalize VWF levels in an *in vitro* model of GLA deficiency. However, recombinant human GLA only partially decreases VWF secretion, while the inhibition of glycosphingolipid synthesis results in an increase in VWF secretion *in vitro*. Together, these results suggest that GLA deficiency may promote VWF secretion through decreased NO bioavailability and elevated ROS, but this abnormality is not readily reversed by normalization of glycosphingolipid levels.

Clinical observations have revealed a high incidence of thrombosis and stroke in Fabry patients (50, 52) and a highly robust sensitivity to inducible thrombogenesis in murine models of Fabry disease (13, 45). VWF may contribute to the pathogenesis of thrombosis and atherosclerosis in Fabry disease due to its role in the formation of platelet thrombi (41). For example, studies using

mouse models of atherosclerosis have demonstrated that platelet adhesion to plaque-prone sites is inhibited by inactivation of VWF or platelet glycoprotein Ib, a receptor for VWF (29, 51). VWF is selectively expressed in WPBs in endothelial cells and α-granules in platelets (20, 34). However, recent studies employing chimeric mice whose VWF was restricted to either endothelial cells or platelets demonstrated that endothelial-derived VWF is a major determinant for thrombus formation (22, 35).

Numerous studies have documented abnormal procoagulant and proinflammatory profiles in Fabry patients (6, 7, 10, 54). Only three studies have reported measurements of VWF levels in this group. In two reports, VWF levels were not different or only slightly elevated in Fabry patients when compared to their control groups (10, 54). In a third study, a significant elevation of VWF in both hemizygous males and heterozygous female carriers (36). The failure to report consistent elevations of VWF in the Fabry population may reflect the small numbers of patients studied, the inclusion of treated and untreated patients in the patients studied, or differences in the analytical methods employed for VWF measurements. More recently, in an initiative to identify biomarkers in large cohorts of untreated pediatric and adult male Fabry patients, VWF was observed to be significantly elevated in both groups (Kevin Mills, UCL Institute of Child Health, unpublished data).

Early studies addressed the observation that Gla null mice lacked a spontaneous vascular phenotype. Three inducible models of vascular disease were identified including arterial thrombosis following intravascular oxidant release from rose Bengal, accelerated atherosclerosis in Gla null mice bred on an apoE null background, and impaired vasorelaxation in pre-contracted aortic and mesenteric rings exposed to acetylcholine (8, 13, 23, 38). Subsequent studies in primary cultures of aortic endothelial cells from Gla null mice demonstrated the accumulation of Gb3 in

caveolar fractions in association with impaired oligomerization of caveolin-1 (48). These structural changes were associated with decreased eNOS expression and activity (47). Based on these prior studies, we hypothesize eNOS dysregulation may be the basis for relationship between GLA deficiency and increased VWF secretion in the current studies.

Generally speaking, eNOS dysregulation refers to one of three distinct changes. These include decreased NO bioavailability, eNOS uncoupling resulting in elevated reactive nitrogen species, and alterations in NO-mediated post-translational protein modification, such as S-nitrosylation. Each of these mechanisms was considered.

Matsushita *et al*. proposed a mechanism whereby NO inhibits WPB exocytosis by inactivation of a vesicle-membrane fusion protein, NSF (30). NO has been shown to nitrosylate cysteine residues of NSF, which blocks NSF disassembly activity of SNARE complex (30). In the current study, however, the inhibitory role of SNO-NSF was not associated with elevated VWF secretion in our *in vitro* models. Rather, we observed that the elevated SNO-NSF was associated with decreased TRX-1 levels, a reductase in the endothelial cells (19). Therefore, the observed SNO-NSF level may not determine NO availability in the setting of Fabry disease.

Several studies have reported an inverse association between flow-mediated vasodilation and plasma VWF levels (16, 25). We have observed that eNOS activity was reduced in endothelial cells following GLA disruption consistent with our previous study (49). NO bioavailability was increased with DETA-NONOate and sepiapterin treatments. Increasing NO by either exogenous or endogenous means was sufficient to normalize the elevated VWF release in GLA-deficient cells, suggesting the increased VWF secretion was secondary to decreased NO level in this setting.

The uncoupling of eNOS has been associated with elevated reactive oxygen and nitrogen species in experimental models and clinical samples from Fabry patients (6, 44, 49). ROS, inflammatory cytokines, and mediators of inflammation induce VWF secretion in endothelial cells (4, 5, 31, 56, 60). In agreement with these observations, we observed that antioxidant treatment with tempol and ebselen negated the effect of GLA deficiency on enhanced VWF release.

Disruption of GLA or Gb3 loading has been shown to promote decreased eNOS activity and ROS production (44, 49). eNOS is then uncoupled and becomes a source of superoxide and peroxynitrite (15). Under this condition, removing Gb3 by ERT or substrate reduction may not be sufficient to "recouple" eNOS. This hypothesis is substantiated by a previous observation that reduction of Gb3 in primary aortic endothelial cells of Gla null mice did not significantly restore eNOS activity (47). In the current study, providing human recombinant GLA back to GLA-null cells only partially decreased VWF secretion, suggesting that the GLA deficient-endothelial cells remained activated. Surprisingly, inhibition of glucosylceramide synthase with eliglustat slightly, but significantly increased VWF secretion despite decreasing globo-series glycosphingolipids (unpublished data). While the basis for inability of these treatments to reverse the VWF secretion is not clear, these findings may be relevant to the continued occurrence of strokes in advanced patients with ERT and will require further study (2, 59).

In summary, the findings from this study are significant for several reasons. First, there is currently a paucity of biomarkers available to specifically assess endothelial dysfunction in Fabry disease. Second, cerebrovascular events continue to occur in Fabry patients receiving enzyme replacement therapy, suggesting that the underlying vasculopathy may not be completely corrected by enzyme replacement and reduction of Gb3 alone. Finally, an elevated urinary Gb3 is associated with near-term mortality in heart disease patients in the absence Fabry disease (42). Therefore, observations

from the current study may support a pathophysiologic link between glycosphingolipid metabolism and vascular disease with relevance to a broader population. Future studies on enhanced VWF release as a predictor of stroke and myocardial infarction, particularly in Fabry patients with and without a history of intravascular thrombotic events, will be important.

Acknowledgements

We are very grateful to Andrew Yee, Ph.D. for his invaluable advice on the experimental protocols on VWF ELISA, and Beth McGee for her general assistance in Dr. David Ginsburg's lab. We also acknowledge Nayiri Kaissarian for sharing the CRISPR/Cas9-mediated GLA-deficient cell lines used in this study. This work was supported by National Institutes of Health grant RO1 DK 055823 awarded to J.A.S.

Figures

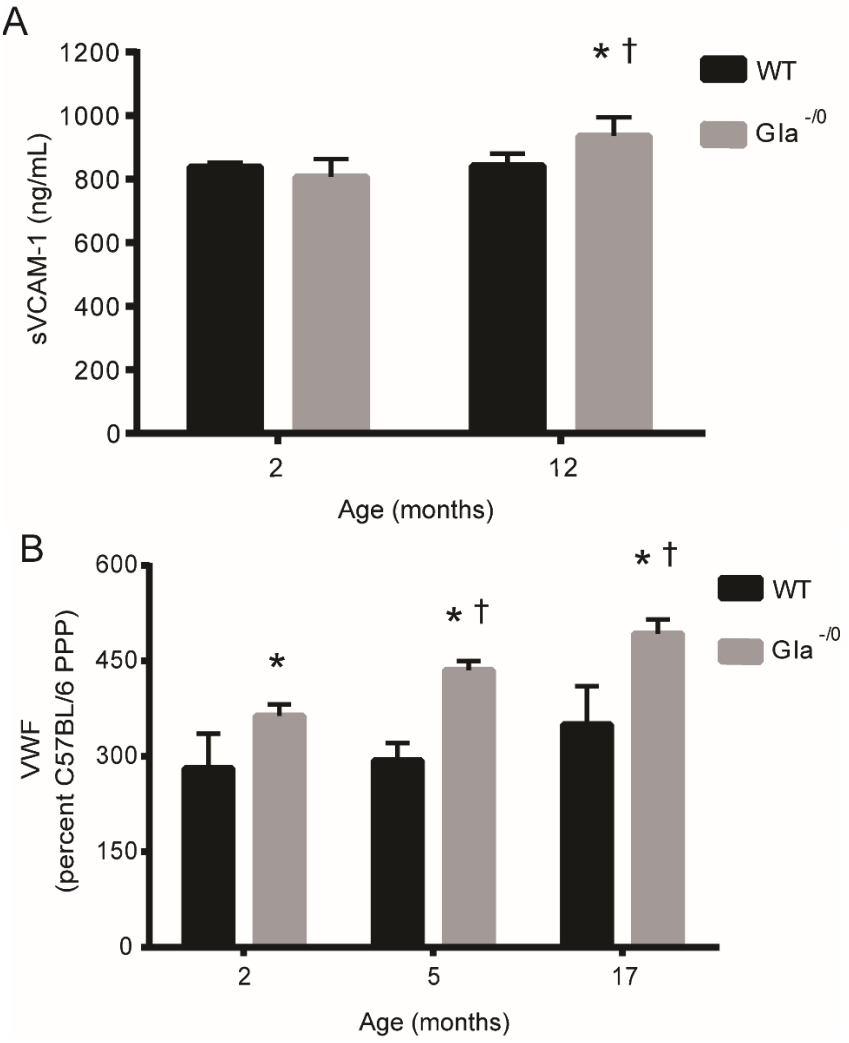

Figure 4 - 1. Age-dependent endothelial activation in mice with Fabry disease

The blood was drawn via the retro-orbital plexus from male wild type and Gla deficient mice at the indicated ages. **A.** Levels of soluble VCAM-1 were measured by ELISA (n=5-10/group). *p < 0.05 compared to the age-matched WT mice, †p < 0.001 compared to the same genotype at 2 months. **B.** Circulating plasma VWF levels were measured by AlphaLISA method as described in the method section (n=4-8 in each age group). A dilution series of pooled platelet-poor plasma (PPP) from C56BL/6 mice (n=10) was used as a reference (100%). *p < 0.05 compared to the age-matched WT. †p < 0.02 compared to the same genotype at 2 months.

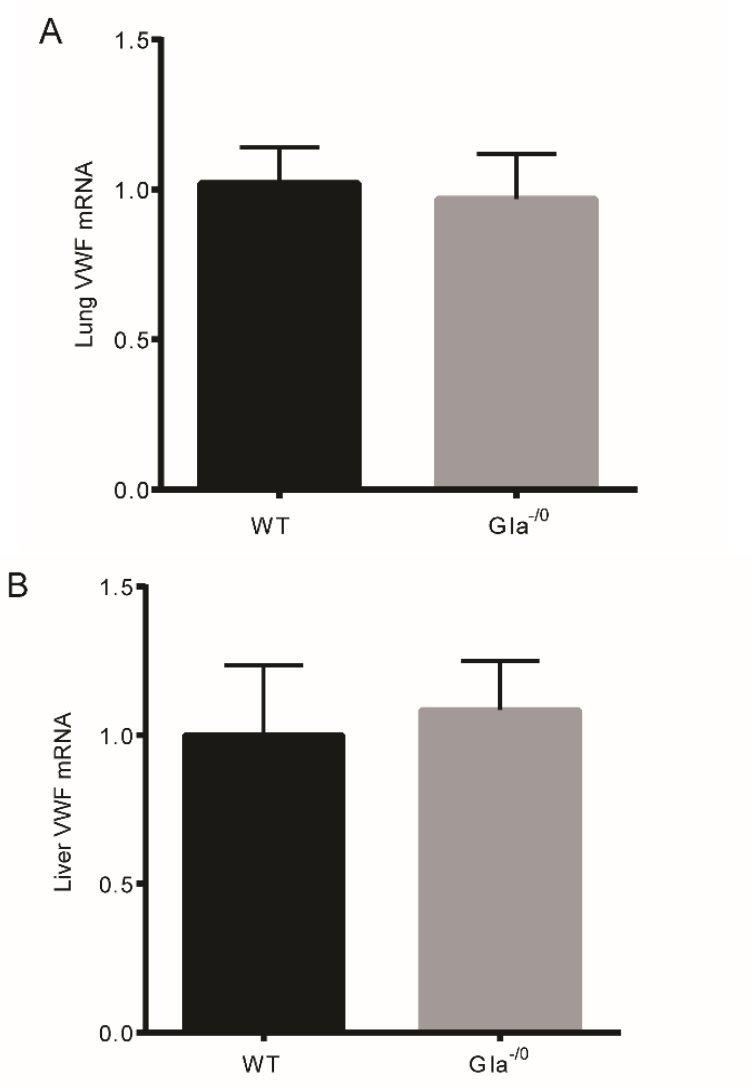

Figure 4 - 2. VWF gene expression in the lung and the liver in WT and Gla deficient mice

A. Expression of mRNA for VWF in the lung homogenates of WT and Gla deficient mice at 10 months. mRNA was determined using real-time PCR, normalized to GAPDH, and expressed relative to the level in WT lung (n=4/group). **B.** Expression of mRNA for VWF in the liver homogenates of WT and Gla deficient mice at 10 months. mRNA was determined using real-time PCR, normalized to GAPDH, and expressed relative to the level in WT liver (n=4/group).

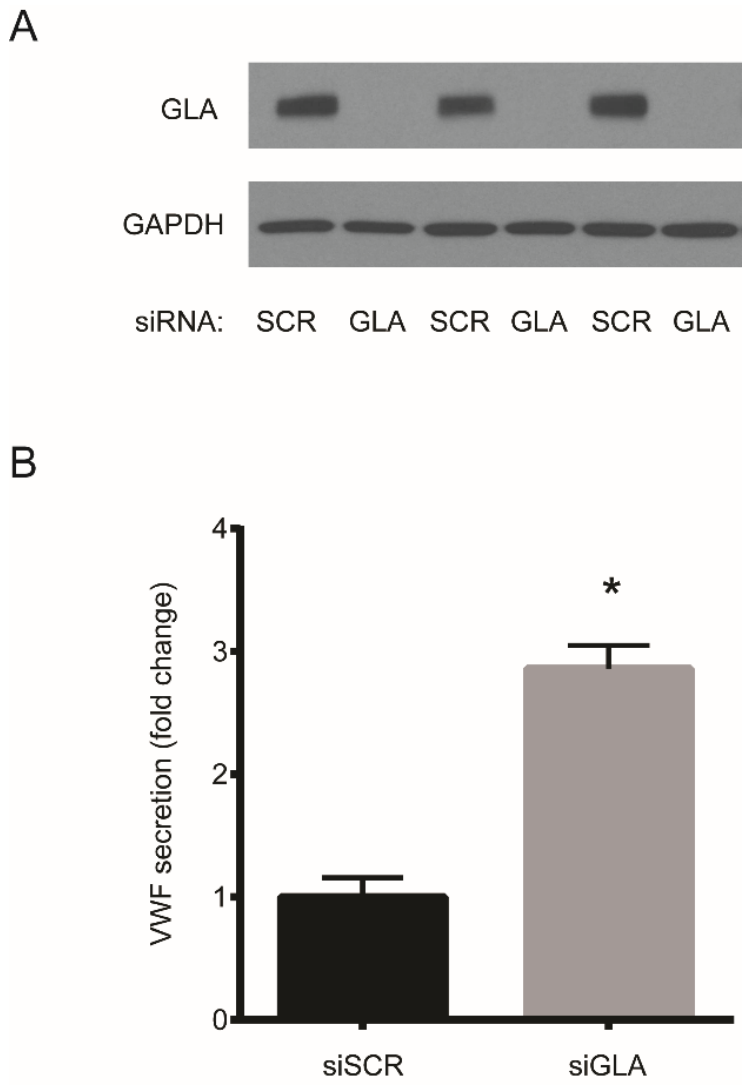

Figure 4 - 3. Elevated VWF secretion in EA.hy926 cells following GLA knockdown

A. Representative western blot showing the knockdown efficiency of siRNA against GLA in EA.hy926 cells. **B.** Cells were transfected with SCR or GLA siRNA. After the second transfection, the transfection media were replaced with 2% serum media and incubated for 3 days. Levels of VWF accumulation in the media were determined by ELISA using a dilution series of pooled normal plasma with known VWF antigen levels as standards and expressed as fold changes with respect to siSCR (n=6-8/group). *$p < 0.00001$

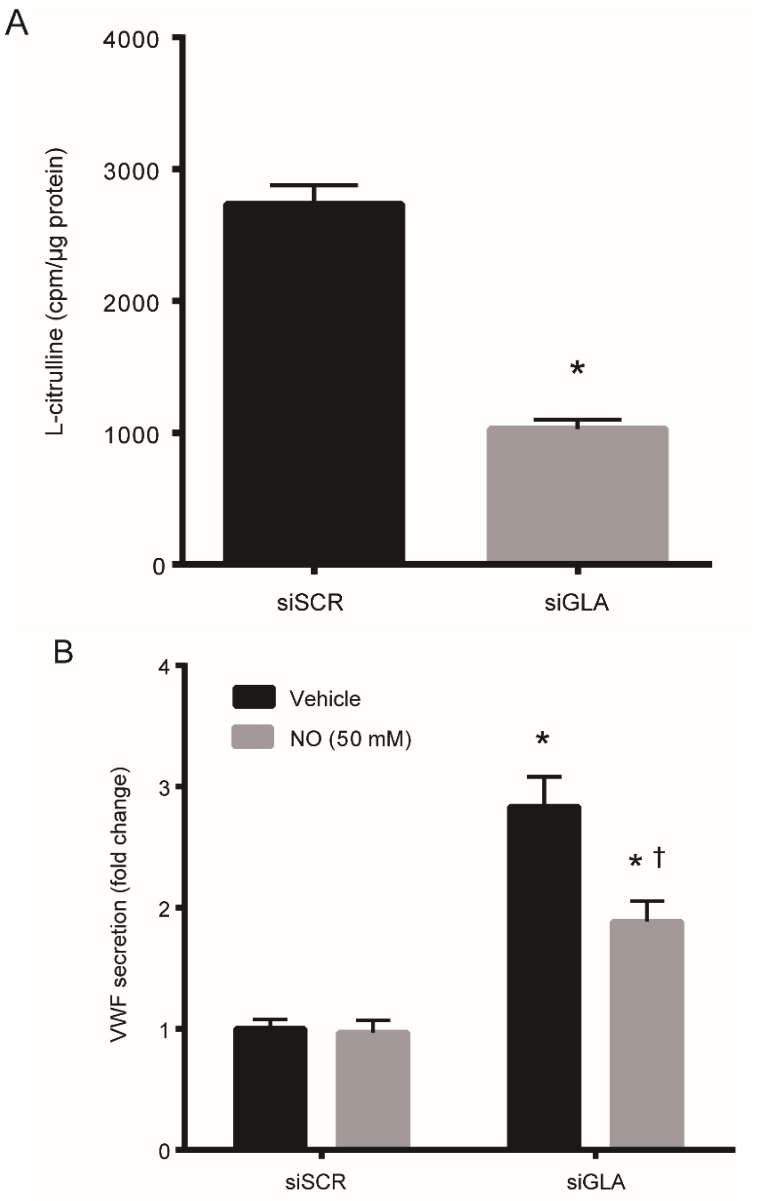

Figure 4 - 4. Decreased NO production and suppression of VWF secretion by an exogenous NO donor, DETA-NONOate

A. The cells were collected after the siRNA transfection. Endothelial nitric oxide synthase activity was measured by monitoring the conversion from radiolabeled L-arginine to the formation of L-citrulline. The activity was expressed as L-citrulline count per minute (cpm), and normalized to each sample's total protein level (n=6/group) *$p < 0.0001$. **B.** After the transfection, cells were incubated with vehicle (10 mM HEPES) or DETA-NONOate (50 µM) for 3 days. VWF levels in the cell culture supernatants were determined by ELISA and expressed as fold changes with respect to siSCR vehicle (n=4/group). *$p < 0.01$ compared to siSCR vehicle, †$p = 0.02$ compared to siGLA vehicle.

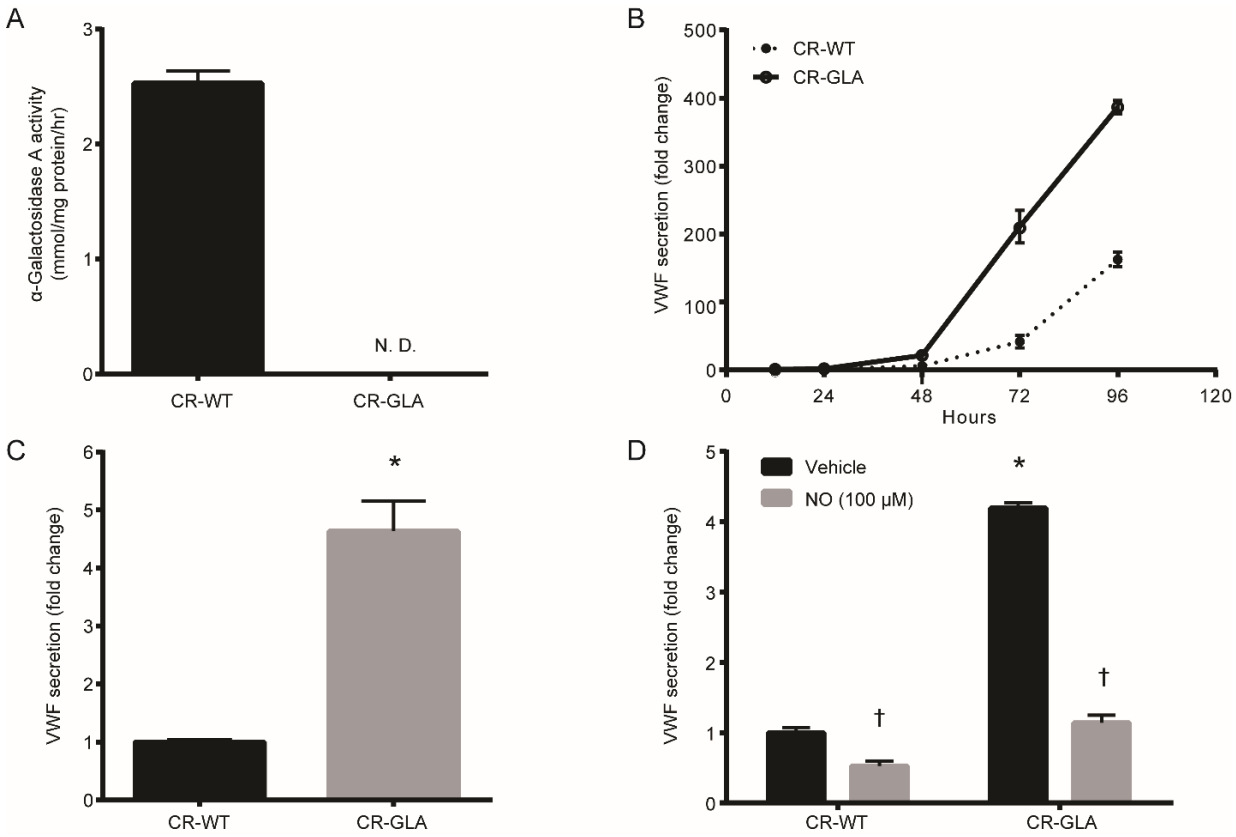

Figure 4 - 5. Time course basal VWF secretion from CRISPR WT and GLA deficient cells

A. An equal amount of protein (3 µg) from cell lysates was used. GLA activity in lysates from CR-WT and CR-GLA was expressed as mmol/mg protein per hr PNP released (n=6/group). N.D.: not detectable. **B.** Normal growth media were replaced with 2% serum media after confluency. The cell culture supernatants were collected at the various time points thereafter (n=4/group). VWF levels were expressed as fold changes with respect to CR-WT at 12 hr. **C.** VWF secretion after 2-3 days (n=11/group). *p<0.00001. **D.** After confluency, cells were incubated with vehicle (10 mM HEPES) or DETA-NONOate (100 µM) for 3 days. VWF levels in the cell culture supernatants were determined by ELISA and expressed as fold changes with respect to CR-WT vehicle (n=8/group). †p < 0.001 compared to vehicle in the same group, *p < 0.00001 compared to WT vehicle.

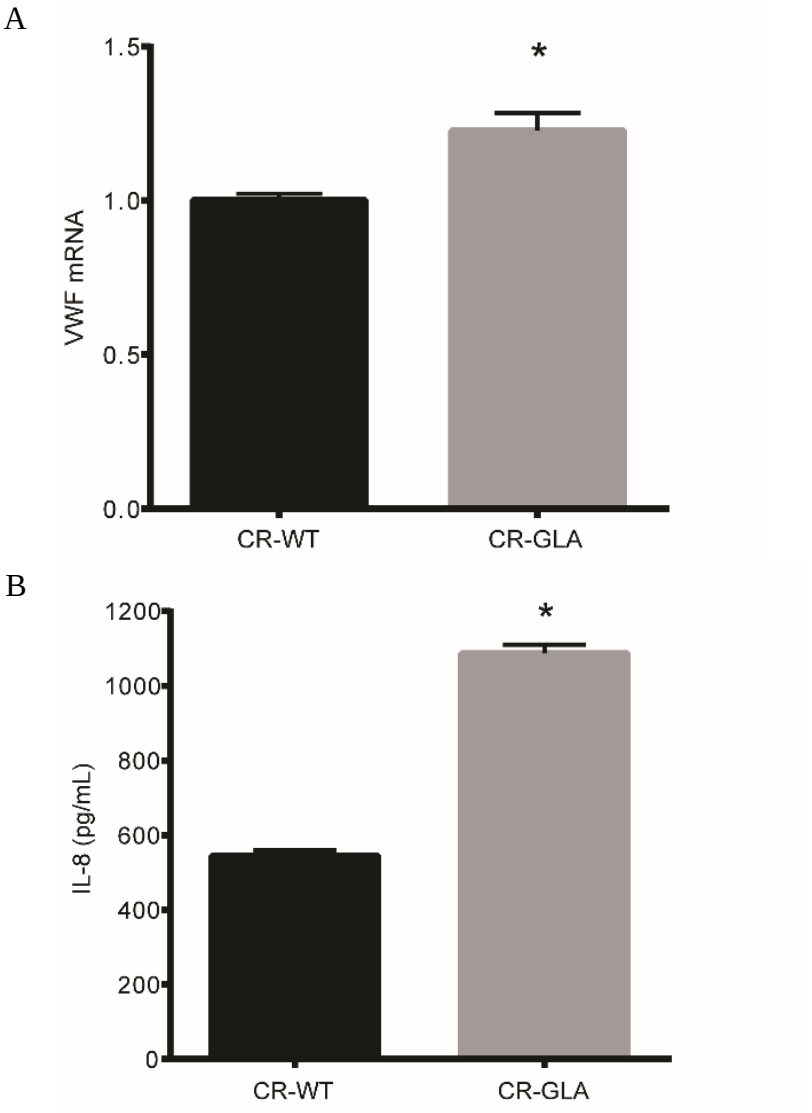

Figure 4 - 6. VWF mRNA and IL-8 levels in CRISPR cells

A. Expression of mRNA for VWF in CR-WT and CR-GLA cells. mRNA was determined using real-time PCR, normalized to TATA-binding protein, and expressed relative to the level in CR-WT (n=6/group). *$p < 0.05$. **B.** IL-8 secretion for 3 days in CR-WT versus CR-GLA cells (n=7/group). *$p<0.00001$.

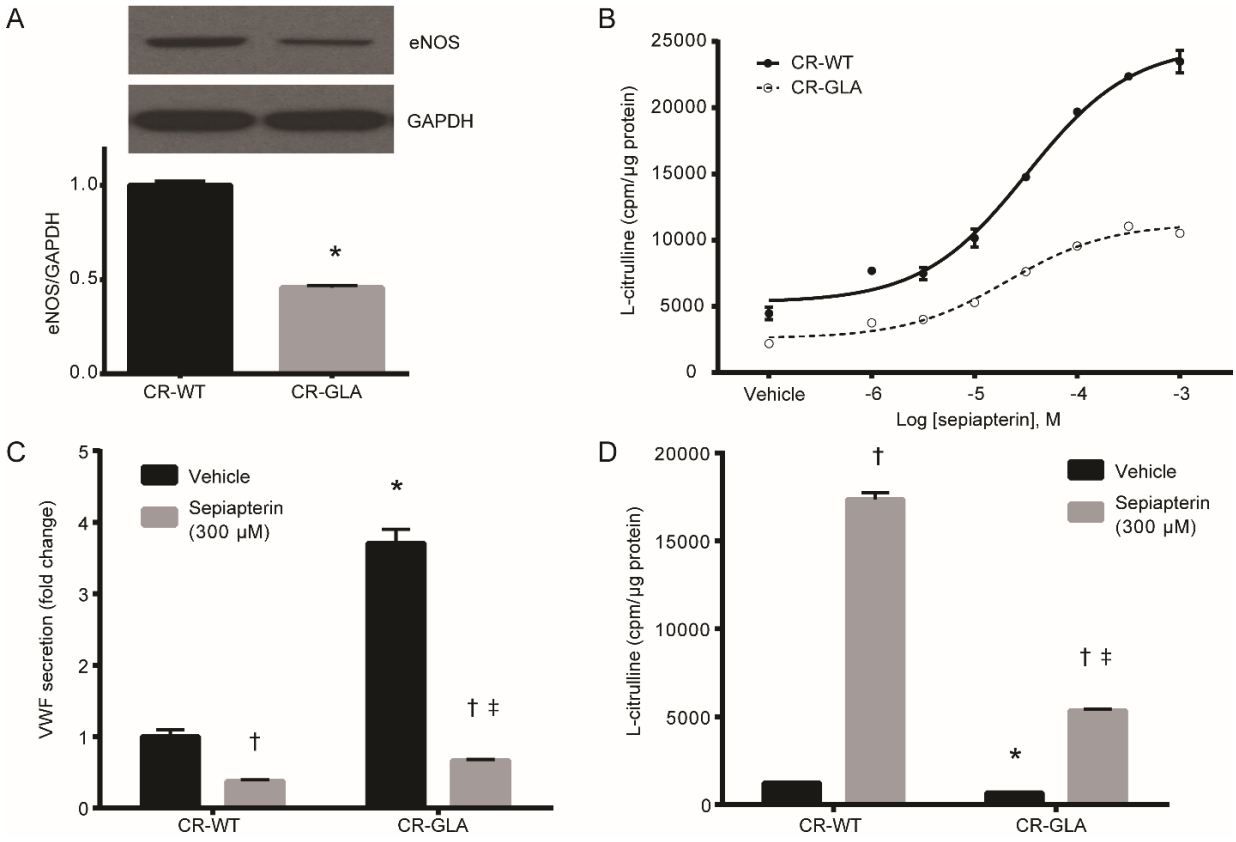

Figure 4 - 7. eNOS dysregulation and sepiapterin treatment in CRISPR WT and GLA cells

A. An equal amount of protein (30 µg) from CR-WT and CR-GLA cells was separated on 4-12% SDS PAGE (n=9/group). *$p < 0.00001$. **B.** Cells were incubated with vehicle (DMSO) or various concentrations of sepiapterin for 24 hours. Trypsinized cells were pelleted and subjected to eNOS activity assay. eNOS activity was determined as described in Figure 4 - 4A. The data are an average of triplicate assays from two separate sets of samples. **C.** After confluency, cells were incubated with vehicle (DMSO) or sepiapterin (300 µM) for 3 days. VWF levels in the cell culture supernatants were determined by ELISA and expressed as fold changes with respect to CR-WT vehicle (n=4/group). $p = 0.01$ between CR-WT vehicle and CR-GLA with sepiapterin, †$p < 0.001$ compared to vehicle in the same group, *$p < 0.0001$ compared to CR-WT vehicle, ‡$p < 0.0001$ compared to CR-WT with sepiapterin. **D.** After confluency, cells were incubated with vehicle (DMSO) or sepiapterin (300 µM) for 3 days. These cells were trypsinized and subjected to eNOS activity assay as described above (n=4/group). †$p < 0.001$ compared to vehicle in the same group, *$p < 0.001$ compared to CR-WT vehicle, ‡$p < 0.001$ compared to CR-WT with sepiapterin.

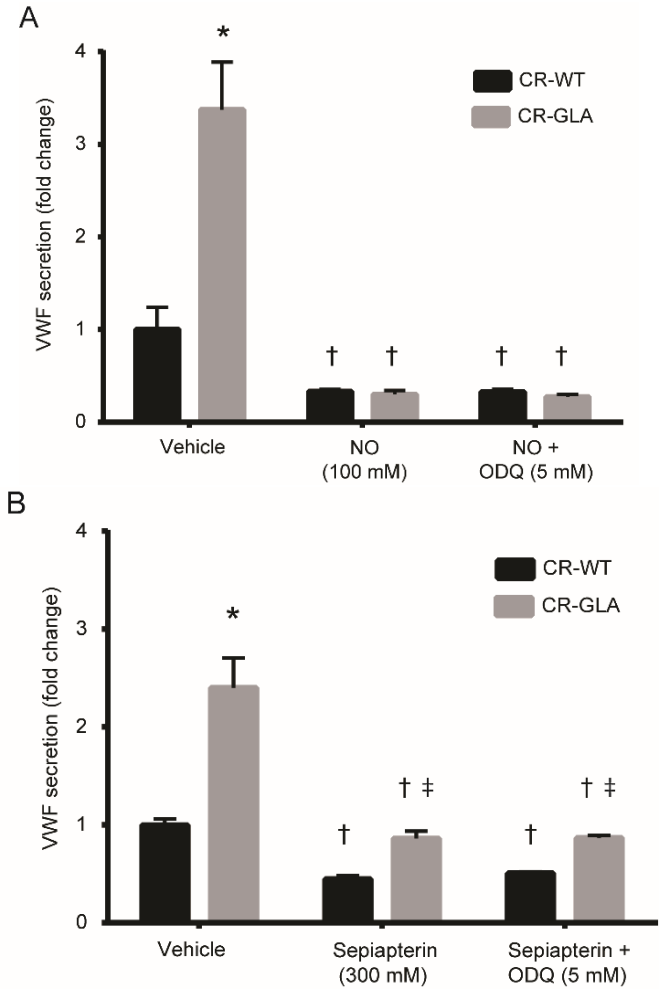

Figure 4 - 8. Effects of ODQ on VWF secretion in CR-WT and CR-GLA cells treated with DETA-NONOate and sepiapterin

A. CR-WT and CR-GLA cells were seeded in a 24-well plate. Cells were incubated with or without DETA-NONOate (100 µM) and/or the sGC inhibitor ODQ (5 µM). ODQ was added 1 hr prior to the addition of DETA-NONOate to inhibit the activation of sGC by NO. VWF levels in the cell culture supernatants were determined by ELISA and expressed as fold changes with respect to CR-WT vehicle (n=4/group). *$p < 0.01$ compared to WT vehicle, †$p < 0.05$ compared to vehicle in the same group. **B.** Cells were treated as described above with or without sepiapterin (300 µM) and/or ODQ (5 µM). VWF levels in the cell culture supernatants were determined by ELISA and expressed as fold changes with respect to CR-WT vehicle (n=4/group). *$p < 0.01$ compared to CR-WT vehicle, †$p < 0.01$ compared to vehicle in the same group, ‡$p < 0.01$ compared to CR-WT with respective treatment.

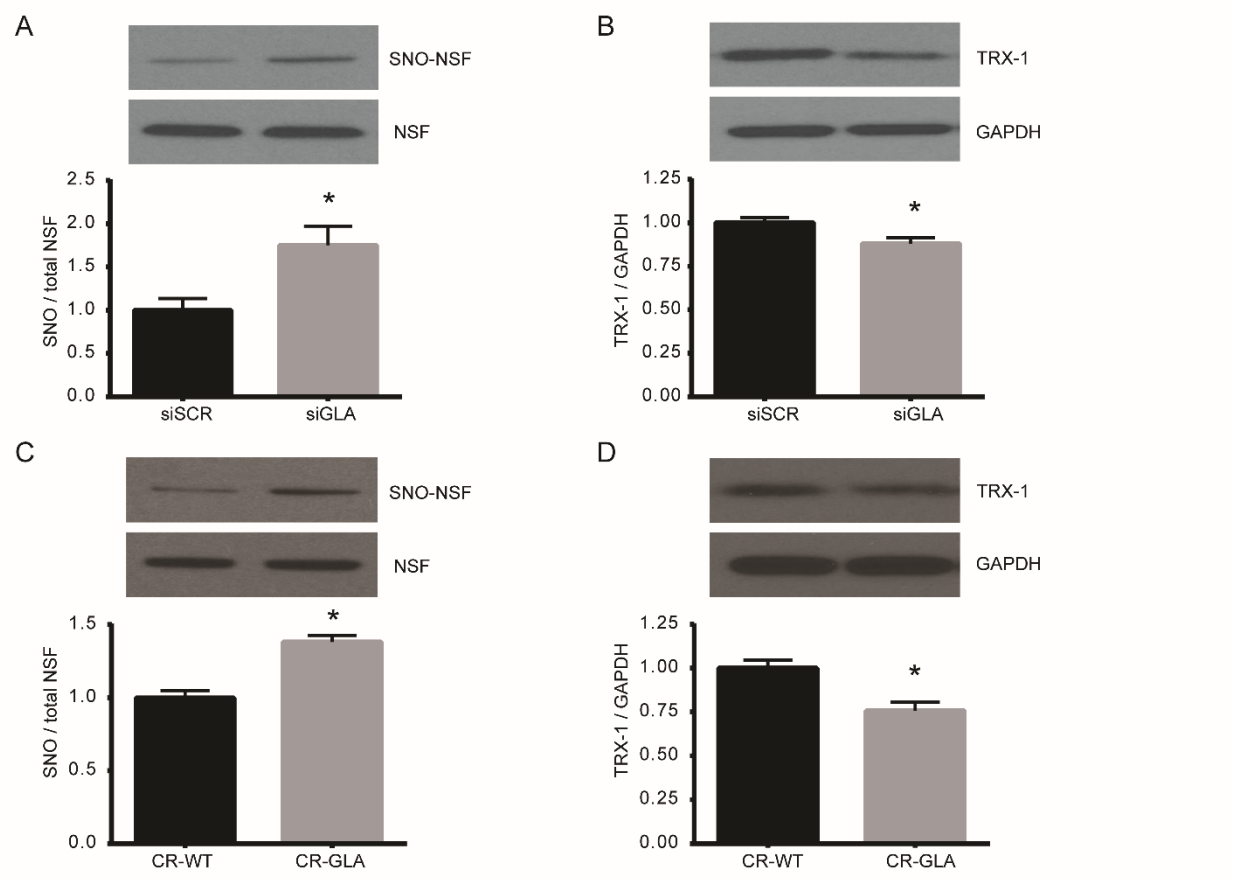

Figure 4 - 9. Increased NSF S-nitrosylation and decreased TRX-1 in GLA deficient cells

A. EA.hy926 cells treated with siSCR or siGLA were subjected to the biotin switch assay as described in the methods section. Isolated biotin-labeled proteins were separated on 4-12% SDS PAGE. The level of S-nitroyslation of NSF was normalized to its total protein level (n=6/group). *$p < 0.02$. **B.** An equal amount of protein from siRNA treated cells was loaded and separated on SDS PAGE (n=6/group). *$p < 0.05$. C. Confluent CR-WT and CR-GLA cells were subjected to the biotin switch assay. Isolated biotin-labeled proteins were separated on 4-12% SDS PAGE. The level of S-nitroyslation of NSF was normalized to its total protein level (n=6/group). *$p < 0.001$. D. An equal amount of protein from CR-WT and CR-GLA cells was loaded and separated on SDS PAGE (n=6/group). *$p < 0.01$.

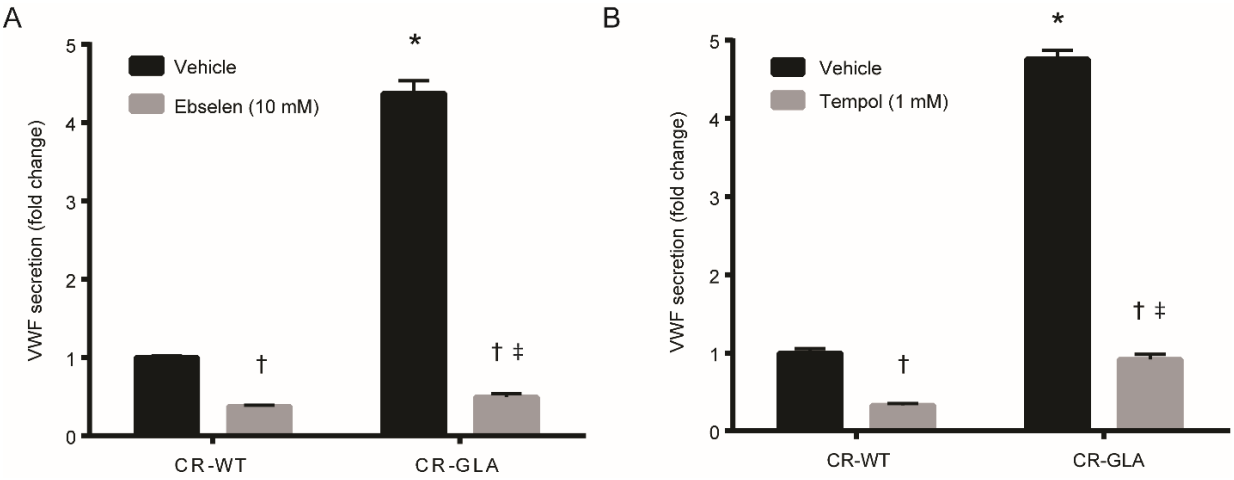

Figure 4 - 10. Decrease in VWF secretion with antioxidant treatments in CRISPR cells

A. After confluency, cells were incubated with vehicle (DMSO 0.2%) or ebselen (10 µM) for 3 days. VWF levels in the cell culture supernatants were determined by ELISA and expressed as fold changes with respect to CR-WT vehicle (n=6/group). $p = 0.0001$ between CR-WT vehicle and CR-GLA with ebselen, †$p < 0.0001$ compared to vehicle in the same group, *$p < 0.0001$ compared to CR-WT vehicle, ‡$p < 0.05$ compared to CR-WT with ebselen. **B.** After confluency, cells were incubated with vehicle or Tempol (1 mM) for 3 days. VWF levels in the cell culture supernatants were determined by ELISA and expressed as fold changes with respect to CR-WT vehicle (n=6/group). †$p < 0.0001$ compared to vehicle in the same group, *$p < 0.0001$ compared to CR-WT vehicle, ‡$p < 0.0001$ compared to CR-WT with Tempol.

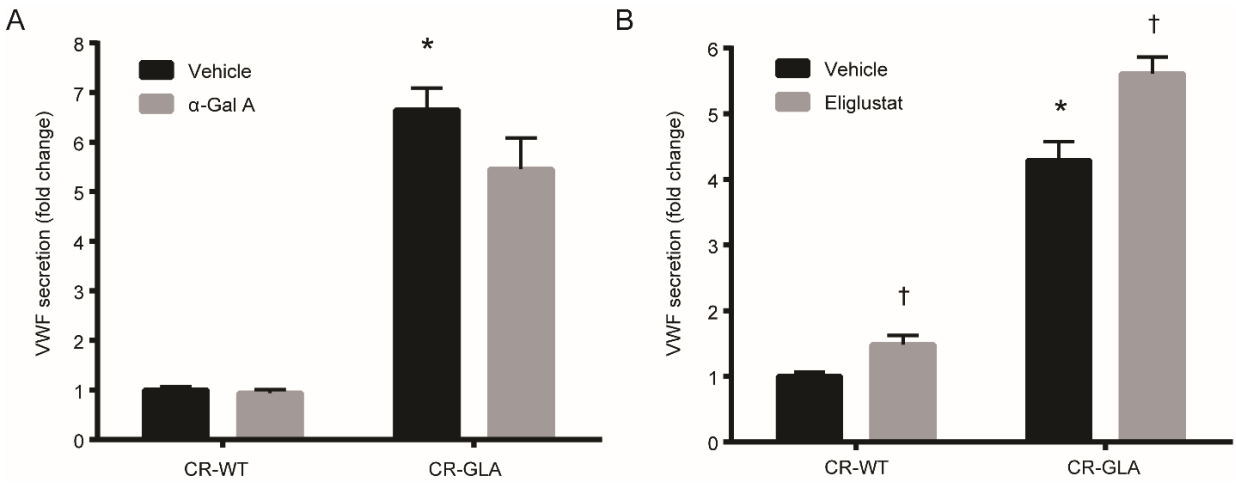

Figure 4 - 11. Treatment of CR-WT and CR-GLA cells with recombinant human α-galactosidase A and eliglustat

A. CR-WT and CR-GLA cells were seeded in a 24-well plate. Next day, vehicle (25 mM Tris and 150 mM NaCl, pH 7.5) or recombinant human GLA (10 µg/mL, α-Gal A) was added to each well. After 2 days of the treatment, the medium was replaced with 2% serum medium containing vehicle or α-Gal A and incubated for 3 days. VWF levels were determined by ELISA and expressed as fold changes with respect to CR-WT vehicle (n=6-10/group). p=0.13 between vehicle- and α-Gal A-treated CR-GLA; *p < 0.00001 compared to CR-WT vehicle. **B.** CR-WT and CR-GLA cells were seeded in a 24-well plate. The following day, vehicle (DMEM media) or Eliglustat (200 nM) was added to each well. After 2 days of the treatment, the medium was replaced with 2% serum medium containing vehicle or eliglustat and incubated for additional 3 days. VWF levels were determined by ELISA and expressed as fold changes with respect to CR-WT vehicle (n=6/group). *p < 0.00001 compared to CR-WT. †p < 0.02 compared to each vehicle condition.

References

1. **Aerts JM, Groener JE, Kuiper S, Donker-Koopman WE, Strijland A, Ottenhoff R, van Roomen C, Mirzaian M, Wijburg FA, Linthorst GE, Vedder AC, Rombach SM, Cox-Brinkman J, Somerharju P, Boot RG, Hollak CE, Brady RO, and Poorthuis BJ.** Elevated globotriaosylsphingosine is a hallmark of Fabry disease. *Proceedings of the National Academy of Sciences of the United States of America* 105: 2812-2817, 2008.

2. **Beck M, Ricci R, Widmer U, Dehout F, de Lorenzo AG, Kampmann C, Linhart A, Sunder-Plassmann G, Houge G, Ramaswami U, Gal A, and Mehta A.** Fabry disease: overall effects of agalsidase alfa treatment. *European journal of clinical investigation* 34: 838-844, 2004.

3. **Benjamin ER, Flanagan JJ, Schilling A, Chang HH, Agarwal L, Katz E, Wu X, Pine C, Wustman B, Desnick RJ, Lockhart DJ, and Valenzano KJ.** The pharmacological chaperone 1-deoxygalactonojirimycin increases alpha-galactosidase A levels in Fabry patient cell lines. *Journal of inherited metabolic disease* 32: 424-440, 2009.

4. **Bernardo A, Ball C, Nolasco L, Moake JF, and Dong JF.** Effects of inflammatory cytokines on the release and cleavage of the endothelial cell-derived ultralarge von Willebrand factor multimers under flow. *Blood* 104: 100-106, 2004.

5. **Bhatia R, Matsushita K, Yamakuchi M, Morrell CN, Cao W, and Lowenstein CJ.** Ceramide triggers Weibel-Palade body exocytosis. *Circulation research* 95: 319-324, 2004.

6. **Biancini GB, Jacques CE, Hammerschmidt T, de Souza HM, Donida B, Deon M, Vairo FP, Lourenço CM, Giugliani R, and Vargas CR.** Biomolecules damage and redox status abnormalities in Fabry patients before and during enzyme replacement therapy. *Clinica Chimica Acta* 461: 41-46, 2016.

7. **Biancini GB, Vanzin CS, Rodrigues DB, Deon M, Ribas GS, Barschak AG, Manfredini V, Netto CB, Jardim LB, Giugliani R, and Vargas CR.** Globotriaosylceramide is correlated with oxidative stress and inflammation in Fabry patients treated with enzyme replacement therapy. *Biochimica et biophysica acta* 1822: 226-232, 2012.

8. **Bodary PF, Shen Y, Vargas FB, Bi X, Ostenso KA, Gu S, Shayman JA, and Eitzman DT.** Alpha-galactosidase A deficiency accelerates atherosclerosis in mice with apolipoprotein E deficiency. *Circulation* 111: 629-632, 2005.

9. **Brady RO, Gal AE, Bradley RM, Martensson E, Warshaw AL, and Laster L.** Enzymatic defect in Fabry's disease. Ceramide trihexosidase deficiency. *N Engl J Med* 276: 1163-1167, 1967.

10. **DeGraba T, Azhar S, Dignat-George F, Brown E, Boutiere B, Altarescu G, McCarron R, and Schiffmann R.** Profile of endothelial and leukocyte activation in Fabry patients. *Annals of neurology* 47: 229-233, 2000.

11. **Desch KC, Ozel AB, Siemieniak D, Kalish Y, Shavit JA, Thornburg CD, Sharathkumar AA, McHugh CP, Laurie CC, Crenshaw A, Mirel DB, Kim Y, Cropp CD, Molloy AM, Kirke PN, Bailey-Wilson JE, Wilson AF, Mills JL, Scott JM, Brody LC, Li JZ, and Ginsburg D.** Linkage analysis identifies a locus for plasma von Willebrand factor undetected by genome-wide association. *Proceedings of the National Academy of Sciences of the United States of America* 110: 588-593, 2013.

12. **Desnick RJ, Brady R, Barranger J, Collins AJ, Germain DP, Goldman M, Grabowski G, Packman S, and Wilcox WR.** Fabry disease, an under-recognized multisystemic disorder: expert recommendations for diagnosis, management, and enzyme replacement therapy. *Ann Intern Med* 138: 338-346, 2003.

13. **Eitzman DT, Bodary PF, Shen Y, Khairallah CG, Wild SR, Abe A, Shaffer-Hartman J, and Shayman JA.** Fabry disease in mice is associated with age-dependent susceptibility to vascular thrombosis. *J Am Soc Nephrol* 14: 298-302, 2003.

14. **Eng CM and Desnick RJ.** Molecular basis of Fabry disease: mutations and polymorphisms in the human alpha-galactosidase A gene. *Hum Mutat* 3: 103-111, 1994.

15. **Forstermann U.** Nitric oxide and oxidative stress in vascular disease. *Pflugers Archiv : European journal of physiology* 459: 923-939, 2010.

16. **Freestone B, Chong AY, Nuttall S, and Lip GY.** Impaired flow mediated dilatation as evidence of endothelial dysfunction in chronic atrial fibrillation: relationship to plasma von Willebrand factor and soluble E-selectin levels. *Thrombosis research* 122: 85-90, 2008.

17. **Gelderman MP, Schiffmann R, and Simak J.** Elevated Endothelial Microparticles in Fabry Children Decreased After Enzyme Replacement Therapy. *Arteriosclerosis, thrombosis, and vascular biology* 27: e138-e139, 2007.

18. **Germain DP.** Fabry disease. *Orphanet journal of rare diseases* 5: 30, 2010.

19. **Ito T, Yamakuchi M, and Lowenstein CJ.** Thioredoxin increases exocytosis by denitrosylating N-ethylmaleimide-sensitive factor. *The Journal of biological chemistry* 286: 11179-11184, 2011.

20. **Jaffe EA, Hoyer LW, and Nachman RL.** Synthesis of antihemophilic factor antigen by cultured human endothelial cells. *The Journal of clinical investigation* 52: 2757-2764, 1973.

21. **Jaffrey SR and Snyder SH.** The biotin switch method for the detection of S-nitrosylated proteins. *Science's STKE : signal transduction knowledge environment* 2001: pl1, 2001.

22. **Kanaji S, Fahs SA, Shi Q, Haberichter SL, and Montgomery RR.** Contribution of platelet vs. endothelial VWF to platelet adhesion and hemostasis. *Journal of thrombosis and haemostasis : JTH* 10: 1646-1652, 2012.

23. **Kang JJ, Shu L, Park JL, Shayman JA, and Bodary PF.** Endothelial nitric oxide synthase uncoupling and microvascular dysfunction in the mesentery of mice deficient in α-galactosidase A. *American journal of physiology Gastrointestinal and liver physiology* 306: G140-G146, 2014.

24. **Keefer LK, Nims RW, Davies KM, and Wink DA.** "NONOates" (1-substituted diazen-1-ium-1,2-diolates) as nitric oxide donors: convenient nitric oxide dosage forms. *Methods in enzymology* 268: 281-293, 1996.

25. **Lee KW, Blann AD, and Lip GY.** High pulse pressure and nondipping circadian blood pressure in patients with coronary artery disease: Relationship to thrombogenesis and endothelial damage/dysfunction. *American journal of hypertension* 18: 104-115, 2005.

26. **LoMonaco MB and Lowenstein CJ.** Enhanced assay of endothelial exocytosis using extracellular matrix components. *Analytical biochemistry* 452: 19-24, 2014.

27. **Lowenstein CJ.** Nitric oxide regulation of protein trafficking in the cardiovascular system. *Cardiovascular research* 75: 240-246, 2007.

28. **MacDermot KD, Holmes A, and Miners AH.** Anderson-Fabry disease: clinical manifestations and impact of disease in a cohort of 60 obligate carrier females. *Journal of medical genetics* 38: 769-775, 2001.

29. **Massberg S, Brand K, Gruner S, Page S, Muller E, Muller I, Bergmeier W, Richter T, Lorenz M, Konrad I, Nieswandt B, and Gawaz M.** A critical role of platelet adhesion in the initiation of atherosclerotic lesion formation. *The Journal of experimental medicine* 196: 887-896, 2002.

30. **Matsushita K, Morrell CN, Cambien B, Yang SX, Yamakuchi M, Bao C, Hara MR, Quick RA, Cao W, O'Rourke B, Lowenstein JM, Pevsner J, Wagner DD, and Lowenstein CJ.** Nitric oxide regulates exocytosis by S-nitrosylation of N-ethylmaleimide-sensitive factor. *Cell* 115: 139-150, 2003.

31. **Matsushita K, Morrell CN, Mason RJ, Yamakuchi M, Khanday FA, Irani K, and Lowenstein CJ.** Hydrogen peroxide regulation of endothelial exocytosis by inhibition of N-ethylmaleimide sensitive factor. *The Journal of cell biology* 170: 73-79, 2005.

32. **Mayes JS, Scheerer JB, Sifers RN, and Donaldson ML.** Differential assay for lysosomal alpha-galactosidases in human tissues and its application to Fabry's disease. *Clinica chimica acta; international journal of clinical chemistry* 112: 247-251, 1981.

33. **Morange PE, Simon C, Alessi MC, Luc G, Arveiler D, Ferrieres J, Amouyel P, Evans A, Ducimetiere P, Juhan-Vague I, and Group PS.** Endothelial cell markers and the risk of coronary heart disease: the Prospective Epidemiological Study of Myocardial Infarction (PRIME) study. *Circulation* 109: 1343-1348, 2004.

34. **Nachman R, Levine R, and Jaffe EA.** Synthesis of factor VIII antigen by cultured guinea pig megakaryocytes. *The Journal of clinical investigation* 60: 914-921, 1977.

35. **Nichols TC, Samama CM, Bellinger DA, Roussi J, Reddick RL, Bonneau M, Read MS, Bailliart O, Koch GG, Vaiman M, and et al.** Function of von Willebrand factor after crossed bone marrow transplantation between normal and von Willebrand disease pigs: effect on arterial thrombosis in chimeras. *Proceedings of the National Academy of Sciences of the United States of America* 92: 2455-2459, 1995.

36. **O'Donnell J, Hughes D, Riddell A, Brown S, Richfield L, and Mehta A.** Marked elevation of plasma von Willebrand factor antigen levels in hemizygous males with Fabry disease. *Acta Pædiatrica* 91: 130, 2002.

37. **Ohshima T, Murray GJ, Swaim WD, Longenecker G, Quirk JM, Cardarelli CO, Sugimoto Y, Pastan I, Gottesman MM, Brady RO, and Kulkarni AB.** alpha-Galactosidase A deficient mice: a model of Fabry disease. *Proceedings of the National Academy of Sciences of the United States of America* 94: 2540-2544, 1997.

38. **Park JL, Whitesall SE, D'Alecy LG, Shu L, and Shayman JA.** Vascular dysfunction in the alpha-galactosidase A-knockout mouse is an endothelial cell-, plasma membrane-based defect. *Clin Exp Pharmacol Physiol* 35: 1156-1163, 2008.

39. **Qian J, Zhang Q, Church JE, Stepp DW, Rudic RD, and Fulton DJ.** Role of local production of endothelium-derived nitric oxide on cGMP signaling and S-nitrosylation. *American journal of physiology Heart and circulatory physiology* 298: H112-118, 2010.

40. **Rombach SM, Smid BE, Bouwman MG, Linthorst GE, Dijkgraaf MGW, and Hollak CEM.** Long term enzyme replacement therapy for Fabry disease: effectiveness on kidney, heart and brain. *Orphanet journal of rare diseases* 8: 47, 2013.

41. **Sadler JE.** von Willebrand factor assembly and secretion. *Journal of thrombosis and haemostasis : JTH* 7: 24-27, 2009.

42. **Schiffmann R, Forni S, Swift C, Brignol N, Wu X, Lockhart DJ, Blankenship D, Wang X, Grayburn PA, Taylor MR, Lowes BD, Fuller M, Benjamin ER, and Sweetman L.** Risk of death in heart disease is associated with elevated urinary globotriaosylceramide. *Journal of the American Heart Association* 3: e000394, 2014.

43. **Sestito S, Ceravolo F, and Concolino D.** Anderson-Fabry disease in children. *Current pharmaceutical design* 19: 6037-6045, 2013.

44. **Shen JS, Meng XL, Moore DF, Quirk JM, Shayman JA, Schiffmann R, and Kaneski CR.** Globotriaosylceramide induces oxidative stress and up-regulates cell adhesion molecule expression in Fabry disease endothelial cells. *Molecular genetics and metabolism* 95: 163-168, 2008.

45. **Shen Y, Bodary PF, Vargas FB, Homeister JW, Gordon D, Ostenso KA, Shayman JA, and Eitzman DT.** Alpha-galactosidase A deficiency leads to increased tissue fibrin deposition and thrombosis in mice homozygous for the factor V Leiden mutation. *Stroke; a journal of cerebral circulation* 37: 1106-1108, 2006.

46. **Shu L, Murphy HS, Cooling L, and Shayman JA.** An in vitro model of Fabry disease. *J Am Soc Nephrol* 16: 2636-2645, 2005.

47. **Shu L, Park JL, Byun J, Pennathur S, Kollmeyer J, and Shayman JA.** Decreased nitric oxide bioavailability in a mouse model of Fabry disease. *J Am Soc Nephrol* 20: 1975-1985, 2009.

48. **Shu L and Shayman JA.** Caveolin-associated accumulation of globotriaosylceramide in the vascular endothelium of alpha-galactosidase A null mice. *The Journal of biological chemistry* 282: 20960-20967, 2007.

49. **Shu L, Vivekanandan-Giri A, Pennathur S, Smid BE, Aerts JM, Hollak CE, and Shayman JA.** Establishing 3-nitrotyrosine as a biomarker for the vasculopathy of Fabry disease. *Kidney Int* 86: 58-66, 2014.

50. **Sims K, Politei J, Banikazemi M, and Lee P.** Stroke in Fabry disease frequently occurs before diagnosis and in the absence of other clinical events: natural history data from the Fabry Registry. *Stroke; a journal of cerebral circulation* 40: 788-794, 2009.

51. **Theilmeier G, Michiels C, Spaepen E, Vreys I, Collen D, Vermylen J, and Hoylaerts MF.** Endothelial von Willebrand factor recruits platelets to atherosclerosis-prone sites in response to hypercholesterolemia. *Blood* 99: 4486-4493, 2002.

52. **Utsumi K, Yamamoto N, Kase R, Takata T, Okumiya T, Saito H, Suzuki T, Uyama E, and Sakuraba H.** High incidence of thrombosis in Fabry's disease. *Internal medicine* 36: 327-329, 1997.

53. **van Schie MC, de Maat MP, Isaacs A, van Duijn CM, Deckers JW, Dippel DW, and Leebeek FW.** Variation in the von Willebrand factor gene is associated with von Willebrand factor levels and with the risk for cardiovascular disease. *Blood* 117: 1393-1399, 2011.

54. **Vedder AC, Biro E, Aerts JM, Nieuwland R, Sturk G, and Hollak CE.** Plasma markers of coagulation and endothelial activation in Fabry disease: impact of renal impairment. *Nephrology, dialysis, transplantation : official publication of the European Dialysis and Transplant Association - European Renal Association* 24: 3074-3081, 2009.

55. **Vischer UM.** von Willebrand factor, endothelial dysfunction, and cardiovascular disease. *Journal of thrombosis and haemostasis : JTH* 4: 1186-1193, 2006.

56. **Vischer UM, Jornot L, Wollheim CB, and Theler JM.** Reactive oxygen intermediates induce regulated secretion of von Willebrand factor from cultured human vascular endothelial cells. *Blood* 85: 3164-3172, 1995.

57. **Weidemann F, Niemann M, Stork S, Breunig F, Beer M, Sommer C, Herrmann S, Ertl G, and Wanner C.** Long-term outcome of enzyme-replacement therapy in advanced Fabry disease: evidence for disease progression towards serious complications. *Journal of internal medicine* 274: 331-341, 2013.

58. **Whybra C, Kampmann C, Willers I, Davies J, Winchester B, Kriegsmann J, Bruhl K, Gal A, Bunge S, and Beck M.** Anderson-Fabry disease: clinical manifestations of disease in female heterozygotes. *Journal of inherited metabolic disease* 24: 715-724, 2001.

59. **Wilcox WR, Banikazemi M, Guffon N, Waldek S, Lee P, Linthorst GE, Desnick RJ, and Germain DP.** Long-term safety and efficacy of enzyme replacement therapy for Fabry disease. *Am J Hum Genet* 75: 65-74, 2004.

60. **Xiang Y, Cheng J, Wang D, Hu X, Xie Y, Stitham J, Atteya G, Du J, Tang WH, Lee SH, Leslie K, Spollett G, Liu Z, Herzog E, Herzog RI, Lu J, Martin KA, and Hwa J.** Hyperglycemia repression of miR-24 coordinately upregulates endothelial cell expression and secretion of von Willebrand factor. *Blood* 125: 3377-3387, 2015.

61. **Xiang Y and Hwa J.** Regulation of VWF expression, and secretion in health and disease. *Current opinion in hematology* 23: 288-293, 2016.

62. **Yamamoto K, de Waard V, Fearns C, and Loskutoff DJ.** Tissue distribution and regulation of murine von Willebrand factor gene expression in vivo. *Blood* 92: 2791-2801, 1998.

63. **Yee A, Gildersleeve RD, Gu S, Kretz CA, McGee BM, Carr KM, Pipe SW, and Ginsburg D.** A von Willebrand factor fragment containing the D'D3 domains is sufficient to stabilize coagulation factor VIII in mice. *Blood* 124: 445-452, 2014.

CHAPTER 5

Voluntary wheel exercise training improves Akt/AMPK/eNOS signaling cascades, but not endothelial dysfunction in aged mice deficient in α-galactosidase A

Abstract

Fabry disease is caused by loss of activity of the lysosomal hydrolase α-galactosidase A (GLA). Premature life-threatening complications in Fabry patients arise from cardiovascular disease, including stroke and myocardial infarction. Exercise training has been shown to improve endothelial dysfunction in various settings including coronary artery disease. However, the effects of exercise training on endothelial dysfunction in Fabry disease have not been investigated. Gla knockout mice were single-housed in a cage equipped with a voluntary wheel (EX) or no wheel (SED) for 12 weeks. Exercised mice ran 10 km/day on average during the voluntary running intervention (VR) period. Despite significantly higher food intake in EX than SED, body weights of EX and SED remained stable during the VR period. After the completion of VR, citrate synthase activity in gastrocnemius muscle was significantly higher in EX than SED. Western blot analyses demonstrated that VR resulted in greater phosphorylation of Akt (S473) and AMPK (T172) in the aorta of EX compared to SED. Furthermore, VR significantly enhanced eNOS protein expression and phosphorylation at S1177 by 20% and 50% in the aorta of EX when compared with SED, suggesting eNOS activation. In contrast, anti- and pro-oxidative enzymes including superoxide

dismutase and p67 subunit of NADPH oxidase were not different between groups. Although the aortic endothelial relaxation to acetylcholine was slightly increased in EX, it did not reach statistical significance. Overall, this study provides the first evidence that VR improves Akt/AMPK/eNOS signaling cascades, but not endothelial function in the aorta of aged Gla deficient mice.

Introduction

Fabry disease is an X-linked lysosomal storage disorder that results from a defective or absent activity of α-galactosidase A (GLA) (8). The enzymatic defect leads to a progressive accumulation of glycosphingolipids including globotriaosylceramide, galabiosylceramide, and globotriaosylsphingosine. This toxic accumulation is observed in a variety of cell types, but especially found in the endothelium and smooth muscle cells (25, 35). Early symptoms of Fabry disease in childhood include episodic acute pain and gastrointestinal involvement with abdominal pain, diarrhea, and nausea (25). However, premature life-threatening complications arise from cardiovascular diseases around fourth decade of life, and include cerebrovascular events, myocardial infarction, hypertrophic cardiomyopathy, and renal failure (18). Whereas enzyme replacement therapy (ERT) with recombinant GLA is the only approved treatment for Fabry disease, there is no clear evidence that ERT alters the natural course of cardiovascular morbidities in patients with advanced Fabry disease (17).

A mouse model of Fabry disease has been used to explore the vascular pathophysiology in the setting of GLA deficiency. Several inducible models of vasculopathy in these mice have demonstrated accelerated atherosclerosis, oxidant-induced occlusive arterial thrombosis, impaired acetylcholine-induced vascular relaxation, and the presence of endothelial nitric oxide synthase

(eNOS) uncoupling (4, 16, 30, 43). A potential link of these experimentally observed abnormalities is decreased nitric oxide (NO) bioavailability. Exercise has been shown to be one of the most effective non-pharmacological interventions for improving NO bioavailability (37). During the last two decades, the beneficial effects of exercise on the vascular endothelium have been extensively studied in various aspects including endothelium-dependent vasodilation, anti-inflammation, and anti-atherosclerosis (7, 15, 46). Furthermore, exercise has been demonstrated to improve acetylcholine-mediated coronary blood flow even in the setting of documented coronary artery disease (26, 27), suggesting that the presence of advanced disease does not preclude improvements in endothelial function resulting from exercise. Although exercise intolerance has been reported in patients with Fabry disease previously (19), a more recent study showed that exercise training could improve exercise capacity and well-being of Fabry patients who refrained from physical activity in the past (45). This suggests that exercise training might be an alternative therapeutic option in Fabry disease. Yet, the benefits of exercise training with respect to vasculopathy in Fabry disease remain unclear.

The purpose of the present study, therefore, was to directly assess the effects of 12 weeks of voluntary wheel exercise training on signaling and functional alterations in the aorta using an established mouse model of Fabry disease. Specifically, we focused on aortic endothelial function, selected enzymes influencing the NO bioavailability in the endothelium (AMPK, Akt, eNOS expression and S1177, superoxide dismutase, and the $p67^{phox}$ subunit of NADPH oxidase) and indirect markers of vascular oxidative/nitrosative stress level (nitrotyrosine).

Methods

Mice

Gla null mice (129/SvJXC57BL/6J) used in this study were bred from mice originally generated and provided by Drs. Ashok Kulkarni and Roscoe Brady (National Institute of Health, Bethesda, MD) as described previously (42). These mice were back-crossed a minimum of six generations to the C57BL/6J strain. The animals were maintained on a 12-h light/dark cycle (0600 h to 1800 h) with free access to food and water ad libitum. A week before the voluntary wheel intervention, groups of male mice (8-11 months) with similar average body weight were single-housed and assigned to either a control sedentary (n=20, SED) or voluntary wheel running group (n=20, EX). Mice in the EX group were provided with a running wheel (5" diameter x 2" width) equipped with an odometer (Bell Dashboard 100-F12) for 12 weeks. Running distance and food intake were monitored daily. Body weight was measured weekly. All animal experiments were conducted according to the protocol of the Institutional Animal Care and Use Committee of the University of Michigan.

Tissue Harvest

Animals in the EX group had access to the voluntary wheel up until the time of tissue collection. Mice were euthanized with an injection of pentobarbital sodium (66.5 mg/kg ip) at approximately 0900 h. Due to the logistics of the functional studies of the aorta, one mouse from each group was euthanized per day on consecutive days at the end of the 12-week intervention.

Aortic protein expression

The thoracic aorta was dissected, cleared of surrounding connective tissues in cold PSS, and frozen in liquid nitrogen. The vessels were pulverized in liquid nitrogen using a pestle. Each powdered sample was lysed with 200 µl RIPA lysis buffer (#R0278, Sigma) with 1X mixture of

phosphatase/protease inhibitors (#P2714, P0044, and P5726, Sigma). Homogenates were then incubated on a rotor at 4°C for 1 hr. Cell debris was removed by centrifugation at 10,000 x g for 10 min at 4°C. Quantification of total protein in each aortic lysate sample was determined by a bicinchoninic acid assay with bovine serum albumin as a standard. For measures of aortic protein expression, 15 µg of protein with LSB were loaded on 4-12% gradient gels, separated by electrophoresis, and transferred onto a nitrocellulose membrane. The membrane was blocked in 5 % non-fat dry milk in Tris-buffered saline with 0.1% Tween-20 (TBST) for at least 1 hr at room temperature. After blocking, the membrane was washed with TBST and incubated with primary antibody overnight at 4°C followed by washing with TBST. The membrane was incubated with appropriate secondary antibody. The immunoreactive bands were detected with ECL western blotting substrate (#32106, Thermo Sci), and quantified by densitometric scanning using ImageJ software.

Citrate synthase activity assay

Gastrocnemius muscles from SED and EX mice were dissected and flash frozen in liquid nitrogen. Frozen muscles were weighed, transferred to pre-chilled glass tissue grinding tubes (Kontes, Vineland, NJ), and homogenized 1:20 (wt:vol) in ice-cold lysis buffer (50mM TRIS-HCl, 1mM EDTA, 0.1% Triton X-100, pH 7.2) using a glass pestle attached to a motorized homogenizer (Caframo, Wiarton, ON). Homogenates were then incubated on a rotor at 4°C for 1 hr. The lysates were centrifuged at 10,000 x g for 10 min at 4°C to remove cell debris. Quantification of total protein in each aortic lysate sample was performed by a bicinchoninic acid assay with bovine serum albumin as a standard. Two micrograms of gastrocnemius homogenate were used. Citrate

synthase activity was determined using an assay kit according to the instructions (#701040, Cayman).

Assessment of aortic endothelial function

Following the tissue harvest, the thoracic aorta was dissected and placed in a dissection petri dish filled with cold physiological salt solution (PSS, mmol/L: 130 NaCl, 4.7 KCl, 1.18 $KHPO_4$, 1.17 $MgSO_4$, 1.6 $CaCl_2$, 14.9 $NaHCO_3$, 5.5 dextrose, and 0.03 EDTA). After removing connective tissue, segments (2-3 mm in length) of aorta were mounted on pins in a myograph system (model 610M, Danish Myo Technology, Aarhus, Denmark). Vessels were slowly warmed (37°C) and aerated (95% O_2 and 5% CO_2) in PSS for 20 min. Rings were set at 700 mg passive tension and equilibrated for 60 min with washing with pre-warmed and aerated PSS every 20 min. Prior to performing concentration response curves, vessels were subjected to osmotically balanced 60 mM potassium physiological salt solution (mmol/l: 14.7 NaCl, 100 KCl, 1.18 $KHPO_4$, 1.17 $MgSO_4$, 1.6 $CaCl_2$, 14.9 $NaHCO_3$, 5.5 dextrose, and 0.03 EDTA). After washing, the vessels were contracted with 100 mmol/L KPSS until plateau, followed by washes. Phenylephrine (PE, 10^{-9} mol/L to 10^{-4} mol/L) was added cumulatively to establish a concentration-response curve, in which PE EC_{80} was calculated for each individual ring. The vessels were contracted with their individual PE EC_{80} values and allowed to reach a stable plateau. Subsequently, acetylcholine (ACh) or sodium nitroprusside (SNP) was added cumulatively to the chamber to determine endothelium-dependent (ACh) or endothelium-independent (SNP) relaxation. All chemicals used in the vascular reactivity study were purchased from Sigma (St. Louis, MO). The vascular reactivity to ACh or SNP was presented on a percent basis according to the following formula: Relaxation (%) = (T_{PE80} – T_d) / (T_{PE80}) x 100, where T_{PE80} is the steady-state tension produced after addition of PE EC80,

and T_d is the steady state tension following addition of vasoactive agent (ACh, SNP). Sensitivity (EC_{50}) was defined as the concentration of the agent that produced 50% of its maximal response. A total of eight mice per group were utilized for these studies.

Statistical analysis

GraphPad Prism software was used for statistical analysis. The data were presented as mean ± standard error of the mean. Results were analyzed using the unpaired t-test for comparison of two groups. For vascular reactivity studies using ACh or SNP, concentration-response data was analyzed using two-way ANOVA (exercise and concentration) to compare the concentration-response curves between the EX and SED groups. Bonferroni's post hoc test was used to assess differences at individual points on the concentration-response curves if the results of the two-way ANOVA comparison between curves was significantly different. Statistical significance was set at $p<0.05$.

Results

Overall effects of voluntary wheel running on non-vascular endpoints

The mice in the voluntary running wheel group (EX) ran on average 10 ± 0.75 km/day (Figure 5 - 1A). During the first week of the exercise intervention, food intake was not different between the mice in the sedentary control (SED) and EX groups (Figure 5 - 1B). In the second week, consistent with the increased running distance, EX mice consumed 24% more food compared to SED mice. Interestingly, body weights were not different at the completion of voluntary wheel running (VR) compared to the beginning of VR in both SED and EX mice (Figure 5 - 1C). Despite no changes in total body mass, 12 weeks of VR resulted in a significantly higher heart to body mass ratio and

lower gonadal fat to body mass ratio in EX mice compared to those in SED mice (Table 5 - 1). The activity of citrate synthase as a marker for mitochondrial content was also measured to confirm an exercise training effect (33, 36). Consistent with the results in running distance, there was a 49% increase in the citrate synthase activity in gastrocnemius muscle of EX mice compared with SED controls (Figure 5 - 2).

VR increases Akt / AMPK / eNOS signaling pathways in the aorta of EX mice

Exercise has been shown to increase eNOS activity, in part, through shear stress (55). Akt and AMPK have been proposed to be critical mediators of shear stress-induced eNOS activation (5). The expression and phosphorylation status of Akt, AMPK, and eNOS were determined to test the hypothesis that VR induced changes in signaling pathways in the aorta. For these measurements, phosphorylation site-specific antibodies were used to probe immunoblots from the aortic homogenates from SED and EX mice. As shown in Figure 5 - 3, the ratio of p-AMPK (Thr-172) / t-AMPK was significantly higher (arbitrary units; 100 $\pm$ 9% vs. 137 $\pm$ 13%: SED vs. EX) in the aorta of EX than SED mice (Figure 5 - 3A). A significant increase in the p-Akt (Ser-473) / t-Akt ratio (arbitrary units; 100 $\pm$ 9% vs. 148 $\pm$ 17%: SED vs. EX) was also noted in the aorta of EX mice in comparison with SED mice (Figure 5 - 3B). It has been shown that phosphorylation of eNOS at Ser1177 is a major downstream target of Akt and AMPK in response to exercise and shear stress (55). Consistent with the previous finding, we observed a significantly higher p-eNOS (Ser-1177) to total eNOS ratio (arbitrary units; 100 $\pm$ 10% vs. 154 $\pm$ 12%: SED vs. EX) in the aorta of EX mice when compared to that of SED mice (Figure 5 - 3C). In addition, eNOS protein expression was significantly elevated (arbitrary units; 100 $\pm$ 2% vs. 120 $\pm$ 4%: SED vs. EX) in the aorta of EX in comparison with SED mice (Figure 5 - 3D). These results suggested that 12

weeks of VR intervention mediated an increase in expression and activity of eNOS and its upstream signaling kinases by which exercise/shear stress exert the beneficial effects on the endothelium.

Nitric oxide and oxidative stress levels

In previous studies increased levels of oxidative/nitrosative stress was observed in tissues of patients with Fabry disease and GLA-deficient mice (10, 39, 49). Thoracic aortae were used to determine the effects of VR on nitrotyrosine (NT) abundance, a cellular marker of peroxinitrite formation, therefore vascular oxidative/nitrosative stress (14). In this study, VR did not alter the level of NT in the aortic tissue (Figure 5 - 4A), suggesting the balance between NO and superoxide did not change significantly by VR. NO level in response to exercise was next determined in the aorta. Soluble guanylate cyclase is the major physiological receptor for NO and catalyzes the synthesis of intracellular cGMP level (3). Activated by cGMP is protein kinase G that preferentially phosphorylates vasodilator-stimulated phosphoprotein (VASP) at Ser-239 (22, 41). We observed no changes in p-VASP (Ser 239) to t-VASP ratio in response to 12 weeks of VR (Figure 5 - 4B). Because VASP is a common marker used for monitoring NO availability (41), this suggests no improvement in NO/cGMP signaling with VR. In addition, VR had no effect on the protein expressions of Mn-, CuZn-, and ec-SOD in the aortae of EX compared to SED mice (Figure 5 - 5A-C). Finally, we determined the effect of VR on NADPH oxidase, a prominent source of vascular-derived reactive oxygen species, in the aorta (23). Phox67 is one of the subunits of NADPH, and has been found to be reduced in aorta of mice following VR training (15). In the present study, VR did not alter phox67 subunit protein expression in EX mice compared to SED (Figure 5 - 5D).

Endothelial function

The vascular contraction mediated by 100 mmol/L KPSS was equivalent in aortae from SED and EX mice (1351.81 ± 117.09 mg vs. 1511.36 ± 105.54 mg, n=8/group, $p>0.05$). Phenylephrine (PE) caused a concentration-dependent contraction in isolated aortic rings from both SED and EX mice (Figure 5 - 6A). The PE-induced contractions were equivalent in aortae from SED and EX mice as demonstrated by similar log EC_{50} values (-6.58 ± 0.01 vs. -6.63 ± 0.02, $p>0.05$) as well as equivalent E_{max} values (140.83 ± 4.71% vs. 140.60 ± 10.01%, $p>0.05$). Based on the PE-induced contraction response, PE EC_{80} was calculated for each aortic ring. Receptor-mediated endothelium-dependent relaxation to acetylcholine (ACh) was examined in aortic rings from SED and EX mice. The vessels from SED and EX mice were dilated to ACh in a dose-dependent manner (Figure 5 - 6B). Both the maximal relaxation elicited by ACh (36.21 ± 7.88% vs. 44.0 ± 7.04%, $p>0.05$) and log EC_{50} values (-6.73 ± 0.14 vs. -6.78 ± 0.12, $p>0.05$) did not differ between the groups. Sodium nitroprusside (SNP) induced a concentration-dependent, endothelium-independent relaxation in isolated aortae from SED and EX mice (Figure 5 - 6C). However, SNP-mediated vasodilation was greater in the aortic rings from both SED and EX mice (67.89 ± 7.48% vs. 74.75 ± 6.05%) than the endothelium-dependent dilation to ACh (Figure 5 - 6B), suggesting the low magnitude of relaxation to ACh was not due to changes in the sensitivity of vascular smooth muscle to NO.

Discussion

Previous research regarding Fabry disease has focused on the pathophysiologic mechanisms using both patients and mouse models (4, 16, 38, 40, 43, 47). However, few studies have investigated the potential effects of exercise training on endothelial dysfunction in Fabry disease (45). In this study, we examined whether 12 weeks of VR intervention could improve endothelial dysfunction in the presence of eNOS uncoupling in a mouse model of Fabry disease. Our results indicate that in aged mice with Fabry disease, VR (a) induced exercise training adaptations, (b) increased Akt/AMPK/eNOS signaling pathways in the aorta, but (c) did not improve endothelial dysfunction and systemic markers of oxidative stress in the aorta and plasma.

Our finding that VR induced training adaptations in tissues was supported by an increase in heart size and skeletal muscle citrate synthase activity. After 12 weeks of VR, a heart to total body mass ratio was higher in EX compared to SED mice. In addition, the magnitude of the increase in citrate synthase activity observed in EX compared to SED mice was comparable with a previous study examining the skeletal muscle of wild-type C57BL/6J mice following voluntary wheel exercise (20).

EX mice had 54% and 20% higher levels of aortic p-eNOS at Ser1177 and protein expression of eNOS, respectively, compared to SED mice. One possible mechanism by which VR augmented eNOS activity as well as protein expression is through an activation of upstream kinases of eNOS by an increase in shear stress during exercise. Several lines of evidence have demonstrated that eNOS mRNA and protein expression are increased in endothelial cells exposed to shear stress (11, 12), in isolated coronary arterioles subjected to elevated intraluminal flow (53, 54), and in the aorta from exercise trained mice (12, 24, 32, 34) and rats (2). In a previous study, shear stress increased eNOS activity, measured by NO production and phosphorylation of eNOS at S1177, via

PI(3)K/Akt-dependent pathway in HUVEC cells, which was prevented by wortmannin and in cells transfected with dominant-negative Akt mutant (13). Zhang et al. showed that arterial p-eNOS S617, which is activated by Akt alone, and p-eNOS S1177, which is activated by both Akt and AMPK, were increased in response to treadmill-running in mice (55). In the same study, intraperitoneal administration of wortmannin before treadmill running revealed either Akt or AMPK alone might be sufficient to activate p-eNOS S1177 during exercise. As such, we determined activation status of Akt and AMPK in the aorta in response to VR in this study. In keeping with the previous findings, we observed elevated levels of phospho -Akt (S473), -AMPK (T172), and -eNOS (S1177) in the aorta of EX in comparison with SED mice.

Previous study in our lab has observed that endothelial dysfunction in the aorta was evident in 3-5 month-old GLA deficient mice, characterized by decreased maximal vasodilation to ACh in the aorta (E_{max}: ~60%) (43). In the present study, the E_{max} to ACh in GLA deficient mice at 11-13 months was approximately 40%. Another group reported 25% of E_{max} to ACh in the same mice at 19 months (28). These results indicate a progressive decline in endothelial function in Fabry disease. Indeed, endothelial dysfunction in the mesenteric artery and accelerated oxidant-induced thrombosis in the setting of GLA deficiency in other studies were all shown to be age-dependent (16, 30). A previous study by Durrant el al. showed that carotid artery vasodilatation to ACh was improved in older mice of an aging model subjected to 10-14 weeks of voluntary running compared to their age-matched sedentary counterparts (15). On the other hand, some studies have reported that exercise did not improve endothelial function and/or arterial stiffness despite significant improvement in VO_2peak or p-eNOS S1177 (31, 50). One possible reason that VR did not improve endothelial relaxation in the aged Fabry mice in the current study might be related to the rapid inactivation of NO by reactive oxygen species (ROS). In the presence of elevated ROS,

NO binds to superoxide to form peroxynitrite, a powerful oxidizing intermediate (21). NT has been used as a specific marker of the presence of reactive oxygen/nitrogen species (15, 29). In a previous study, an age-related increase in NT in the aorta of older mice of an aging model was attenuated by VR with a corresponding increase in SOD and decreased NADPH oxidase activity (15). However, in the current study, the levels of NT were unaltered by VR. Furthermore, the phospho/total VASP ratio and the expressions of SODs and p67phox, an important regulatory subunit of NADPH oxidase, did not differ significantly between EX and SED mice, indicating no changes in the balance between NO availability and oxidative/nitrosative stress. In previous studies NT levels of GLA deficient mice were significantly elevated even at 2 months of age compared to wild type mice, suggesting oxidative stress in this setting does not simply represent normal age-related alterations (30, 49). Rather, the changes likely represent direct and/or indirect consequences resulting from Gb3 accumulation and related pro-inflammatory conditions, such as elevated ROS and eNOS uncoupling (47, 49). These results suggest that the expected shear stress-induced benefits on endothelial function may have been prevented by the presence of elevated ROS level in these aged Fabry mice.

Another potential reason that the elevated eNOS activity did not translate to improvement in endothelial function in the aorta might be advanced morphological alterations of the smooth muscle cells and extracellular matrix preceding the VR intervention. For example, the aortae from GLA deficient mice displayed less sensitive endothelium-independent relaxation with an NO donor compared to wild type mice, suggesting alterations in vascular smooth muscle cells (SMC) (43). Heare et al. reported that aortic wall thickness of GLA-deficient mice was significantly increased with high Gb3 storage level in endothelium and vascular SMC compared with wild type mice (28). Progressive thickening of the intima-media layers of radial arteries was also observed

in patients with Fabry disease (6). One hypothesis is that accumulation of lyso-Gb3 (globotriaosylsphingosine) in the SMC promotes SMC proliferation resulting in increased intima-media thickness in the setting of Fabry disease (1). Gb3 accumulation in the endothelial cells has also been reported to increase ROS and cellular adhesion molecules (47). Often, these pathological conditions are associated with inflammation, hypertrophy, apoptosis, and replacement fibrosis in older patients with Fabry disease (48, 51). Thus, VR may not be able to reverse the age-related alterations that have accumulated before the initiation of the intervention in Fabry disease. Taken together, these data indicate that our exercise intervention does not reverse endothelial dysfunction and oxidative stress level in these aged GLA-deficient mice.

Several limitations exist in our study. First, age-matched wild-type mice were not included for a direct comparison of the measurements with GLA-deficient mice. However, we and others have previously demonstrated endothelial dysfunction in younger and older mice with Fabry disease compared to age-matched wild-type mice (28, 30, 43). In addition, the primary goal of the present study was to gain initial insight into the effects of exercise on endothelial dysfunction and changes in signaling pathways in aged mice with Fabry disease. Finally, we assessed the levels of signaling kinases in aortic homogenates rather than in the aortic endothelial cells alone. However, a recent study, using phospho-protein-specific antibodies with immunohistochemistry analysis, demonstrated that exercise induced an activation of AMPK with concurrent elevation of p-eNOS S1177 in the endothelial cells to a greater extent than those in the smooth muscle cells in the aorta of mice (9). Although our study bears some limitations, this is the first study to evaluate the influence of voluntary running on endothelial function in a mouse model of Fabry disease.

In conclusion, VR significantly improved Akt/AMPK/eNOS signaling pathways without improvement of the severe endothelial dysfunction evident in the aorta of aged mice with Fabry

disease. This finding has clinical relevance to Fabry disease treatment by supporting the notion that early intervention may be necessary for clinical improvements. Emerging clinical data evaluating the effectiveness of long-term enzyme replacement therapy indicated that this therapy does not prevent the occurrence of new cardiovascular complications in Fabry patients with more advanced disease (44). Furthermore, another recent study demonstrated that Fabry patients without myocardial fibrosis, compared to those with myocardial fibrosis, showed better outcomes regarding left ventricular mass, improved myocardial function, and a higher exercise capacity during 3 years of enzyme replacement therapy (52). Similarly, the findings of this study raise a primary question of whether exercise might suppress the progression of endothelial dysfunction in this setting if started earlier in this disease process. Future studies examining the effects of exercise in younger age or as an adjuvant treatment with enzyme replacement therapy will further our understanding of the effects of exercise as a potential strategy for preventive and therapeutic interventions for vasculopathy in Fabry disease.

Acknowledgements

We are very grateful to Taylour A. Treadwell for her outstanding assistance with the voluntary wheel data collection. This research was supported by grants from the National Institutes of Health grant RO1 DK 055823 awarded to J.A.S. and Rackham Graduate Student Research Grant to J.J.K.

Figures

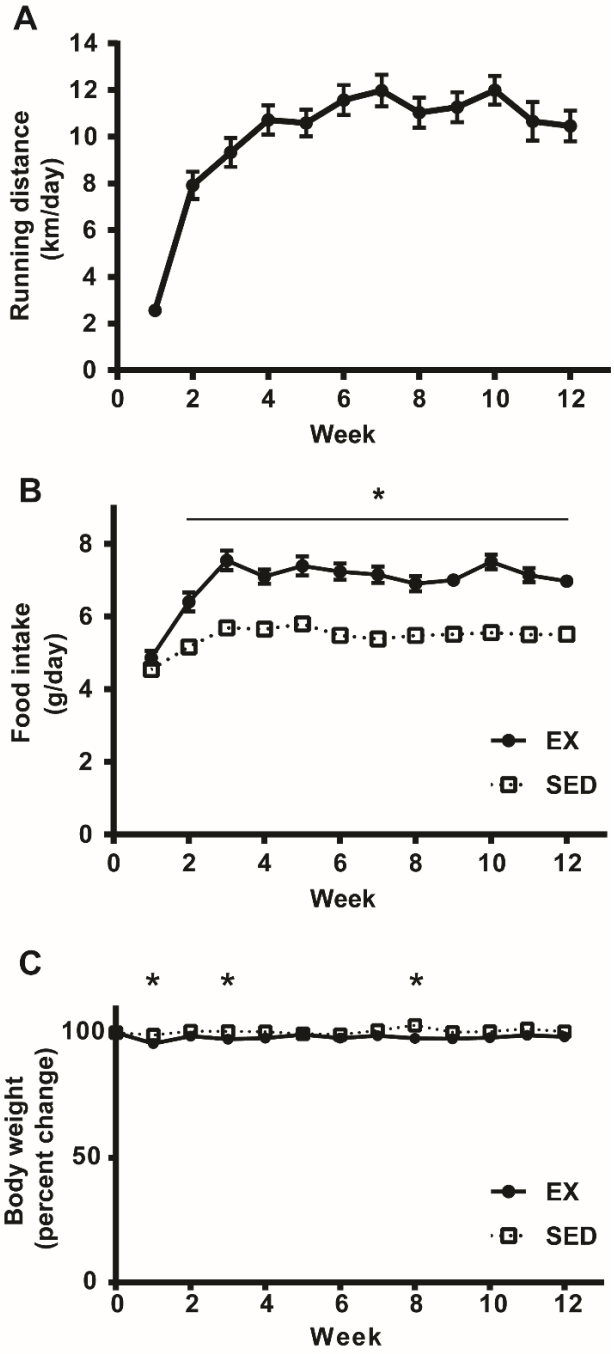

Figure 5 - 1. Daily running distance and changes in food intake and body weight in SED and EX mice during 12-week voluntary wheel intervention

Graphs show **A.** the average daily running distance (km/day), **B.** food intake (g/day); *p<0.001 compared to SED mice, and **C.** changes in body weight expressed as percent of that at the beginning of the 12-week voluntary wheel intervention (n=19/group). *p<0.05 compared to SED mice. The data represent the mean ± SEM.

Table 5-1. Summary of parameters of SED and EX mice

	SED	EX
Final body weight (g)	35.1 ± 0.6	34.0 ± 0.6
Food intake (g/day)	5.4 ± 0.1	6.9 ± 0.2*
Heart (mg)	198.4 ± 5.6	225.0 ± 6.2*
Heart:BW (g/g x 100)	0.57 ± 0.01	0.66 ± 0.01*
Gonadal fat (mg)	533.7 ± 46.1	277.9 ± 18.7*
GF:BW (g/g x 100)	1.50 ± 0.12	0.82 ± 0.06*

Data are shown as mean ± SEM (n=19/group). *$p < 0.01$ compared to SED mice.

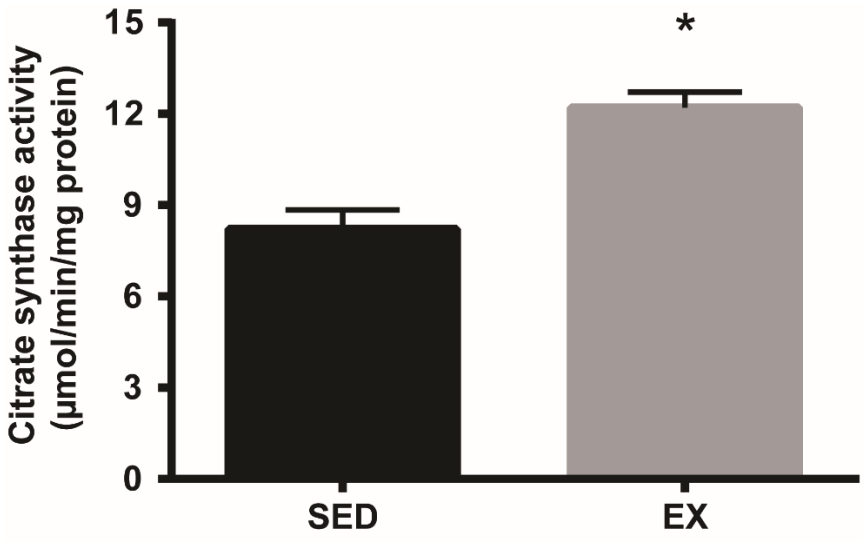

Figure 5 - 2. Increased citrate synthase activity in gastrocnemius muscle from EX mice

Gastrocnemius muscle was homogenized as described in the method section. Citrate synthase activity in muscle homogenate was determined by measuring the production of SH-CoA from the condensation of dicarboxylate oxaloacetate and acetyl CoA by citrate synthase (n=8/group). The data was expressed as µmol/min/mg protein. *$p < 0.001$ compared to SED mice.

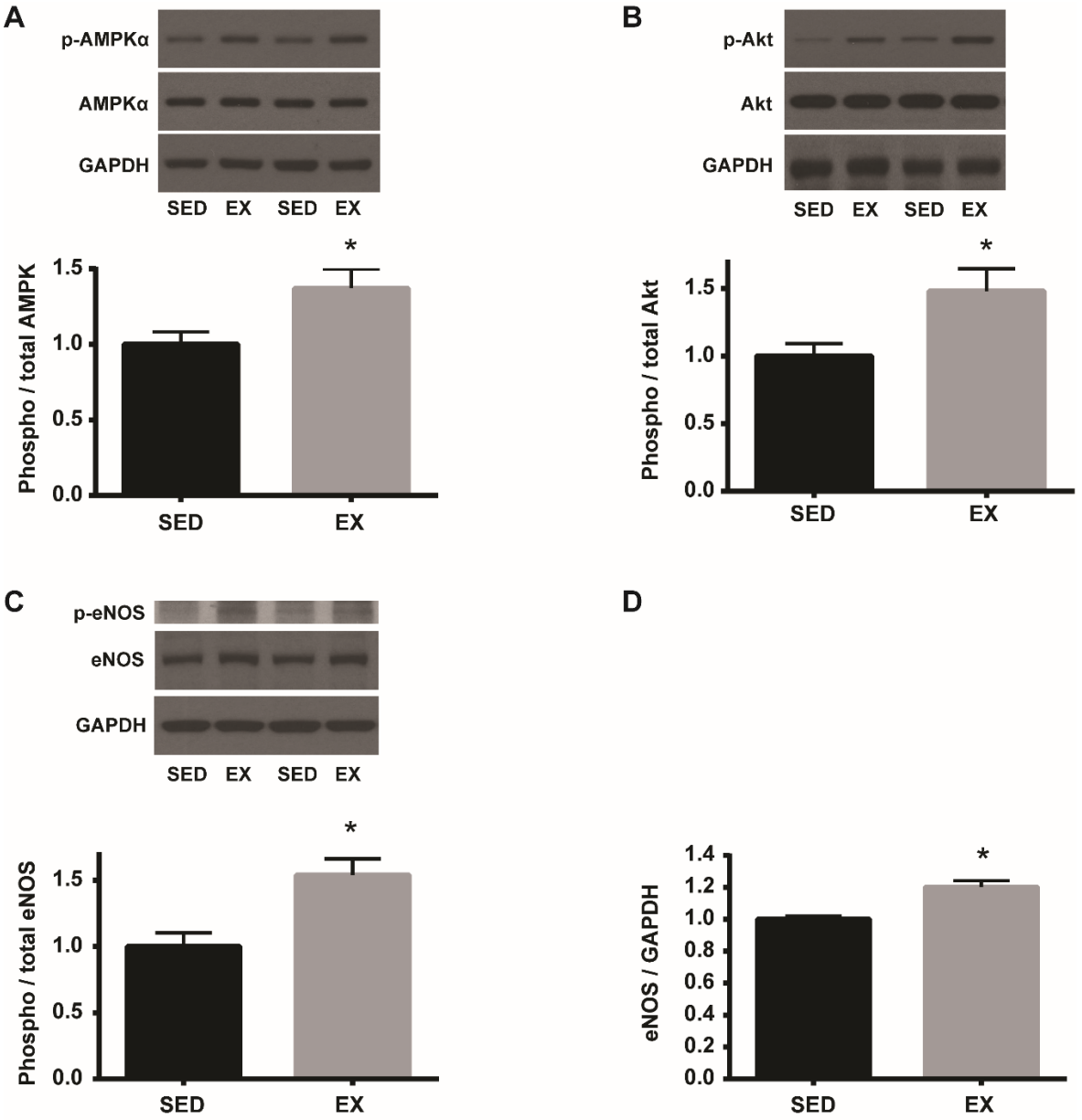

Figure 5 - 3. Increased p-AMPK, p-Akt, and p-eNOS in the aorta of EX mice

An equal amount of aortic homogenates was separated by SDS-PAGE. Representative blots were shown above each summary graph. **A.** Phospho-AMPKα (Thr172) was normalized to total AMPKα expression and expressed relative to SED mean (n=7/group). *p<0.05. **B.** Phospho-Akt (Ser473) was normalized to total Akt expression and expressed relative to SED mean (n=7/group). *p<0.05. **C.** Phospho-eNOS (Ser1177) was normalized to total eNOS expression and expressed relative to SED mean (n=7/group). *p<0.01. **D.** Total eNOS protein expression was normalized to GAPDH and expressed relative to SED mean (n=7/group). *p<0.001.

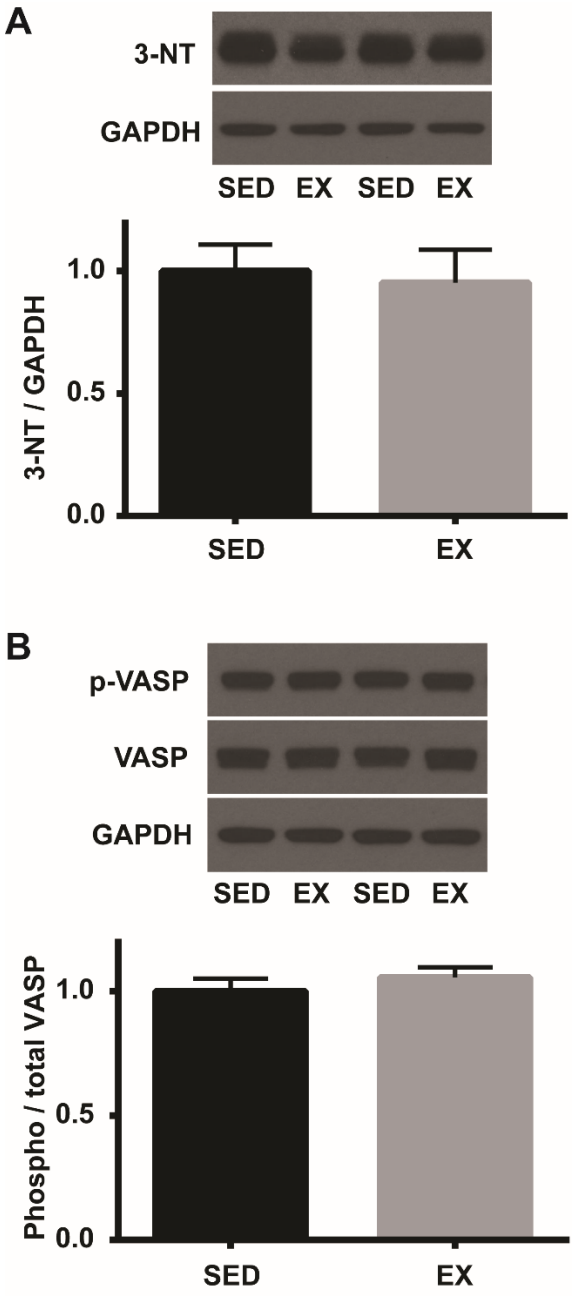

Figure 5 - 4. Levels of ROS/RNS and NO bioavailability in the aortic tissue

An equal amount of aortic homogenates was separated by SDS-PAGE. Representative blots were shown above each summary graph. **A.** Nitrotyrosine abundance was normalized to GAPDH and expressed relative to SED mean (n=7/group). **B.** Phospho-VASP (Ser239) level was normalized to total VASP expression and expressed relative to SED mean (n=7/group).

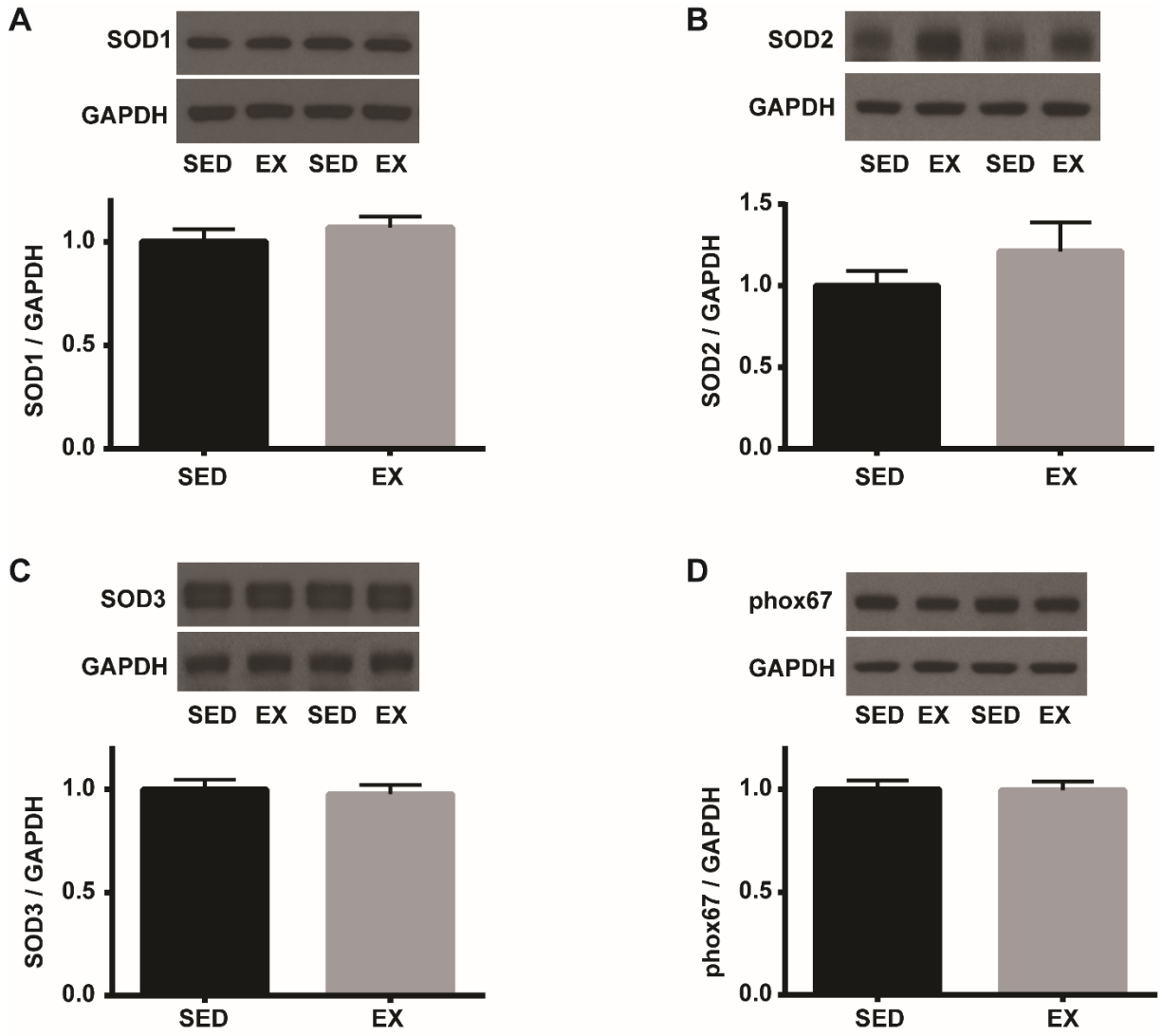

Figure 5 - 5. Levels of SOD and phox67 subunit of NADPH oxidase in the aorta of SED and EX mice

An equal amount of aortic homogenates was separated by SDS-PAGE. Representative blots were shown above each summary graph. **A.** SOD1 was normalized to GAPDH and expressed relative to SED mean (n=7/group). **B.** SOD2 was normalized to GAPDH and expressed relative to SED mean (n=7/group). **C.** SOD3 was normalized to GAPDH and expressed relative to SED mean (n=7/group). **D.** The level of phox67, a subunit of NADPH oxidase, was normalized to GAPDH and expressed relative to SED mean (n=7/group).

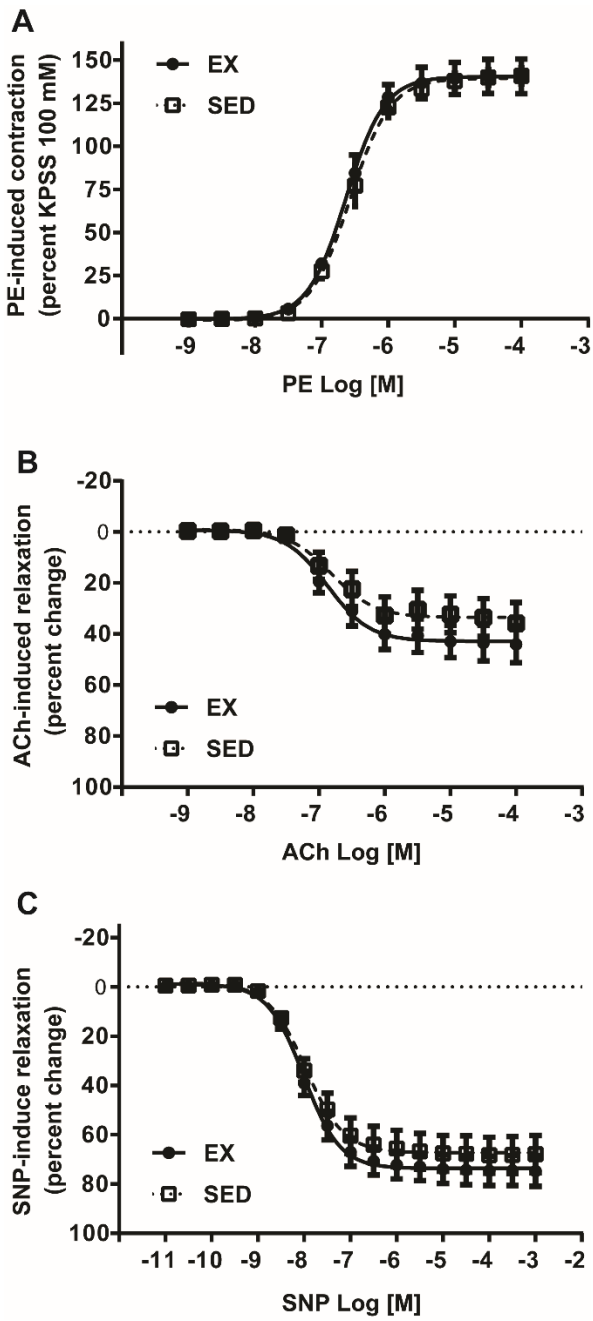

Figure 5 - 6. Endothelium-dependent and -independent aortic vascular relaxation in SED and EX mice with Fabry disease

A. Phenylephrine (PE)-mediated vascular contraction in aortic rings from SED and EX mice was expressed as percentage maximum response to KPSS (n=8/group). **B.** Acetylcholine (ACh)-mediated endothelium-dependent relaxation in the aortic rings from SED and EX mice was expressed as a percentage relaxation of the pre-contraction elicited by PE EC_{80} (n=8/group). **C.** Sodium nitroprusside (SNP)-mediated endothelium-independent relaxation in the aortic rings from SED and EX mice was expressed as a percentage relaxation of the pre-contraction elicited by PE EC_{80} (n=8/group).

References

1. **Aerts JM, Groener JE, Kuiper S, Donker-Koopman WE, Strijland A, Ottenhoff R, van Roomen C, Mirzaian M, Wijburg FA, Linthorst GE, Vedder AC, Rombach SM, Cox-Brinkman J, Somerharju P, Boot RG, Hollak CE, Brady RO, and Poorthuis BJ.** Elevated globotriaosylsphingosine is a hallmark of Fabry disease. *Proceedings of the National Academy of Sciences of the United States of America* 105: 2812-2817, 2008.

2. **Barbosa VA, Luciano TF, Marques SO, Vitto MF, Souza DR, Silva LA, Santos JP, Moreira JC, Dal-Pizzol F, Lira FS, Pinho RA, and De Souza CT.** Acute exercise induce endothelial nitric oxide synthase phosphorylation via Akt and AMP-activated protein kinase in aorta of rats: Role of reactive oxygen species. *International journal of cardiology* 167: 2983-2988, 2013.

3. **Bellamy TC and Garthwaite J.** Pharmacology of the nitric oxide receptor, soluble guanylyl cyclase, in cerebellar cells. *British journal of pharmacology* 136: 95-103, 2002.

4. **Bodary PF, Shen Y, Vargas FB, Bi X, Ostenso KA, Gu S, Shayman JA, and Eitzman DT.** Alpha-galactosidase A deficiency accelerates atherosclerosis in mice with apolipoprotein E deficiency. *Circulation* 111: 629-632, 2005.

5. **Boo YC and Jo H.** Flow-dependent regulation of endothelial nitric oxide synthase: role of protein kinases. *American journal of physiology Cell physiology* 285: C499-508, 2003.

6. **Boutouyrie P, Laurent S, Laloux B, Lidove O, Grunfeld JP, and Germain DP.** Non-invasive evaluation of arterial involvement in patients affected with Fabry disease. *Journal of medical genetics* 38: 629-631, 2001.

7. **Bowles DK and Laughlin MH.** Mechanism of beneficial effects of physical activity on atherosclerosis and coronary heart disease. *Journal of applied physiology* 111: 308-310, 2011.

8. **Brady RO, Gal AE, Bradley RM, Martensson E, Warshaw AL, and Laster L.** Enzymatic defect in Fabry's disease. Ceramide trihexosidase deficiency. *N Engl J Med* 276: 1163-1167, 1967.

9. **Cacicedo JM, Gauthier MS, Lebrasseur NK, Jasuja R, Ruderman NB, and Ido Y.** Acute exercise activates AMPK and eNOS in the mouse aorta. *American journal of physiology Heart and circulatory physiology* 301: H1255-1265, 2011.

10. **Chimenti C, Scopelliti F, Vulpis E, Tafani M, Villanova L, Verardo R, De Paulis R, Russo MA, and Frustaci A.** Increased oxidative stress contributes to cardiomyocyte

dysfunction and death in patients with Fabry disease cardiomyopathy. *Human pathology* 46: 1760-1768, 2015.

11. **Davis ME, Cai H, Drummond GR, and Harrison DG.** Shear stress regulates endothelial nitric oxide synthase expression through c-Src by divergent signaling pathways. *Circulation research* 89: 1073-1080, 2001.

12. **Davis ME, Cai H, McCann L, Fukai T, and Harrison DG.** Role of c-Src in regulation of endothelial nitric oxide synthase expression during exercise training. *American journal of physiology Heart and circulatory physiology* 284: H1449-1453, 2003.

13. **Dimmeler S, Fleming I, Fisslthaler B, Hermann C, Busse R, and Zeiher AM.** Activation of nitric oxide synthase in endothelial cells by Akt-dependent phosphorylation. *Nature* 399: 601-605, 1999.

14. **Donato AJ, Eskurza I, Silver AE, Levy AS, Pierce GL, Gates PE, and Seals DR.** Direct evidence of endothelial oxidative stress with aging in humans: relation to impaired endothelium-dependent dilation and upregulation of nuclear factor-kappaB. *Circulation research* 100: 1659-1666, 2007.

15. **Durrant JR, Seals DR, Connell ML, Russell MJ, Lawson BR, Folian BJ, Donato AJ, and Lesniewski LA.** Voluntary wheel running restores endothelial function in conduit arteries of old mice: direct evidence for reduced oxidative stress, increased superoxide dismutase activity and down-regulation of NADPH oxidase. *The Journal of physiology* 587: 3271-3285, 2009.

16. **Eitzman DT, Bodary PF, Shen Y, Khairallah CG, Wild SR, Abe A, Shaffer-Hartman J, and Shayman JA.** Fabry disease in mice is associated with age-dependent susceptibility to vascular thrombosis. *J Am Soc Nephrol* 14: 298-302, 2003.

17. **El Dib RP, Nascimento P, and Pastores GM.** Enzyme replacement therapy for Anderson-Fabry disease. *The Cochrane database of systematic reviews* 2: CD006663, 2013.

18. **Eng CM, Fletcher J, Wilcox WR, Waldek S, Scott CR, Sillence DO, Breunig F, Charrow J, Germain DP, Nicholls K, and Banikazemi M.** Fabry disease: baseline medical characteristics of a cohort of 1765 males and females in the Fabry Registry. *Journal of inherited metabolic disease* 30: 184-192, 2007.

19. **Eng CM, Germain DP, Banikazemi M, Warnock DG, Wanner C, Hopkin RJ, Bultas J, Lee P, Sims K, Brodie SE, Pastores GM, Strotmann JM, and Wilcox WR.** Fabry disease: guidelines for the evaluation and management of multi-organ system involvement. *Genetics in medicine : official journal of the American College of Medical Genetics* 8: 539-548, 2006.

20. **Fentz J, Kjobsted R, Kristensen CM, Hingst JR, Birk JB, Gudiksen A, Foretz M, Schjerling P, Viollet B, Pilegaard H, and Wojtaszewski JF.** AMPKalpha is essential for

acute exercise-induced gene responses but not for exercise training-induced adaptations in mouse skeletal muscle. *American journal of physiology Endocrinology and metabolism* 309: E900-914, 2015.

21. **Forstermann U.** Nitric oxide and oxidative stress in vascular disease. *Pflugers Archiv : European journal of physiology* 459: 923-939, 2010.

22. **Francis SH, Busch JL, Corbin JD, and Sibley D.** cGMP-dependent protein kinases and cGMP phosphodiesterases in nitric oxide and cGMP action. *Pharmacological reviews* 62: 525-563, 2010.

23. **Frey RS, Ushio-Fukai M, and Malik AB.** NADPH oxidase-dependent signaling in endothelial cells: role in physiology and pathophysiology. *Antioxidants & redox signaling* 11: 791-810, 2009.

24. **Fukai T, Siegfried MR, Ushio-Fukai M, Cheng Y, Kojda G, and Harrison DG.** Regulation of the vascular extracellular superoxide dismutase by nitric oxide and exercise training. *The Journal of clinical investigation* 105: 1631-1639, 2000.

25. **Germain DP.** Fabry disease. *Orphanet journal of rare diseases* 5: 30, 2010.

26. **Hambrecht R, Adams V, Erbs S, Linke A, Krankel N, Shu Y, Baither Y, Gielen S, Thiele H, Gummert JF, Mohr FW, and Schuler G.** Regular physical activity improves endothelial function in patients with coronary artery disease by increasing phosphorylation of endothelial nitric oxide synthase. *Circulation* 107: 3152-3158, 2003.

27. **Hambrecht R, Wolf A, Gielen S, Linke A, Hofer J, Erbs S, Schoene N, and Schuler G.** Effect of exercise on coronary endothelial function in patients with coronary artery disease. *N Engl J Med* 342: 454-460, 2000.

28. **Heare T, Alp NJ, Priestman DA, Kulkarni AB, Qasba P, Butters TD, Dwek RA, Clarke K, Channon KM, and Platt FM.** Severe endothelial dysfunction in the aorta of a mouse model of Fabry disease; partial prevention by N-butyldeoxynojirimycin treatment. *Journal of inherited metabolic disease* 30: 79-87, 2007.

29. **Heinecke JW.** Oxidized amino acids: culprits in human atherosclerosis and indicators of oxidative stress. *Free radical biology & medicine* 32: 1090-1101, 2002.

30. **Kang JJ, Shu L, Park JL, Shayman JA, and Bodary PF.** Endothelial nitric oxide synthase uncoupling and microvascular dysfunction in the mesentery of mice deficient in alpha-galactosidase A. *American journal of physiology Gastrointestinal and liver physiology* 306: G140-146, 2014.

31. **Kitzman DW, Brubaker PH, Herrington DM, Morgan TM, Stewart KP, Hundley WG, Abdelhamed A, and Haykowsky MJ.** Effect of endurance exercise training on endothelial function and arterial stiffness in older patients with heart failure and preserved

ejection fraction: a randomized, controlled, single-blind trial. *Journal of the American College of Cardiology* 62: 584-592, 2013.

32. **Kojda G, Cheng YC, Burchfield J, and Harrison DG.** Dysfunctional regulation of endothelial nitric oxide synthase (eNOS) expression in response to exercise in mice lacking one eNOS gene. *Circulation* 103: 2839-2844, 2001.

33. **Konopka AR, Suer MK, Wolff CA, and Harber MP.** Markers of human skeletal muscle mitochondrial biogenesis and quality control: effects of age and aerobic exercise training. *The journals of gerontology Series A, Biological sciences and medical sciences* 69: 371-378, 2014.

34. **Lauer N, Suvorava T, Ruther U, Jacob R, Meyer W, Harrison DG, and Kojda G.** Critical involvement of hydrogen peroxide in exercise-induced up-regulation of endothelial NO synthase. *Cardiovascular research* 65: 254-262, 2005.

35. **Linhart A.** The heart in Fabry disease. In: *Fabry Disease: Perspectives from 5 Years of FOS*, edited by Mehta A, Beck M and Sunder-Plassmann G. Oxford, 2006.

36. **Lopez-Lluch G, Hunt N, Jones B, Zhu M, Jamieson H, Hilmer S, Cascajo MV, Allard J, Ingram DK, Navas P, and de Cabo R.** Calorie restriction induces mitochondrial biogenesis and bioenergetic efficiency. *Proceedings of the National Academy of Sciences of the United States of America* 103: 1768-1773, 2006.

37. **McAllister RM and Laughlin MH.** Vascular nitric oxide: effects of physical activity, importance for health. *Essays in biochemistry* 42: 119-131, 2006.

38. **Moore DF, Kaneski CR, Askari H, and Schiffmann R.** The cerebral vasculopathy of Fabry disease. *Journal of the neurological sciences* 257: 258-263, 2007.

39. **Moore DF, Scott LT, Gladwin MT, Altarescu G, Kaneski C, Suzuki K, Pease-Fye M, Ferri R, Brady RO, Herscovitch P, and Schiffmann R.** Regional cerebral hyperperfusion and nitric oxide pathway dysregulation in Fabry disease: reversal by enzyme replacement therapy. *Circulation* 104: 1506-1512, 2001.

40. **Moore DF, Ye F, Brennan ML, Gupta S, Barshop BA, Steiner RD, Rhead WJ, Brady RO, Hazen SL, and Schiffmann R.** Ascorbate decreases Fabry cerebral hyperperfusion suggesting a reactive oxygen species abnormality: an arterial spin tagging study. *J Magn Reson Imaging* 20: 674-683, 2004.

41. **Oelze M, Mollnau H, Hoffmann N, Warnholtz A, Bodenschatz M, Smolenski A, Walter U, Skatchkov M, Meinertz T, and Munzel T.** Vasodilator-stimulated phosphoprotein serine 239 phosphorylation as a sensitive monitor of defective nitric oxide/cGMP signaling and endothelial dysfunction. *Circulation research* 87: 999-1005, 2000.

42. **Ohshima T, Murray GJ, Swaim WD, Longenecker G, Quirk JM, Cardarelli CO, Sugimoto Y, Pastan I, Gottesman MM, Brady RO, and Kulkarni AB.** alpha-Galactosidase A deficient mice: a model of Fabry disease. *Proceedings of the National Academy of Sciences of the United States of America* 94: 2540-2544, 1997.

43. **Park JL, Whitesall SE, D'Alecy LG, Shu L, and Shayman JA.** Vascular dysfunction in the alpha-galactosidase A-knockout mouse is an endothelial cell-, plasma membrane-based defect. *Clin Exp Pharmacol Physiol* 35: 1156-1163, 2008.

44. **Rombach SM, Twickler TB, Aerts JM, Linthorst GE, Wijburg FA, and Hollak CE.** Vasculopathy in patients with Fabry disease: current controversies and research directions. *Molecular genetics and metabolism* 99: 99-108, 2010.

45. **Schmitz B, Thorwesten L, Lenders M, Duning T, Stypmann J, Brand E, and Brand SM.** Physical Exercise in Patients with Fabry Disease - a Pilot Study. *International journal of sports medicine* 37: 1066-1072, 2016.

46. **Seals DR, Desouza CA, Donato AJ, and Tanaka H.** Habitual exercise and arterial aging. *Journal of applied physiology* 105: 1323-1332, 2008.

47. **Shen JS, Meng XL, Moore DF, Quirk JM, Shayman JA, Schiffmann R, and Kaneski CR.** Globotriaosylceramide induces oxidative stress and up-regulates cell adhesion molecule expression in Fabry disease endothelial cells. *Molecular genetics and metabolism* 95: 163-168, 2008.

48. **Sheppard MN, Cane P, Florio R, Kavantzas N, Close L, Shah J, Lee P, and Elliott P.** A detailed pathologic examination of heart tissue from three older patients with Anderson-Fabry disease on enzyme replacement therapy. *Cardiovascular pathology : the official journal of the Society for Cardiovascular Pathology* 19: 293-301, 2010.

49. **Shu L, Vivekanandan-Giri A, Pennathur S, Smid BE, Aerts JM, Hollak CE, and Shayman JA.** Establishing 3-nitrotyrosine as a biomarker for the vasculopathy of Fabry disease. *Kidney Int* 86: 58-66, 2014.

50. **Steppan J, Sikka G, Jandu S, Barodka V, Halushka MK, Flavahan NA, Belkin AM, Nyhan D, Butlin M, Avolio A, Berkowitz DE, and Santhanam L.** Exercise, vascular stiffness, and tissue transglutaminase. *Journal of the American Heart Association* 3: e000599, 2014.

51. **Weidemann F, Breunig F, Beer M, Sandstede J, Stork S, Voelker W, Ertl G, Knoll A, Wanner C, and Strotmann JM.** The variation of morphological and functional cardiac manifestation in Fabry disease: potential implications for the time course of the disease. *European heart journal* 26: 1221-1227, 2005.

52. **Weidemann F, Niemann M, Breunig F, Herrmann S, Beer M, Stork S, Voelker W, Ertl G, Wanner C, and Strotmann J.** Long-term effects of enzyme replacement therapy

on fabry cardiomyopathy: evidence for a better outcome with early treatment. *Circulation* 119: 524-529, 2009.

53. **Woodman CR, Muller JM, Laughlin MH, and Price EM.** Induction of nitric oxide synthase mRNA in coronary resistance arteries isolated from exercise-trained pigs. *The American journal of physiology* 273: H2575-2579, 1997.

54. **Woodman CR, Muller JM, Rush JW, Laughlin MH, and Price EM.** Flow regulation of ecNOS and Cu/Zn SOD mRNA expression in porcine coronary arterioles. *The American journal of physiology* 276: H1058-1063, 1999.

55. **Zhang QJ, McMillin SL, Tanner JM, Palionyte M, Abel ED, and Symons JD.** Endothelial nitric oxide synthase phosphorylation in treadmill-running mice: role of vascular signalling kinases. *The Journal of physiology* 587: 3911-3920, 2009.

CHAPTER 6

OVERALL DISCUSSION

It is very clear that cardiovascular disease and stroke contribute to the immense health and economic burdens in the United States and globally (11). Although the rates of cardiovascular disease have declined over decades, heart disease, stroke, and related vascular deaths still remain as the leading causes of morbidity and mortality in the United States (10). Endothelial dysfunction has been associated with the primary risk factors for cardiovascular disease, including smoking, physical inactivity, obesity, diabetes, hypertension, and dyslipidemia. Endothelial dysfunction is characterized by reduced bioavailability of vasodilators, in particular nitric oxide (NO), and considered as a key early step in atherosclerosis and a contributor to arterial thrombosis. Fabry disease is caused by α-galactosidase A (GLA) deficiency, which has pleiotropic effects on multiple organ tissues, resulting in renal disease, cardiomyopathy, and vasculopathy associated with accumulation of globo-series glycosphingolipids including globotriaosylceramide (Gb3). However, Gb3 has been implicated in other pathological conditions as well. For example, hemolytic-uremic syndrome (HUS), characterized by the classic presentation of acute renal injury, microangiopathic hemolytic anemia, and thrombocytopenia, is the leading cause of acute renal failure in children and associated with enteric infection by Shiga toxin-producing organisms, predominantly Escherichia coli (13). Although most patients of hemolytic-uremic syndrome

normally recover from kidney damage completely, approximately 5% of patients with hemolytic-uremic syndrome die by damage to the brain (18). A previous study has shown that elevated levels of inflammatory cytokines markedly increased brain endothelial cell surface Gb3 expression, a receptor for Shiga toxin, and brain endothelial cell damage (19). Furthermore, a recent study has revealed that elevated urinary Gb3 is positively associated with near-term mortality in heart disease patients who do not have Fabry disease (15), suggesting abnormalities in glycosphingolipid metabolism are associated with cardiovascular diseases beyond this rare lysosomal storage disorder. Therefore, Fabry disease provides a unique model to explore the link between Gb3 accumulation and endothelial dysfunction, findings of which may be applied to a broader population with cardiovascular disease. Using this Fabry model, my dissertation projects were designed to further characterize the causes and consequences of endothelial dysfunction and inflammation in Fabry disease. Furthermore, the effects of an exercise intervention on endothelial function were examined in the setting of eNOS uncoupling as present in mice with Fabry disease.

Together, the three of my dissertation projects discussed herein have enhanced our understanding of the effects of: *1)* GLA deficiency on microvascular endothelial dysfunction; *2)* the disruption of GLA on the secretion of endothelial-derived VWF; and *3)* exercise on aortic endothelial function and signaling alterations related to eNOS activity in the setting of GLA deficiency. Important findings of my dissertation studies include that: *A)* the GLA deficiency resulted in an early endothelial dysfunction in the mesenteric artery associated with Gb3 accumulation and eNOS uncoupling (STUDY 1); *B)* the genetic disruption of GLA in endothelial cells directly promoted decreased eNOS activity and elevated VWF secretion (STUDY 2); *C)* improving NO level or scavenging reactive oxygen species (ROS) inhibited VWF release in the setting of GLA deficiency (STUDY 2); and D*)* 12 weeks of voluntary wheel exercise improved signaling cascades of selected

kinases that are known to activate eNOS in the aorta without alterations of endothelial function in older mice with Fabry disease (STUDY 3). In this overall summary of my dissertation, I will attempt to expand on the findings of my projects and provide an integrative discussion of the collective implications that can be derived from my dissertation studies.

The key underlying component of all three of my dissertation studies was the examination of the hypothesis that dysregulation of eNOS is an important underlying basis for the vasculopathy in Fabry disease. The basis for this hypothesis was largely generated from previous studies of Gla-deficient mice and in vitro endothelial models of Fabry disease. Briefly, Gla deficient mice demonstrated a marked increase in atherosclerotic plaque lesion on an apoE1-deficient background compared to wild type mice (1). In another model, when arterial injury was induced in the carotid artery by the release of photochemical-mediated reactive oxygen species, Gla knockout mice exhibited a higher propensity for thrombosis than wild type mice (5). In a third model, aortic rings from Gla-deficient mice demonstrated impaired relaxation to acetylcholine (12). Finally, disruption of GLA in a human endothelial cell line, EA.hy926, showed decreased eNOS activity and robust elevation in 3-nitrotyrosine, a marker for eNOS uncoupling (17). Both STUDY 1 and STUDY 2 of my dissertation provide further support for the previous hypothesis. In STUDY 1, I reported that Gla-deficiency promoted an early profound reduction (~70%) in acetylcholine-mediated, endothelium-dependent relaxation in the mesenteric artery of Gla-null mice at 2 months of age compared to wild type mice. In an older age (8 months), the endothelium-dependent relaxation in the mesenteric artery of Gla knockout mice was completely absent. These conditions were associated with increased eNOS uncoupling at the younger age and changes in eNOS-regulatory phosphorylation sites at the older age. In STUDY 2, both short-term and permanent deletion of GLA from cultured endothelial cells promoted a decrease in eNOS activity (~60%)

similar to a previous study (17). Subsequently, a robust increase in VWF release from endothelial cells was observed when GLA was disrupted. Using VWF as a biomarker for endothelial dysfunction in these cells, I have found that pharmacological treatments that increase eNOS activity and NO level or decrease reactive oxygen and nitrogen species completely normalized the elevated VWF secretion in GLA deficient cells. However, recombinant GLA, the current standard of care for Fabry disease, did not improve endothelial dysfunction. This finding is important because strokes continue to occur in advanced Fabry disease patients while receiving recombinant GLA replacement therapy. The findings of STUDY 2 support the previous hypothesis of eNOS dysregulation as an important basis of the underlying vasculopathy in GLA deficiency and advocate for new possible strategies to improve endothelial dysfunction in Fabry disease.

Although my dissertation studies generally reaffirmed the major concepts of the current hypothesis, the widely accepted dogma that exercise can reverse an existing endothelial dysfunction in pathological conditions, was not supported in STUDY 3. For example, several studies examining patients with CAD have demonstrated that aerobic exercise training improves endothelium-dependent coronary artery dilatation as well as blood flow in CAD patients (7, 8). This improvement in endothelial function was associated with elevated eNOS expression and phosphorylation at serine1177 (S1177), a major eNOS activating phosphorylation site. The beneficial effects of exercise on endothelial dysfunction through activation of eNOS were also observed in the setting of sedentary aging (4, 20). In these studies, 3 months of aerobic exercise intervention restored the impaired arterial compliance and endothelium-dependent vasodilatation in sedentary middle-aged and older men to the level of those in healthy young men. It is important to note that beginning an exercise program in healthy men at any stage of life yielded significant cardiovascular health benefits (4, 20). However, in STUDY 3, I have found that 12 weeks of

exercise intervention did not improve endothelial dysfunction in the aorta of GLA deficient mice despite the activation of AMPK/Akt/eNOS signaling pathways. A previous study demonstrated that activating eNOS through S1177 phosphorylation under a complete BH4 depletion, a condition known to induce eNOS uncoupling, leads to increased superoxide production from the enzyme *in vitro* (3). However, in STUDY 3, the activation of eNOS in the setting of severe eNOS uncoupling (i.e. Fabry diease) *in vivo* was found not to be detrimental.

Several important findings from STUDY 3 gave rise to questions as to 1) why was the endothelial function not improved despite the eNOS activation?, and 2) does this portend that endothelial dysfunction is not reversible in this setting? One possible explanation would be the presence of advanced morphological alterations of the smooth muscle cells and/or extracellular matrix that may have preceded the exercise intervention. This notion is supported by several previous observations. For example, aortic wall thickness of GLA-deficient mice has been reported to be significantly increased compared with wild-type mice (9). In addition, progressive thickening of the intima-media layer of radial arteries was also observed in patients with Fabry disease (2). These previous observations together with the results of STUDY 3 raise another question of whether exercise can delay/prevent the development of endothelial dysfunction and eNOS uncoupling if started earlier in this disease process. This hypothesis that timing of intervention would be important is substantiated by previous observations. Weidemann et al. studied the effects of enzyme replacement therapy (ERT) over a period of 3 years on disease progression and clinical outcomes (left ventricular mass, myocardial function, and exercise capacity) in three groups of Fabry patients with no, mild, and severe fibrosis (21). ERT resulted in a significant improvement in all of these clinical outcomes only in the patients without left ventricular fibrosis. In comparison, the patients with mild or severe fibrosis revealed only a minor reduction in left ventricular mass

and no improvement in myocardial function or exercise capacity in response to ERT. This observation indicates that once irreversible structural changes such as fibrosis are present, ERT has only minor effects in Fabry patients. It follows, therefore, that an early intervention with ERT could provide greater protection regarding important cardiovascular complications, including stroke. Gb3 accumulation has been hypothesized to be the main mechanism that causes the vasculopathy in Fabry disease. This hypothesis seems reasonable because the metabolites that accumulate as a result of GLA deficiency, such as Gb3 and lyso-Gb3, have been demonstrated to directly or indirectly promote decreased NO level and elevated ROS production (14, 16). However, despite the efficacy of ERT on clearing stored globo-series glycosphingolipids from endothelium, it has become clear that enzyme replacement has limited impact on the prevention of important cardiovascular complications in Fabry disease. This suggests that even though Gb3 could be the causal basis for the initial ROS production and decreased NO level, the more complex alterations in vascular function occur once the disease is far advanced. Under chronically elevated ROS, bioavailability of NO is decreased by a reaction with superoxide, leading to the formation of peroxynitrite (6). Peroxynitrite is a potent oxidant, capable of oxidizing BH_4, an important cofactor for eNOS (6). With reduced BH_4 level, eNOS becomes uncoupled, producing more superoxide and less NO, which promotes further uncoupling of the enzyme. Thus, the endothelial cells enter a vicious cycle (Figure 6) where eNOS dysregulation is exacerbated. Therefore, in the advanced stage of Fabry disease, it is possible that simply removing Gb3 may not be sufficient to "recouple" eNOS in the presence of elevated ROS. The findings of STUDY 2 support this hypothesis. Using VWF as a marker for endothelial dysfunction, I have shown that GLA deficiency can directly promote eNOS dysregulation and VWF release in cell culture. Furthermore, providing human recombinant GLA back to the deficient cells resulted in only a partial decrease in the VWF

secretion, suggesting endothelial cells remained dysfunctional. In contrast, the pharmacological agents that are known to increase exogenous NO availability, correct eNOS uncoupling, or to decrease ROS level were demonstrated to inhibit VWF exocytosis in cell culture. Therefore, the clinical observation of continued cardiovascular disease complications during ERT, including cerebrovascular events, may be due to an incomplete restoration of the balance between NO and ROS, and endothelial inflammation. In Study 3, the exercise intervention (non-pharmacological approach) was observed to improve signaling cascades of eNOS activation. Considering these observations together, it is plausible to hypothesize that adjuvant therapies improving NO levels by (non)pharmacological approaches with ERT in an earlier stage of the disease process may have beneficial effects in Fabry disease.

Currently, it is challenging to demonstrate the efficacy of ERT or alternate treatment strategies specifically for Fabry disease due to the following reasons: *1)* a heterogeneous phenotype of patients, *2)* a difficulty to recruit enough number of patients with this rare disease, and *3)* the necessity of long-term follow-up studies that use stroke, myocardial infarction, and death as endpoint measures due to the lack of biomarkers. In STUDY 1, I have found an early endothelial dysfunction in the mesenteric artery, which was exacerbated in an age-dependent manner. Plasma VWF, but not sVCAM-1, of GLA-deficient mice was associated with the presence of endothelial dysfunction and eNOS uncoupling (STUDY 1 and 2). These results collectively suggest that VWF may reveal the presence and/or degree of endothelial dysfunction in Fabry disease. Future studies should evaluate whether VWF levels may be useful to determine the risk of stroke and myocardial infarction, particularly in Fabry patients with and without a history of intravascular thrombotic events.

In summary, my dissertation projects support our current understanding that endothelial dysfunction is an important mechanism contributing to the accelerated cardiovascular disease complications in Fabry disease. Specifically, my dissertation projects provide the first evidence that: *A)* GLA-deficiency causes profound endothelial dysfunction in the mesenteric artery in an early stage of the disease, *B)* the disruption of GLA in endothelial cells directly promotes endothelial inflammation and VWF secretion, which is inhibited by restoration of NO level, and *C)* exercise increases signaling cascades that are shown to activate eNOS without significant improvement in aortic endothelial relaxation in GLA deficient mice. My dissertation STUDIES 1-3 collectively reaffirm the notion that the endothelium, as a primary interface between blood and body tissues, is an active organ whose normal function is crucial for maintaining vascular health. The results of my dissertation studies lay the foundation for future experiments to further understand the mechanisms of endothelial dysfunction and inflammation in Fabry disease, and may provide a platform to study the efficacy of new treatment strategies.

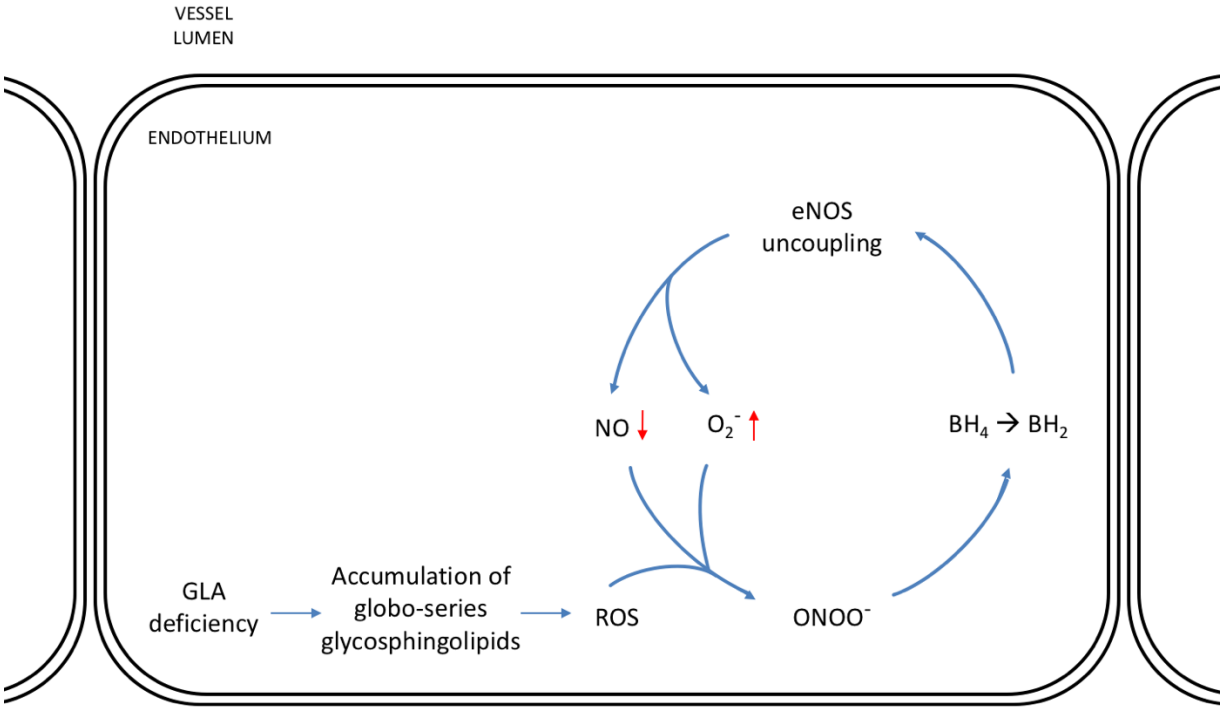

Figure 6 - 1. GLA deficiency promotes eNOS uncoupling

The loss of activity of the lysosomal GLA results in a toxic accumulation of globo-series glycosphingolipids in vascular endothelial cells. The Gb3 accumulation induces the formation of reactive oxygen species and oxidative stress. eNOS-derived NO binds to superoxide to form peroxynitrite, which reduces an important cofactor of eNOS, BH_4, to BH_2. In the absence of BH_4, eNOS generates less NO and more superoxide and produces peroxynitrite, which promotes further uncoupling of eNOS. In this vicious cycle, replacement of GLA or removing Gb3 may not be sufficient to "recouple" eNOS. *Abbreviations*: *GLA*: α-galactosidase A; *ROS*: reactive oxygen species; *$ONOO^-$*: peroxynitrite; *BH_4*: tetrahydrobiopterin; *BH_2*: dihydrobiopterin; *eNOS*: endothelial nitric oxide synthase; *NO*: nitric oxide; *O_2^-*: superoxide.

References

1. **Bodary PF, Shen Y, Vargas FB, Bi X, Ostenso KA, Gu S, Shayman JA, and Eitzman DT.** Alpha-galactosidase A deficiency accelerates atherosclerosis in mice with apolipoprotein E deficiency. *Circulation* 111: 629-632, 2005.

2. **Boutouyrie P, Laurent S, Laloux B, Lidove O, Grunfeld JP, and Germain DP.** Non-invasive evaluation of arterial involvement in patients affected with Fabry disease. *Journal of medical genetics* 38: 629-631, 2001.

3. **Chen CA, Druhan LJ, Varadharaj S, Chen YR, and Zweier JL.** Phosphorylation of endothelial nitric-oxide synthase regulates superoxide generation from the enzyme. *The Journal of biological chemistry* 283: 27038-27047, 2008.

4. **DeSouza CA, Shapiro LF, Clevenger CM, Dinenno FA, Monahan KD, Tanaka H, and Seals DR.** Regular aerobic exercise prevents and restores age-related declines in endothelium-dependent vasodilation in healthy men. *Circulation* 102: 1351-1357, 2000.

5. **Eitzman DT, Bodary PF, Shen Y, Khairallah CG, Wild SR, Abe A, Shaffer-Hartman J, and Shayman JA.** Fabry disease in mice is associated with age-dependent susceptibility to vascular thrombosis. *J Am Soc Nephrol* 14: 298-302, 2003.

6. **Forstermann U.** Nitric oxide and oxidative stress in vascular disease. *Pflugers Archiv : European journal of physiology* 459: 923-939, 2010.

7. **Hambrecht R, Adams V, Erbs S, Linke A, Krankel N, Shu Y, Baither Y, Gielen S, Thiele H, Gummert JF, Mohr FW, and Schuler G.** Regular physical activity improves endothelial function in patients with coronary artery disease by increasing phosphorylation of endothelial nitric oxide synthase. *Circulation* 107: 3152-3158, 2003.

8. **Hambrecht R, Wolf A, Gielen S, Linke A, Hofer J, Erbs S, Schoene N, and Schuler G.** Effect of exercise on coronary endothelial function in patients with coronary artery disease. *N Engl J Med* 342: 454-460, 2000.

9. **Heare T, Alp NJ, Priestman DA, Kulkarni AB, Qasba P, Butters TD, Dwek RA, Clarke K, Channon KM, and Platt FM.** Severe endothelial dysfunction in the aorta of a mouse model of Fabry disease; partial prevention by N-butyldeoxynojirimycin treatment. *Journal of inherited metabolic disease* 30: 79-87, 2007.

10. **Lloyd-Jones DM, Hong Y, Labarthe D, Mozaffarian D, Appel LJ, Van Horn L, Greenlund K, Daniels S, Nichol G, Tomaselli GF, Arnett DK, Fonarow GC, Ho PM, Lauer MS, Masoudi FA, Robertson RM, Roger V, Schwamm LH, Sorlie P, Yancy CW, Rosamond WD, American Heart Association Strategic Planning Task F, and**

Statistics C. Defining and setting national goals for cardiovascular health promotion and disease reduction: the American Heart Association's strategic Impact Goal through 2020 and beyond. *Circulation* 121: 586-613, 2010.

11. **Mozaffarian D, Benjamin EJ, Go AS, Arnett DK, Blaha MJ, Cushman M, de Ferranti S, Despres JP, Fullerton HJ, Howard VJ, Huffman MD, Judd SE, Kissela BM, Lackland DT, Lichtman JH, Lisabeth LD, Liu S, Mackey RH, Matchar DB, McGuire DK, Mohler ER, 3rd, Moy CS, Muntner P, Mussolino ME, Nasir K, Neumar RW, Nichol G, Palaniappan L, Pandey DK, Reeves MJ, Rodriguez CJ, Sorlie PD, Stein J, Towfighi A, Turan TN, Virani SS, Willey JZ, Woo D, Yeh RW, Turner MB, American Heart Association Statistics C, and Stroke Statistics S.** Heart disease and stroke statistics--2015 update: a report from the American Heart Association. *Circulation* 131: e29-322, 2015.

12. **Park JL, Whitesall SE, D'Alecy LG, Shu L, and Shayman JA.** Vascular dysfunction in the alpha-galactosidase A-knockout mouse is an endothelial cell-, plasma membrane-based defect. *Clin Exp Pharmacol Physiol* 35: 1156-1163, 2008.

13. **Robson WL, Leung AK, and Kaplan BS.** Hemolytic-uremic syndrome. *Current problems in pediatrics* 23: 16-33, 1993.

14. **Rombach SM, Twickler TB, Aerts JM, Linthorst GE, Wijburg FA, and Hollak CE.** Vasculopathy in patients with Fabry disease: current controversies and research directions. *Molecular genetics and metabolism* 99: 99-108, 2010.

15. **Schiffmann R, Forni S, Swift C, Brignol N, Wu X, Lockhart DJ, Blankenship D, Wang X, Grayburn PA, Taylor MR, Lowes BD, Fuller M, Benjamin ER, and Sweetman L.** Risk of death in heart disease is associated with elevated urinary globotriaosylceramide. *Journal of the American Heart Association* 3: e000394, 2014.

16. **Shen JS, Meng XL, Moore DF, Quirk JM, Shayman JA, Schiffmann R, and Kaneski CR.** Globotriaosylceramide induces oxidative stress and up-regulates cell adhesion molecule expression in Fabry disease endothelial cells. *Molecular genetics and metabolism* 95: 163-168, 2008.

17. **Shu L, Vivekanandan-Giri A, Pennathur S, Smid BE, Aerts JM, Hollak CE, and Shayman JA.** Establishing 3-nitrotyrosine as a biomarker for the vasculopathy of Fabry disease. *Kidney Int* 86: 58-66, 2014.

18. **Siegler RL, Pavia AT, Christofferson RD, and Milligan MK.** A 20-year population-based study of postdiarrheal hemolytic uremic syndrome in Utah. *Pediatrics* 94: 35-40, 1994.

19. **Stricklett PK, Hughes AK, Ergonul Z, and Kohan DE.** Molecular basis for up-regulation by inflammatory cytokines of Shiga toxin 1 cytotoxicity and globotriaosylceramide expression. *The Journal of infectious diseases* 186: 976-982, 2002.

20. **Tanaka H, Dinenno FA, Monahan KD, Clevenger CM, DeSouza CA, and Seals DR.** Aging, habitual exercise, and dynamic arterial compliance. *Circulation* 102: 1270-1275, 2000.

21. **Weidemann F, Niemann M, Breunig F, Herrmann S, Beer M, Stork S, Voelker W, Ertl G, Wanner C, and Strotmann J.** Long-term effects of enzyme replacement therapy on fabry cardiomyopathy: evidence for a better outcome with early treatment. *Circulation* 119: 524-529, 2009.

APPENDICES

Appendix I: Study 2

This section contains additional figures for data collected from Study 2 that were not included in Chapter 4.

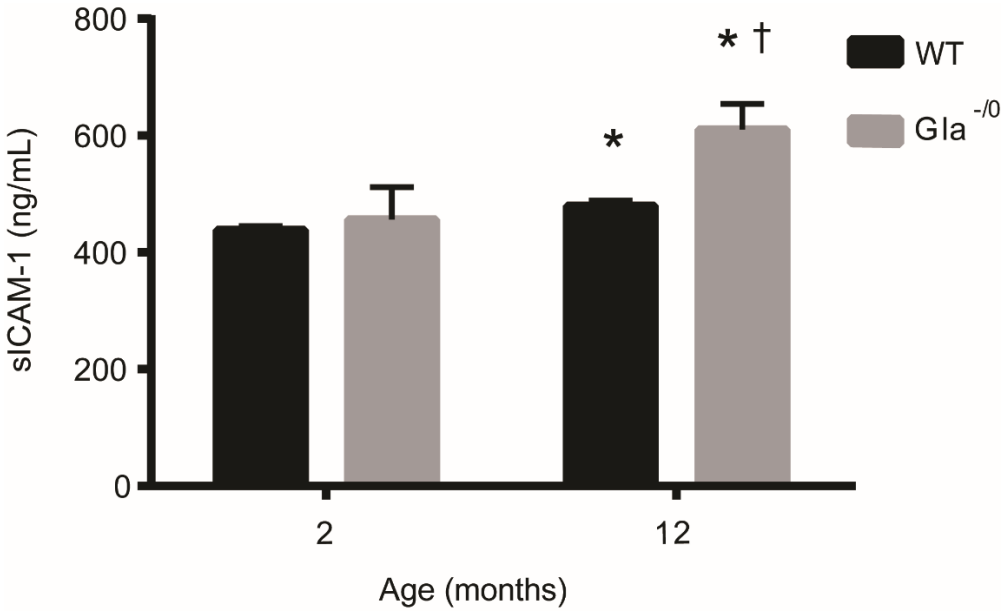

Figure A - I 4 - 1. Elevated sICAM-1 level in WT and Gla deficient mice

The blood was drawn via the retro-orbital plexus from male wild type (WT) and Gla deficient mice at the indicated ages. Levels of soluble intercellular adhesion molecule 1 (sICAM-1) were measured by ELISA (n=6/group and n=2-3/group at 2 and 12 months, respectively). *$p < 0.02$ compared to the same genotype at 2 months, †$p < 0.05$ compared to the age-matched WT mice.

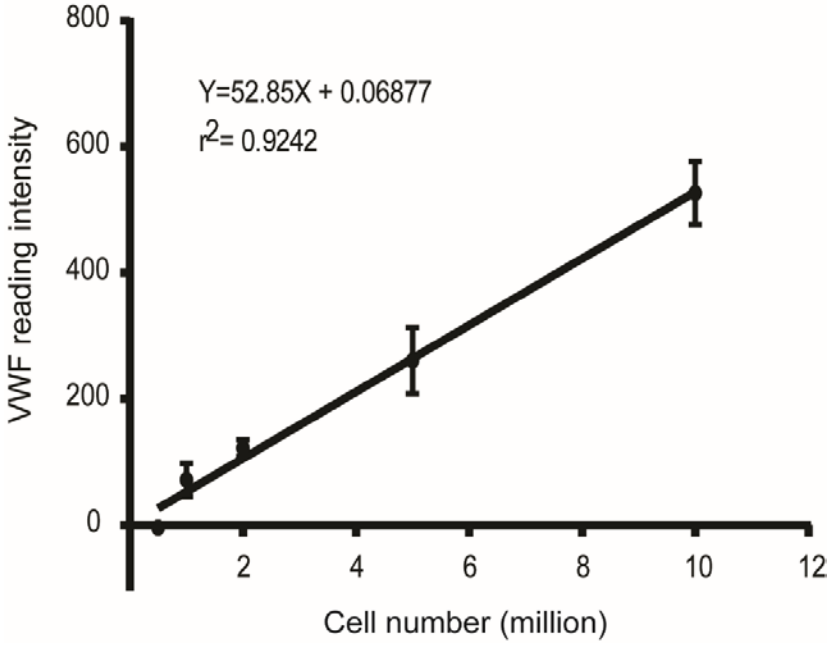

Figure A - I 4 - 2. Correlation between VWF and the number of cells

EA.hy926 cells were grown in 75 cm^2 flasks and trypsinized. Cell number was counted by hemocytometer. The indicated number of cells were lysed with lysis buffer, and VWF levels in the lysate samples were measured by AlphaLISA (n=3/group).

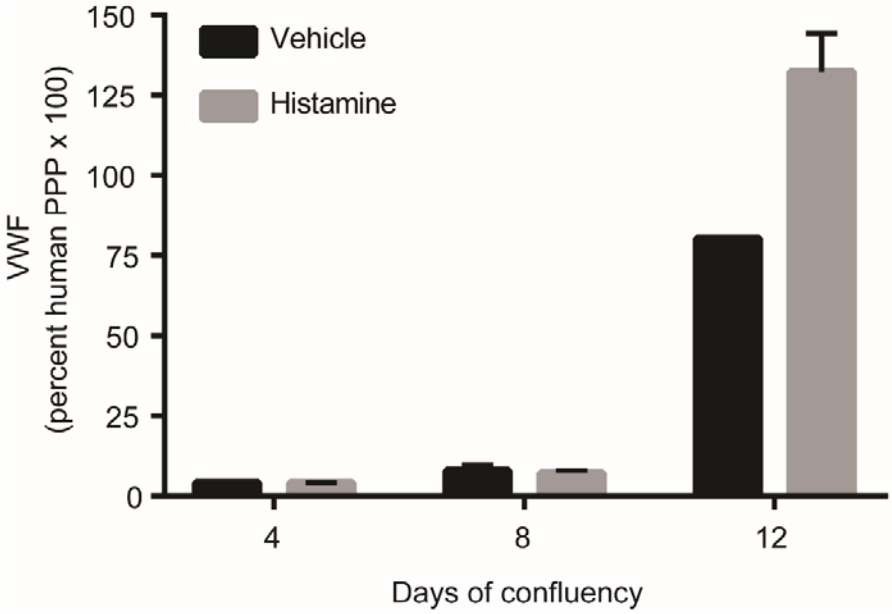

Figure A - I 4 - 3. Histamine-evoked VWF release from EA.hy926 cells with different days of confluency

EA.hy926 cells were plated at 6 x 10^6 density in a 100 cm^2 petri dish. The cells were grown for the indicated days above after cell confluency was attained. The cells were washed twice with 0% FBS DMEM media and incubated in vehicle (DMEM) or histamine (100 µM) for 90 minutes. The concentration of VWF released into media was determined by ELISA using a dilution series of pooled normal plasma with known VWF antigen levels as standards (n=2/group).

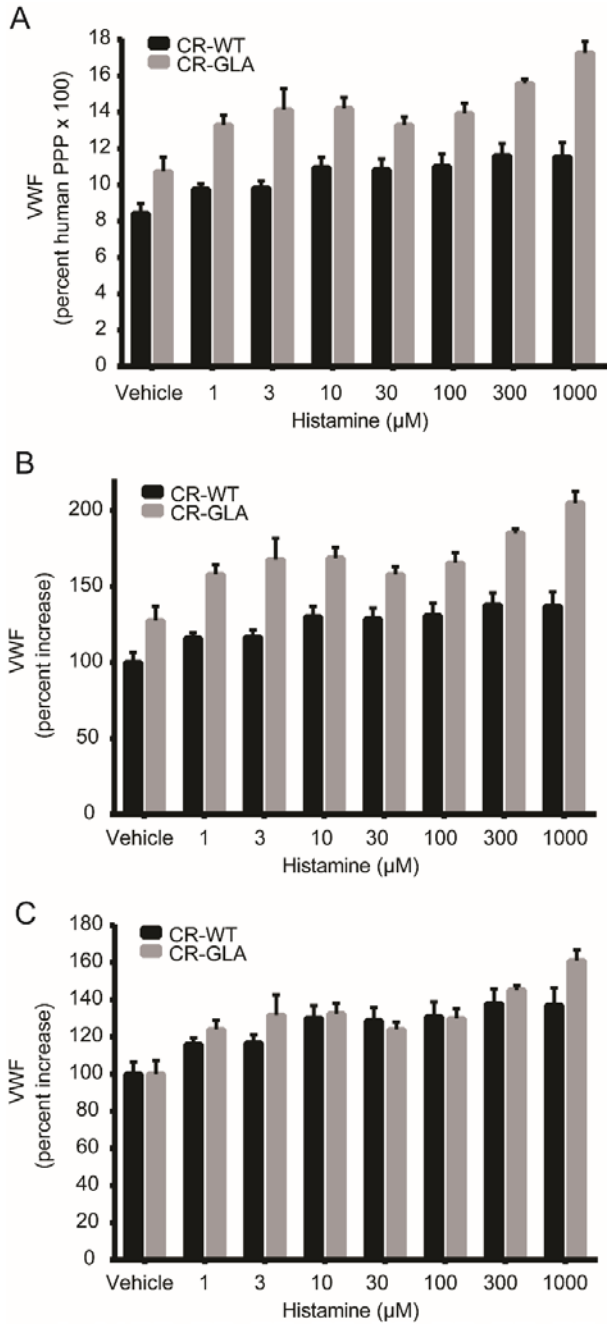

Figure A - I 4 - 4. Histamine-evoked VWF release in CRISPR cells

CR-WT and CR-GLA cells were plated at 2 x 10^5 density in a 24-well plate. The cells were grown for 10 days after cell confluency was attained. The cells were washed twice with 0% FBS DMEM media and incubated in vehicle (DMEM) or histamine for 60 minutes. A. The concentration of VWF released into media was determined by ELISA using a dilution series of pooled normal plasma with known VWF antigen levels as standards (n=3/group). B. The VWF levels were expressed as fold changes with respect to CR-WT vehicle. C. The VWF levels were expressed as fold changes with respect to each vehicle condition.

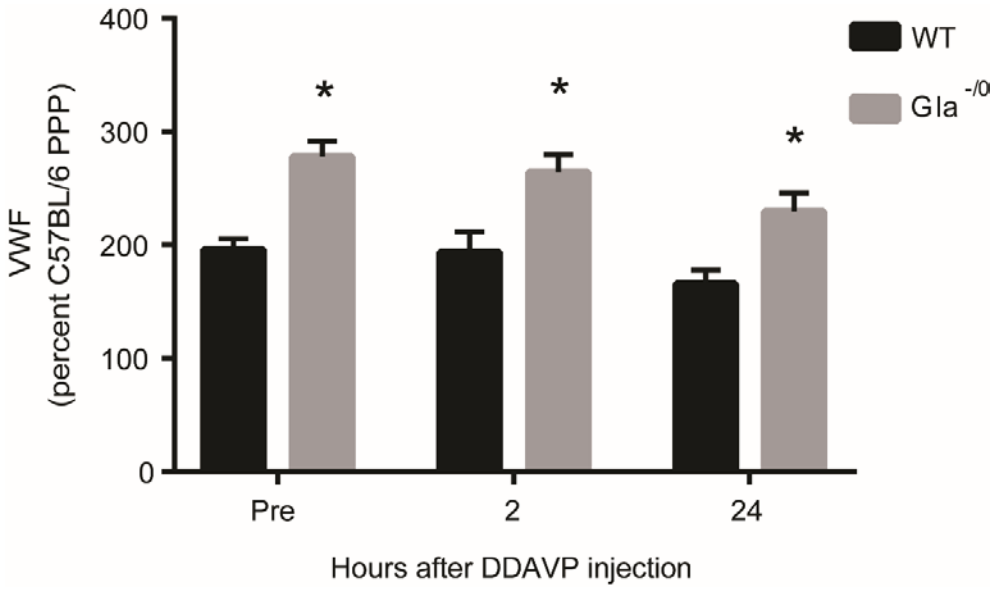

Figure A - I 4 - 5. The effect of DDAVP on VWF secretion in WT and Gla deficient mice

The blood was drawn via the retro-orbital plexus from female wild type (WT) and Gla deficient mice at 10 months of age before an intravenous injection of desmopressin (DDAVP) at 3 µg/kg body weight. The blood was drawn again, 2 and 24 hours post DDAVP injection. Circulating plasma VWF levels were measured by ELISA (n=6-8/group). A dilution series of pooled platelet-poor plasma (PPP) from C56BL/6 mice (n=10) was used as a reference (100%). *$p < 0.02$ compared to the time-matched WT.

Appendix II: Study 3

This section contains additional figures for data collected from Study 3 that were not included in Chapter 5.

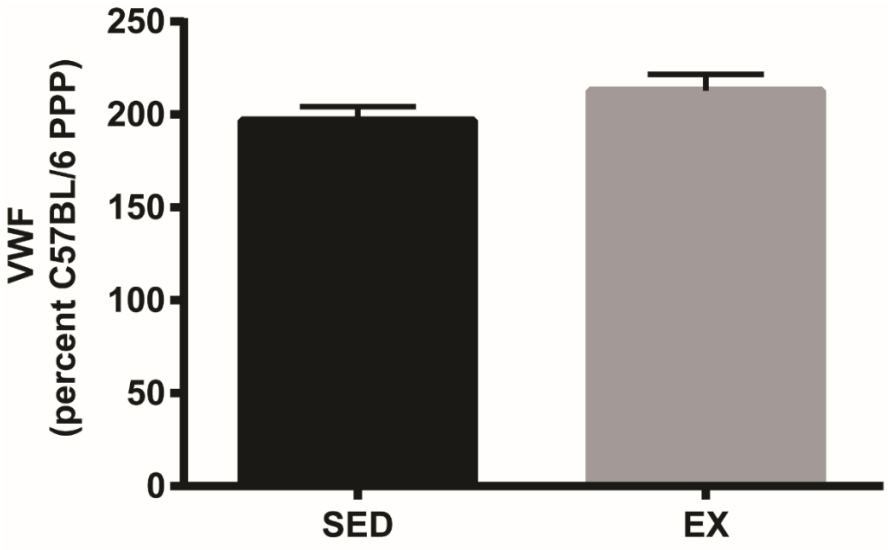

Figure A - II 5 - 1. VWF levels in EX and SED mice at the completion of 12 weeks of voluntary wheel exercise training

The blood was drawn from mice via the left ventricle using a 3 mL syringe and a 21 gauge needle preloaded with sodium citrate (1:9, v/v to blood) (n=19/group). Blood was centrifuged at 2,000 x g for 10 min at room temperature to obtain platelet-poor plasma. VWF antigen levels in the plasma was determined by ELISA. A dilution series of pooled platelet-poor plasma (PPP) from C56BL/6 mice (n=10) was used as a reference (100%).